**Ph.D. Dissertation of Natural Science**

# Characteristics and Cognitive Functions of Another Hippocampal Subregion: *Fasciola Cinereum*

해마의 또다른 하위 영역인 소대회의 특징과 인지적 기능

**February 2020**

**Graduate School of Natural Sciences**

**Seoul National University**

**Brain and Cognitive Sciences Major**

**Seong-Beom Park**

# Abstract

The *fasciola cinereum* (FC) is a small subregion of the hippocampus, relatively unattended compared to the other hippocampal subregions. It is known that each subregion of the hippocampus plays a key role in cognitive function, especially in learning and memory, through its unique connections and physiological characteristics. However, the connectivity and physiological characteristics of FC has rarely been studied, so it is hard to predict what the cognitive function is. In this anatomy study, it was revealed that FC receives input from the lateral entorhinal cortex and perirhinal cortex and projects into DG. Taking into account the anatomical connections of FC, it can have a cognitive function related to contextual memory and object associative memory. To test if FC involved in learning, a contextual learning experiment, which was known as DG-dependent learning, was performed with rats whose FC was selectively damaged. The retrieval performance with the pre-learned scenes was not impaired, while acquisition performance with the new scenes was impaired in the lesion group, comparing to control rats, suggesting that FC is essential for contextual memory acquisition. In addition, FC showed important roles in other memory tasks, including object-place association tasks, suggesting that FC has a more general role in learning as well as contextual learning. In the freely moving rats, the neurons of the FC showed a place field like those in the other hippocampal subregions, while detailed electrophysiological characteristics differed from those of CA1. Also, when the place field was observed in the FC cells of rats during shuttling on the T-maze with alternating of contextual scenes, it was observed that the place field showed global remapping. **Significance Statement**: This study is critical because it revealed the connectivity, physiological characteristics, and cognitive function in memory of FC, which was seldom noticed in the past, and newly suggested learning mechanism of dentate gyrus including FC. This finding not only broadened the understanding of the structure and function of the

hippocampus but also found a possible cause of anterograde amnesia, which is meaningful in that it can be the beginning of treatment of the disease. The newly presented model may also inspire the construction of brain-like AI.

**Keywords:** hippocampus, *fasciola cinereum*, contextual memory, associative memory

**Student Number :** 2014-21335

# Table of Contents

# List of Figures

# List of Tables

# Background

## The importance of the hippocampus in cognition

A pair of sea horses, also known as the hippocampus, in our heads are experts in navigating the sea of memory. Without this, we are lost in the sea of memory. The fact that the hippocampus is important for memory was first known to the world by Scoville and Millner in 1957 (Scoville and Milner, 1957).Since this study first reported that patients who had surgery to remove both hippocampi due to epilepsy had difficulty in forming new memories, many studies have shown that hippocampus is important for episodic memory (Morris et al., 1982; Parkinson et al., 1988; Kim and Fanselow, 1992; Nyberg et al., 1996).

Meanwhile, another breakthrough for hippocampus study is the discovery of place cell. In 1971, it was reported that a neuron in the hippocampus has a receptive field in a specific place (O'Keefe and Dostrovsky, 1971). The presence of place cell in the hippocampus is a critical basis of cognitive map theory (O'Keefe and Nadel, 1978). The theory claims that there is a map in the hippocampus that tells the subject where it is by integrating allocentric and egocentric information. The hippocampal place cell has been confirmed by many studies afterward, and several studies that revealed various spatial and non-spatial representations have been conducted (Muller and Kubie, 1987; Muller and Kubie, 1989; Mehta et al., 2000; Wood et al., 2000; Lee and Kesner, 2004b; Leutgeb et al., 2004; Pastalkova et al., 2008; Aronov et al., 2017).

## The importance of the hippocampal subfields

Since it is known that the hippocampus is important for memory, a topic that many researchers have interested in is the mechanism that the hippocampus process memory. Researchers who focused on the unique connection and structure

of the hippocampus note that each subfield of the hippocampus had its unique cognitive functions and physiological characteristics as well as anatomical connections (Marr, 1971; O'Reilly and McClelland, 1994; Treves and Rolls, 1994; Witter et al., 2000; Gilbert et al., 2001; Lee et al., 2004b; Leutgeb et al., 2004; Vazdarjanova and Guzowski, 2004; Neunuebel and Knierim, 2014). The pioneer who noted the structure of the subfields and argued that they have a unique role based on the anatomical connection was David Marr (Marr, 1971). In his paper, he noted the anatomical connections and structures of EC, DG, and CA3, and predicted orthogonal and sparse representations of the memory in the DG based on the connection (Figure 1). Besides, he argued that CA3's recurrent collaterals maintain a robust representation of memory even when some noisy inputs are mixed. Even though this model was too simplified to explain the roles of detailed connectional features (e.g. direct projection from EC to CA3 called perforant pathway, CA3 to EC connection via CA1 and subiculum), these ideas later inspired many models which explain mechanism of hippocampus, and different functions and physiological representations between subfields were revealed by actual physiological experiments (Marr, 1971; O'Reilly and McClelland, 1994; Treves and Rolls, 1994; Lee et al., 2004b; Leutgeb et al., 2004; Vazdarjanova and Guzowski, 2004; Neunuebel and Knierim, 2014). Also, the understanding of how the hippocampus process memory has been continuously updated by findings of novel connections such as the connection from frontal cortex to hippocampus and observations about the areas which have been less noticed such as mossy cell in DG and CA2 (Jinde et al., 2012; Mankin et al., 2015; Rajasethupathy et al., 2015; GoodSmith et al., 2017; Senzai and Buzsaki, 2017). To sum up, knowing the connections and characteristics of the subfields of the hippocampus is important for understanding its function and working mechanism.

# A novel hippocampal subfield: *Fasciola Cinereum*

Despite the importance of study for hippocampal subfields, *fasciola cinereum* (FC), a subfield of the hippocampus, has been ignored and its anatomical and physiological characteristics and cognitive function in memory are largely unknown. The structure located along the midline of the dorsal hippocampus in the longitudinal axis and makes a border with CA1 and subiculum(Paxinos and Watson, 2009; Swanson, 2018). The name of FC depicted the shape of the structure. *Fasciola* denoted a small band while *cinereum* (or *cinerea*) denoted gray matter, so the name means a small band-shaped gray matter. The shape in the coronal section differs by anterior to posterior. In the anterior, right posterior to the point, where CA subfields and the septal tip of DG are separated, it lies (Figure 6. The second row). It looks like a check-shape (✓) rather than 'I' shape in the middle (Figure 6. The third row) and become a dot in posterior and meet the indusium griseum (IG) at the end of splenium, which is the posterior part of the corpus callosum (Figure 6. The fifth row). As its name, the area seems small in the coronal section, but the length in the longitudinal axis is about 2 mm (Figure 7). Even though the name and location of the structure have been known from 1838, little is known about its function and connectivity (Arnold, 1838). A summary of what has been reported so far is as follows.

Since the name of the area was first reported by Arnold (Arnold, 1838; Swanson, 2014), few studies described FC in various species. Before the 1990s, researchers addressed FC in a structural view. Thanks to Hjorth-Simonsen and Zimmer, it is possible to track the point of view about FC (Hjorth-Simonsen and Zimmer, 1975). They reported that Giacomini considered FC as an extension of the dentate gyrus (DG), while Ganser, Zuckerkandl, and Retzius considered the hippocampal subregion as a part of Cornu Ammonis, and reported that the structure

is composed of pyramidal neurons in human[1]. Giorgio reported that FC in humans appeared in the prenatal stage. In the rabbit, a region called accessory fascia dentate classified by Das was introduced as FC by Hjorth-Simonsen (Hjorth-Simonsen and Zimmer, 1975). Besides, Hjorth-Simonsen reported that the structure is composed of granule cells and considered as a continuation of the dentate gyrus in rats (Hjorth-Simonsen and Laurberg, 1977). Also, he reported the synaptic connection from LEC to FC (Hjorth-Simonsen, 1972) by making lesion in LEC and observing the degeneration of the synaptic terminal in FC. Hill and Mark also considered FC as a part of DG (Hill, 1895; Mark et al., 1993). In summary, the topic about FC at an early age was whether it is part of the dentate gyrus or *Cornu Ammonis*.

Despite the attention for FC, Specific physiological characteristics were scarcely reported. From 1993, several genetic markers were reported about FC, starting with bFGF (Humpel et al., 1993; Lippoldt et al., 1993; Itoh et al., 1994; Dalley et al., 2008) (Table 1). Many of them noted that the genetic similarity between FC and CA2. Therefore, some researchers raise the possibility that FC is a continuation of CA2 (Laeremans et al., 2013).

Another issue about FC is the lateral border with CA1 in rats and mice. Several studies make the lateral boundary of FC wider than that reported in previous studies (Henriksen et al., 2010; Kjonigsen et al., 2011; von Heimendahl et al., 2012; Witter, 2012; Igarashi et al., 2014; Boccara et al., 2015; Kjonigsen et al., 2015). The trend has recently emerged that defined the laterally extended area as FC or FC-CA

---

[1] However, it should be noted that in human, the tail of hippocampus is not only composed of *fasciola cinereum* but also other structures including gyrus fasciolaris. Even though Hjorth-Simonsen reported that Retzius re-named FC to gyrus fasciolaris because the structure is independent from dentate gyrus, it is possible that he intended other area next to FC called gyrus fasciolaris, which is reported as continuation of *cornu ammonis* (Mark et al., 1993).

area, which was considered CA1 or subiculum in other previous studies (Stephan, 1975; Hunsaker et al., 2008; Paxinos and Watson, 2009; Swanson, 2018).

The reason why this area is so diversely interpreted might be due to a lack of knowledge for the area. It is difficult to study in this area. FC is located under the superior sagittal sinus, which is huge vessel on the brain (Huang et al., 2013). Its small size makes it challenging to insert electrodes or inject drugs. In addition, it is difficult to establish a hypothesis due to the lack of basic knowledge for the area. The goal of this study is to reveal fundamental knowledge for FC such as anatomical connection, cognitive function, and physiological characteristics. This information can solve several issues and can be the basis for further studies.

The first issue to be addressed in this study is to confirm whether FC is a part of orthodox subregions in the hippocampus or independent subfield. The aforementioned studies interpreted the structure as CA2 or DG. The tendency seems to have been concluded regardless of omnifaceted comparisons with other areas of the hippocampus. In order to be sure that FC is a part of another well-known subregion or independent structure, it is necessary to identify the FC in various aspects, including anatomical, physiological, and functional aspects.

Another issue with FC is that the boundary between FC and adjacent CA1 differ by research. The distalmost continuation of the pyramidal cell layer of dorsal CA1 is confusing due to its several names: CA1, subiculum, and FC (Stephan, 1975; Hunsaker et al., 2008; Paxinos and Watson, 2009; Henriksen et al., 2010; Kjonigsen et al., 2011; von Heimendahl et al., 2012; Witter, 2012; Boccara et al., 2015; Kjonigsen et al., 2015; Swanson, 2018). It needs to be examined that this newly extended area is FC or not. Knowing the exact boundary of FC and CA1 is essential not only for understanding FC but also for understanding CA1 because the anatomical and physiological characteristics of CA1 vary along the transverse axis.

**Table 1. Genetic expression in FC**

| Gene | Full name | Reference | Note |
|---|---|---|---|
| **Genes expressed in the both FC and CA2** | | | |
| Pcp4 | Purkinje cell protein 4 | (Lein et al., 2005) | Also observed in the DG |
| Amigo2 | Adhesion molecule with Ig-like domain 2 | (Laeremans et al., 2013) | Also observed in the CA3a |
| bFGF | Fibroblast growth factor 2 | (Humpel et al., 1993; Lippoldt et al., 1993; Itoh et al., 1994) | |
| NT-3 | Neurotrophin-3 | (Vigers et al., 2000) | |
| RGS14 | Regulator of G-protein signaling 14 | (Lee et al., 2010) | |
| $OX_1R$ | Orexin receptor 1 | (Marcus et al., 2001) | Also observed in the crest of the septal DG |
| Cx30.2 | Connexin 30.2 | (Kreuzberg et al., 2008) | |
| Nestin | Nestin | (Hendrickson et al., 2011) | |
| Ncald | Neurocalcin-δ | (Girard et al., 2015) | |
| **Gene expressed in the FC, but not in CA2** | | | |
| RgmA | Repulsive guidance molecule A | (Schmidtmer and Engelkamp, 2004) | RgmA is restricted to the FC in adult mice, but not in young animals(Brinks et al., 2004; Li et al., 2016). However, it should be clarified in that another study reported that RgmA was found in other hippocampal subregions in adult mice (van den Heuvel et al., 2013). |
| Fam163b | Family with sequence similarity 163 member b | (Lein et al., 2007) | Figure 13. (A). Also observed in DG. |
| **Genes expressed in the CA2, but not in the FC** | | | |
| S100b | S100 protein, beta polypeptide, neural | (Dalley et al., 2008) | |

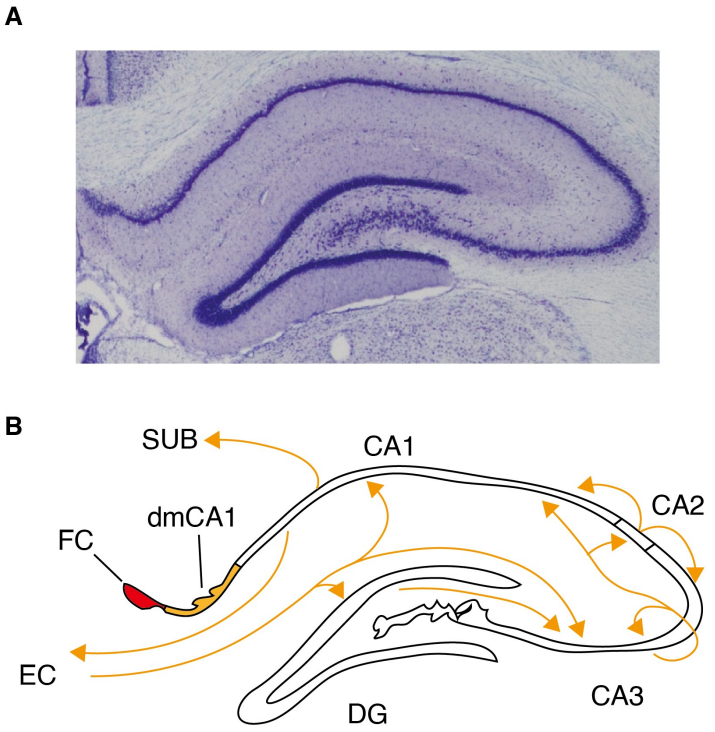


**Figure 1. Anatomical connections of the dorsal hippocampus and *fasciola cinereum*** A coronal section of hippocampi (A) and connectivity diagram (B) is presented. The distalmost CA1 (dmCA1), which is referred to CA1, FC, or subiculum by previous studies, is also presented (see 'Discussion' section in Chapter 1).

# Chapter 1. The anatomical characteristics of the *fasciola cinereum*

# Introduction

In order to study FC, it is necessary to know its exact boundary. The boundary between FC and CA1, however, has been set differently for each research (Paxinos and Watson, 2009; Henriksen et al., 2010; Boccara et al., 2015; Swanson, 2018). The discordance of the boundary does not only make it difficult to reveal the properties of the FC but also result in missing the critical characteristics of CA1. It is known that for CA1, anatomical connections and physiological characteristics are different along the transverse axis (Steward, 1976; Henriksen et al., 2010; Sun et al., 2018). In anatomically, proximal CA1 close to CA3 receives more projection from MEC than LEC, whereas distal CA1 receives relatively more projection from LEC (Steward, 1976). The firing patterns of pyramidal neurons also varied along the transverse axis (Henriksen et al., 2010). Unless the exact boundary is set appropriately, the characteristics of FC and CA1 should be reported differently from experiment to experiment, creating confusion.

To distinguish different subfields of the hippocampus, several dyeing methods were used. In particular, it has been found that each area of the hippocampus has its own genetic markers. For example, RGS14 is a genetic marker for FC/CA2, while WFS1 is a typical genetic marker for CA1 (Lein et al., 2005; Kohara et al., 2014). These markers make clear boundaries between hippocampal subfields. Even though some previous researches suggested anatomical marker for FC by genetic expression or reactivity of metal, the studies had a limitation that they defined FC using only fragmentary information (Haug, 1974; Lein et al., 2005; Lee et al., 2010). For example, FC was considered an extension of CA2 on the grounds that it shares a genetic marker with CA2, or an extension of DG possibly due to its similar cellular morphology to granule cell in DG and anatomical location (Hjorth-Simonsen, 1972; Laeremans et al., 2013). However, defining FC with only partial information results

in conflicting results. Therefore, it is necessary to examine the anatomical characteristics of FC in various ways and make a comparison with previously well-known areas.

It has also been known that each subfield of the hippocampus has its own anatomical connection — for instance, CA1get information from CA3 and EC, and project to subiculum(Andersen, 2007). CA3 receives information from DG and EC, and project to CA1. In the case of DG, it is characterized by receiving information from EC layer II and project CA3(Andersen, 2007). Comparing the anatomical connections of FC to other subfields previously discovered there is storing evidence whether FC is part of CA2 and DG or a separate area.

Studying the anatomical connection has more important meaning than just checking the boundaries of FC or making sure that they are part of other areas or independent subfields. Identifying the anatomical connections gives an idea about the operation and function of the subfield. For example, the pattern separation and pattern completion in DG and CA3 were predicted by anatomical connection even before the physiological evidence had been found (Marr, 1971; O'Reilly and McClelland, 1994; Treves and Rolls, 1994). Therefore, in order to understand the information flow and function of FC, it is essential to identify anatomical connections first.

In the experiment, it was confirmed that FC and CA1 have a distinct boundary in various dyeing methods through Timm’s staining, thionin staining, and immunohistochemistry (IHC). Also, it confirmed that FC got a projection from the lateral entorhinal cortex and perirhinal cortex and made a projection to the crest of the septal dentate gyrus. CA1 and subiculum did not receive the projection from the FC, that the connectional properties are never reported in the previously well-known hippocampal subregions. Further, no adult neurogenesis was found in FC, which suggests that FC and DG are distinct areas.

# Materials and methods

### Subjects

Long-Evans (LE; n = 2) and Sprague-Dawley (SD; n = 51) rats were used in the study. Rats were individually housed with a 12-12 h light-dark cycle. All protocols complied with the Institutional Animal Care and Use Committee of the Seoul National University.

### Anatomical tracing

SD rats (9–24 weeks old) were used in the retrograde-tracing study (n = 31) and anterograde-tracing study (n=7). Rats were initially anesthetized with sodium pentobarbital (Nembutal, 65 mg/kg), and anesthesia was maintained by 1-2% isoflurane (Piramal, Bethlehem, PA) in a stereotaxic frame for cannula implantation. Small burr holes were drilled and commercial guide cannulae (26 G, Plastics One, Roanoke, VA) were implanted targeting the fasciola cinereum (FC), distalmost CA1 or DG. One or two cannulae were inserted using the following coordinates: (1) FC: -3.4 mm from bregma, 1.1-1.2 mm from midline, and 3.7 or 4.0 mm deep from dura at 20° angle, (2) CA1: -3.4 mm from bregma, -1.2 mm from midline, 3.0 mm deep from dura, (3) DG: -3.0 mm from bregma, 2.4 mm from midline, 4.3 mm deep from dura at 20° angle. (4) SUB: -5.2 mm from bregma, ±1.2 mm from the midline, 3.4 mm deep from the skull and -5.8 mm from bregma, ±5.8 mm from the midline, 3.2 mm deep from the skull. Guide cannulae were used in our tracing experiments to prevent the upward spread of tracer. Cannulae were fixed to the skull with dental cement and skull screws. Then, retrobeads were injected through the injection cannula (33G, Plastics One), protruding less than 0.5 mm from the tip of the guide cannula. The injection cannula was connected with 10 μl Hamilton syringe via polyethylene tubing (PE20, Becton Dickinson), and the injection was controlled by a micropump (KDS-101, KD Scientific). For retrograde tracing, retrobeads (30 nL

of red or green retrobeads, Lumafluor) were injected at each injection site at 10 μL/h rate. The rat was sacrificed 3-10 days after the injection of retrobeads. For anterograde tracing, AAV–CMV-mCherry or eGFP1 (Addgene plasmid # 49055; 0.03 or 0.05 μL; KIST, Seoul, Korea) was injected into the FC, and the rat was sacrificed three weeks after the injection. For four rats, AAV2/9.CaMKII.-hChR2(E123A).mCherry.WPRE.hGH (0.02 μL; Catalog#: AV-9-35506, Addgene plasmid # 35506, Penn Vector Core, PA, USA) was injected into the right FC via glass pipette controlled by a micropump (Legato 130, KD Scientific, MA, USA) (Mattis et al., 2011). The injection coordinates for the four rats were as follows: 3.5 mm posterior from bregma, 0.1 mm from the midline and 3.6 mm deep from dura without angle through the superior sagittal sinus.

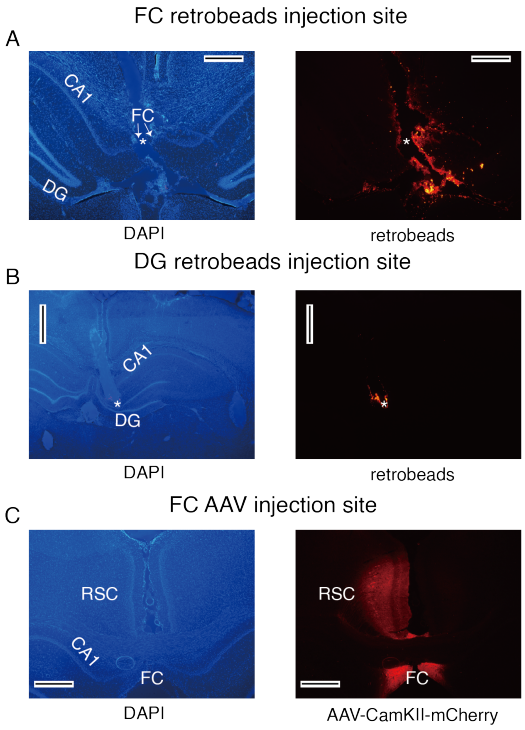


**Figure 2. Injection sites for tracing studies** Injection sites for each tracer are displayed. (A) Retrograde tracer injected into FC. Nucleus (left, DAPI) and retrobeads in the same section are presented. Black scale bar denotes 0.5 mm (B) Retrograde tracer injected into DG. Black scale bar denotes 1 mm (C) Anterograde tracer (AAV-CamKII-mCherry) injected into FC. The black scale bar denotes 0.5 mm.

**Histological procedures**

Rats were sacrificed by the inhalation of $CO_2$ overdose and were perfused transcardially with 0.1 M PBS, followed by 4% v/v formaldehyde. The brain was extracted and fixed in 30% sucrose-formalin at 4 °C. The brain was coated with gelatin with sucrose solution after it sank and was fixed again in sucrose formaldehyde solution for 1-2 days. The brain was sectioned at 35 μm using a freezing microtome (HM 430; Thermo Fisher Scientific). Every third section was first stained for Nissl substances (Thionin staining). The adjacent sections were used for fluorescent photomicrography and staining for nuclei (Hoechst, Cat No. 33342, Thermo Fisher, 1:1000; DAPI, H-1200, Vectashield). Photomicrography was conducted using a fluorescent microscope (Eclipse 80i, Nikon) or confocal microscope (Leica TCS SP8, Leica). For delineating the boundaries, serial sections from one LE rat were stained with Thionin staining, Timm's staining, and myelin staining.

**Neurogenesis**

SD rats (12 weeks old; n = 10) were used. BrdU was dissolved in saline solution (30-50 mg/mL) and injected into a rat with 100 mg/kg concentration (intraperitoneal injection). The injection was performed at 1 pm – 4 pm for seven consecutive days. Five rats were transcardially perfused with 0.1M PBS solution followed by 4% formaldehyde solution at seven days after the last injection, and the others were sacrificed at 21 days after perfused with 4% paraformaldehyde. The brains were post-fixed in the same fixative for 24 h. Brains were then cryoprotected in 30% sucrose, sectioned serially (40um), and stored in 50% PBS solution with 50% glycerol at -20 ºC until use. For BrdU staining, 10mM sodium citrate buffer (pH 6.0) was pre-heated in the microwave for 7min, slides were immersed in the hot buffer. After 5 min, the buffer (with immersed slides) was reheated for 5 min using a

microwave. The buffer with slides still immersed was allowed to cool for 30 min at room temperature. Immunohistochemical processing was then initiated beginning with a PBS wash of the slides and then blocking as described below. Primary antibodies against BrdU (1:300, Thermo Fisher Scientific, 1:500, Abcam), NeuN (1:500, Millipore) and NG2 (1:500, Millipore) were applied for overnight at 4°C with gentle shaking. After several washes with PBS, appropriate secondary antibodies were applied for 1 h by matching the primary antibody host for fluorescence imaging. Subsequently, sections were washed and mounted. Images were acquired using a TCS SP8 confocal laser-scanning microscope (Leica, Germany).

**Immunohistochemistry**

To mark the boundaries between the FC and CA1, two SD rats (8 weeks old) were used in immunohistochemistry. Rats were anesthetized with an intraperitoneal injection of urethane and transcardially perfused with saline solution, followed by 4% paraformaldehyde (PFA) solution. The brain was extracted, and stored in 4% paraformaldehyde solution until it sank to the bottom of the tube, and transferred into 30% sucrose-formaldehyde solution or 30% sucrose solution. Coronal sections (40 μm) were frozen and cut on a sliding microtome. Then, sections were incubated with primary antibodies against RGS14 (1:300, NeuroMab) and WFS1(1:300, Proteintech), or Parvalbumin (PV, 1:300, Swant) diluted in 3% BSA and 0.2% TritonX-100 in PBS for overnight at 4°C. Sections were rinsed 3 times with PBS and incubated with the appropriate secondary antibodies (1:500, Invitrogen and Jackson immunoresearch laboratories) and Hoechst33342 (1:1000, Thermo Fisher Scientific) for 1 h at room temperature. The image was acquired using a TCS SP8 confocal laser-scanning microscope (Leica, Germany).

**Table 2. Primary antibodies used in the current study**

| Antibodies | Host | Working dilution | Company | Catalog number |
|---|---|---|---|---|
| RGS14 | Mouse IgG2a | 1:300 | NeuroMab | #75-170 (RRID: AB_2179931) |
| WFS1 | Rabbit | 1:300 | proteintech | 11558-1-AP |
| NeuN | Mouse IgG1 | 1:500 | millipore | cat.MAB377 |
| NG2 | Rabbit | 1:500 | millipore | cat.AB5320 |
| BrdU | Mouse | 1:300 | Thermo Fisher Scientific | MA3-071 |
| BrdU | Rat | 1:500 | Abcam | Ab6326 |
| PV | Rabbit | 1:300 | Swant | PV27 |

# Results

In some previous mouse studies, it is reported that CA2 and FC have a similarity in terms of gene expression or peptides such as PCP4 and RGS14 while CA1 has wfs1$^{+}$ neurons (Lein et al., 2005; Lee et al., 2010; Kohara et al., 2014). To check the boundaries between FC and CA1, I conducted immunohistochemistry (IHC) with CA1 marker (WFS1) and CA2/FC marker (RGS14) in rats (Figure 3.C). As expected, the boundary between FC and CA1 is clearly distinguished. The dmCA1 which was described as FC or CA1 in previous reports showed the expression of WFS1, a marker of CA1. The boundaries were also confirmed by other staining methods. In thionin staining, the density of cells was lowered at the boundaries (Figure 3. A-B; Figure 4). Also, the boundary was clearly visible through Timm's staining, as previously reported (Haug, 1974). The boundaries defined by several methods have corresponded altogether (Figure 3. B). But the area is not distinguished by PV staining (Figure 5). Although the structure seems small in the coronal section, the length of the structure is about 2mm in the longitudinal axis (Figure 6; Figure 7).

Next, I investigated the efferent and afferent connection of FC. For the afferent connection of FC, retrobeads, a retrograde tracer, were injected into the FC (Figure 8. A). Most of the retrobeads were found in layer II of the lateral entorhinal cortex (LEC), while some found in layer II/III of perirhinal cortex A35 (Figure 8. A-C). In posterior, retrobeads were also found a deep layer of LEC along the border between the LEC and postrhinal cortex (POR). The finding that FC receives input from LEC is congruent to the previous report that reported degeneration in FC after LEC lesion, suggesting a synaptic connection between LEC and FC (Hjorth-Simonsen, 1972). In addition, the intrinsic connection within FC following the longitudinal axis was found (Figure 8. D). Also, the tracer sparsely found in the lateral part of the supramammillary body (Figure 8. E).

To investigate the efferent projection of the FC, AAV-CamKII-mCherry (or EGFP) was injected into FC (Figure 9. A). The neurites of FC were found in about one-fifth inner molecular layer of the septal crest of the dentate gyrus and FC itself following the longitudinal axis as reported above (Figure 9. A-C). Besides, the neurites of the FC were also found in Indusium griseum (IG), Septohippocampal nucleus (SHi), Septofimbrial nucleus (SFi), and the septal tip of the hippocampus (Figure 9. D-E). However, the axons of FC were scarcely found in other hippocampal subregions such as CA1, the primary efferent target of CA2, which means the anatomical characteristics of FC and CA2 are different.

The afferent and efferent connections also confirmed the lateral boundary of the FC because the intrinsic connections did not found in dmCA1 but only in FC. When retrobeads were injected into the crest of DG to confirm the efferent connection to DG of FC, the tracer only appeared in FC but not in dmCA1, which confirmed the anatomical difference between FC and dmCA1 (Figure 10. A). Further, the retrobeads in PER were found as well as EC that the existence of the projection is controversial (Figure 10. B). To find a piece of evidence that dmCA1 is CA1, retrobeads were also injected into the subiculum. If it is, the retrobeads will be found in dmCA1 as well as CA1. As expected, the retrograde tracer was found in dmCA1, which is another evidence that the area has similar connectional properties with CA1 ( Figure 11).

FC has also been interpreted as an extension of DG in the previous study (Hjorth-Simonsen, 1972). However, it was confirmed that one of the most critical characteristics of DG, adult neurogenesis, was invisible in FC. BrdU was injected intraperitoneally, one of the markers of neurogenesis, in adult rats for seven days. Three weeks later, the existence of BrdU was investigated in both DG and FC. In DG, the BrdUs were found and merged with NeuN+ cells as expected (Figure 12. A). In FC, however, the BrdU was found sparsely and did not merge with NeuN+ cells (Figure 12. B). Instead, the BrdUs were merged with oligodendroblast (NG2+),

which is a kind of glial cell (Figure 12. C). To sum up, I did not find the evidence of adult neurogenesis in FC, suggesting a significant difference exists between FC and DG.

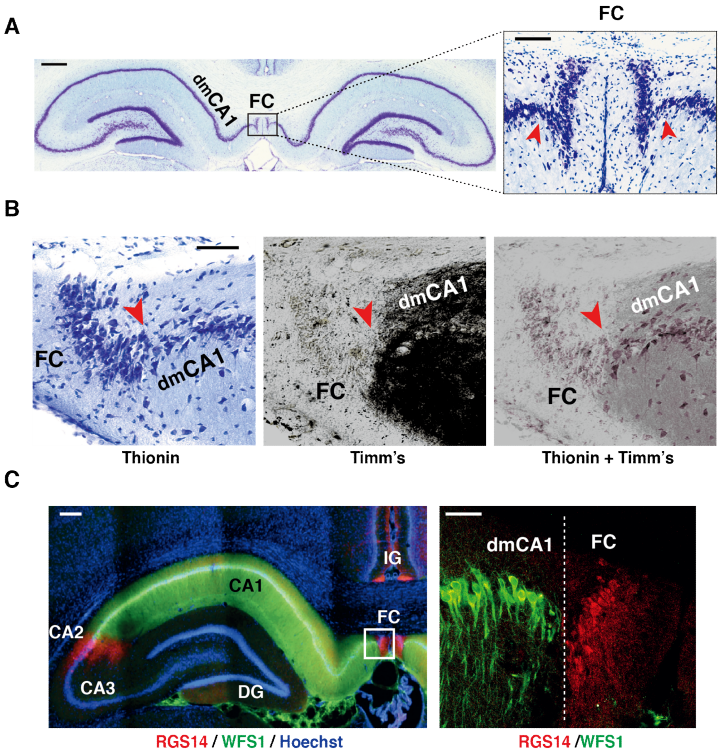


**Figure 3. The anatomical boundary of FC by several staining methods** (A) FC in the hippocampus. The FC is located at the midline of the dorsal hippocampus and the distalmost region of the CA1 (dmCA1) in Nissl-stained tissue. Scale bar: 500 μm. Inset: Magnified view of the FC and its boundaries (red arrowheads). Scale bar: 100 μm. (B) The border between the FC and dmCA1. The lateral border of the FC is clearly visible (red arrowhead) in thionin-stained (left), Timm's-stained (middle), and merged (right) sections. Scale bar: 50 μm. (C) Differential gene expression across hippocampal subfields. The expression of RGS14 (red) was only detected in the FC and CA2 in the hippocampus, whereas WFS1 expression (green) was only found in the CA1. RGS14 is also detected in indusium griseum (IG). Scale bar: 250 μm. Inset: Magnified view of the white-boxed area. Scale bar: 50 μm.

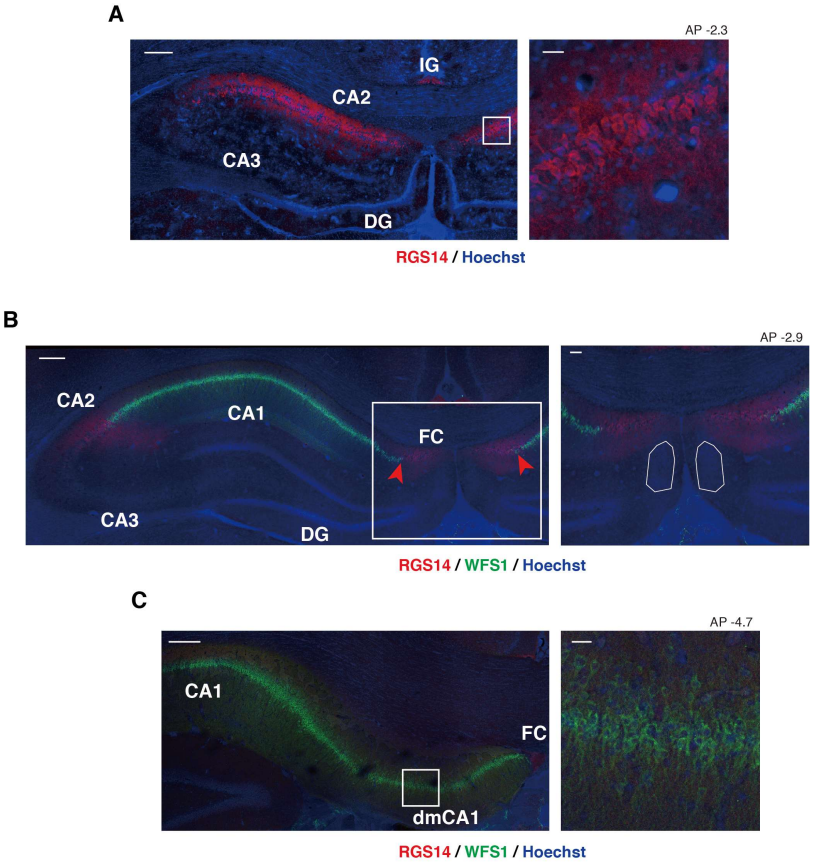


**Figure 4. Additional IHC staining** The figure represent additional RGS14 and WFS1 IHC results. (A) RGS14 in the most septal area of the hippocampus. Unlike the posterior part, the RGS14 positive area did not separate by CA1 (WFS1 positive neurons) as shown in (B). The enlarged figure of the white box is shown in right. Scale bars denote 250 μm and 25 μm, separately. (B) The non-RGS14$^{+}$ area below FC. An isolated cluster of neurons below FC (white polygon) did not express RGS14 (red), suggesting that the areas are not FC as described in an atlas (Paxinos and Watson, 2009). For better inspection of the area please refer to the second row in Figure 6. Scale bars denote 250 μm and 75 μm, separately. (C) WFS1$^{+}$ neurons in distalmost CA1 (dmCA1). Because WFS1 is a genetic marker of CA1, this picture is a piece of strong evidence that the area is CA1. Scale bars denote 250 μm and 25 μm, separately.

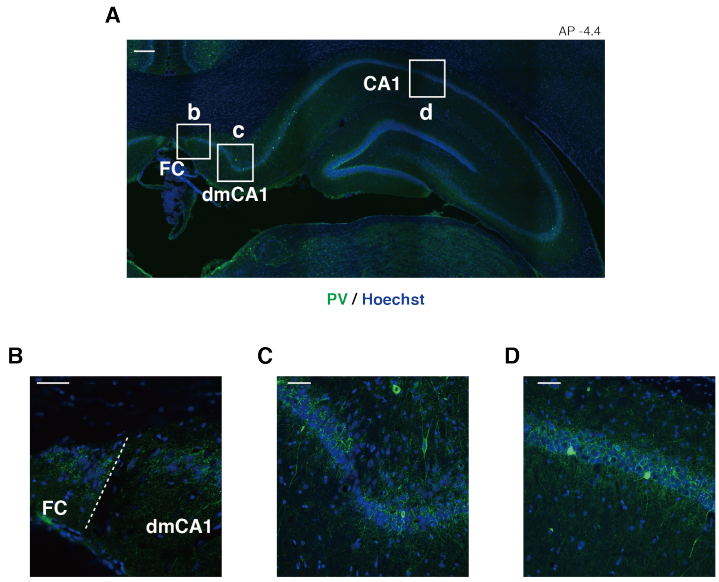


**Figure 5. PV staining (A)** parvalbumin+ neurons or neurites are distributed in the hippocampus including (B) FC, (C) dmCA1, and (D) CA1 as described in a previous study (Callahan et al., 2013). Scale bars denote 250 μm (A) and 50 μm (B-D), separately.

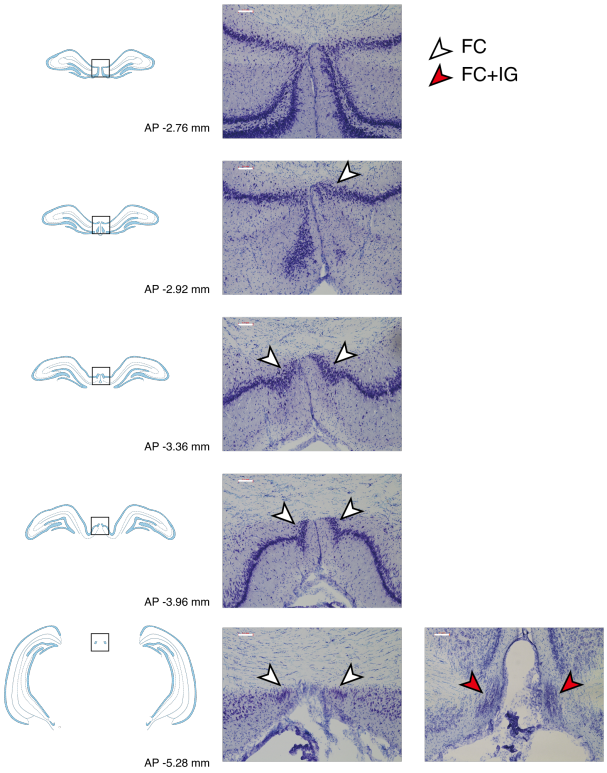


**Figure 6. FC by longitudinal axis** The representation figure shows the FC by longitudinal axis. White arrowhead indicates FC while the red arrowhead indicates the junction between FC and IG at the end of splenium (posterior end of corpus callosum). Scale bar: 0.1 mm.

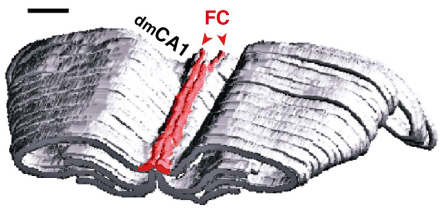


**Figure 7. 3D structure of the dorsal hippocampus and *fasciola cinereum*** The FC region (red) exists along the longitudinal axis of the dorsal hippocampus, adjoining the dmCA1 (arrowheads). Scale bar: 1 mm.

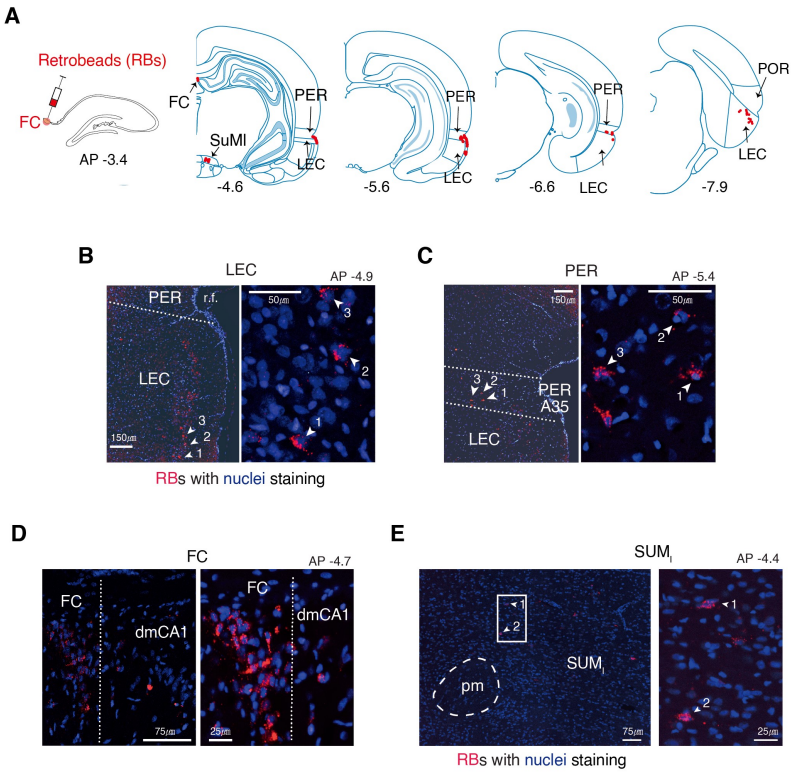


**Figure 8. Afferent connection of FC** (A) Afferent regions of the FC. Retrograde tracing of afferent connectivity was conducted by injecting Retrobeads (RBs) in the FC. Locations with RB-containing cells (red dots) were marked on the atlas (modified from the study of Paxinos and Watson; parahippocampal boundaries are after the Burwell study(Burwell, 2001; Paxinos and Watson, 2009)). Numbers indicate the relative positions of sections from bregma. RBs were detected mostly in layer II of the LEC and the layer II-III in the PER (A35). Posteriorly, RBs were found in deeper layers of the LEC adjoining the borders with the postrhinal cortex (POR). (B-E). Retrograde labeling of cells projecting to the FC. Nuclei and RBs are shown in blue (Hoechst staining) and red, respectively. Cells projecting to the FC were found in the LEC (B) and PER (C). Intrinsic connections within the FC are also shown (D). Sparsely labeled cells were also found in supramamillary body, lateral part ($SUM_l$) (E).

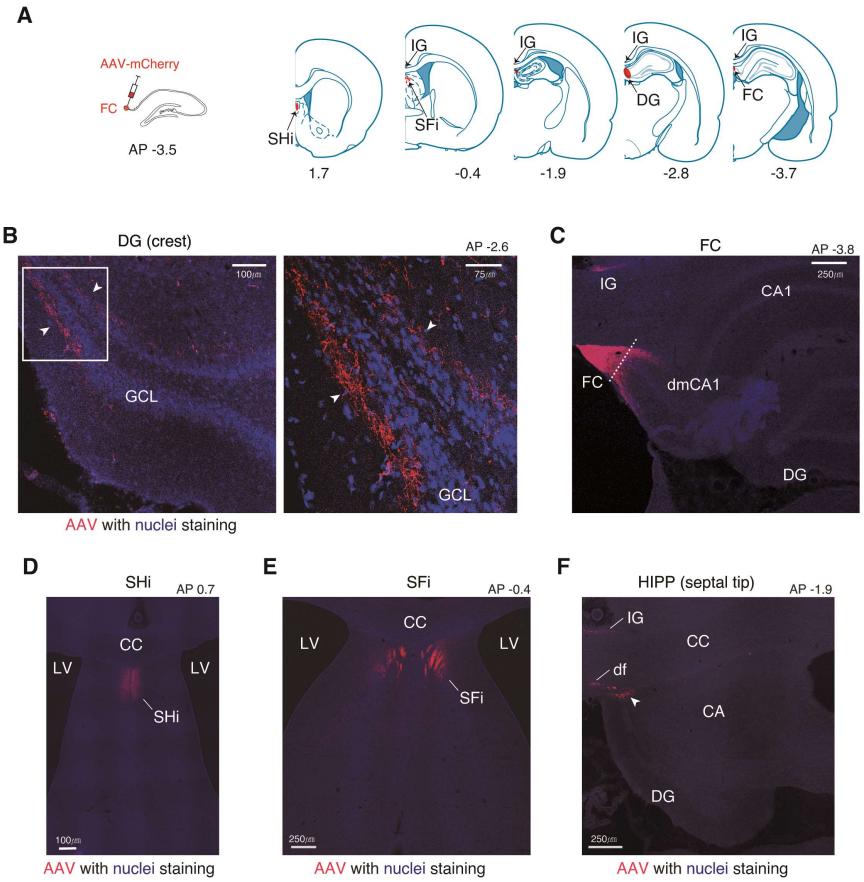


**Figure 9. Efferent connections of FC** (A) Efferent regions of FC. Tracing of efferent excitatory connectivity was conducted by injecting AAV (AAV-CamKII-mCherry) in FC. Locations of AAV neurites were marked on the atlas (modified from the study of Paxinos and Watson. Numbers indicate the relative positions of sections from bregma. (B-F) FC projections to DG and other areas. Axons of FC cells containing AAV-mCherry (red; injected into the FC) were detected in the molecular layer (ML) of the crest of the septal DG (B). White arrowheads indicate axons immediately adjacent to the granule cell layer (blue; stained with DAPI). An enlarged figure of the white box is displayed in right. GCL, granule cell layer. (C) Anterograde transport of AAV-mCherry within the FC itself via intrinsic connections was also detected. IG, indusium griseum. The axons of FC also found in SHi (D), SFi (E), and the septal tip of the hippocampus (F).

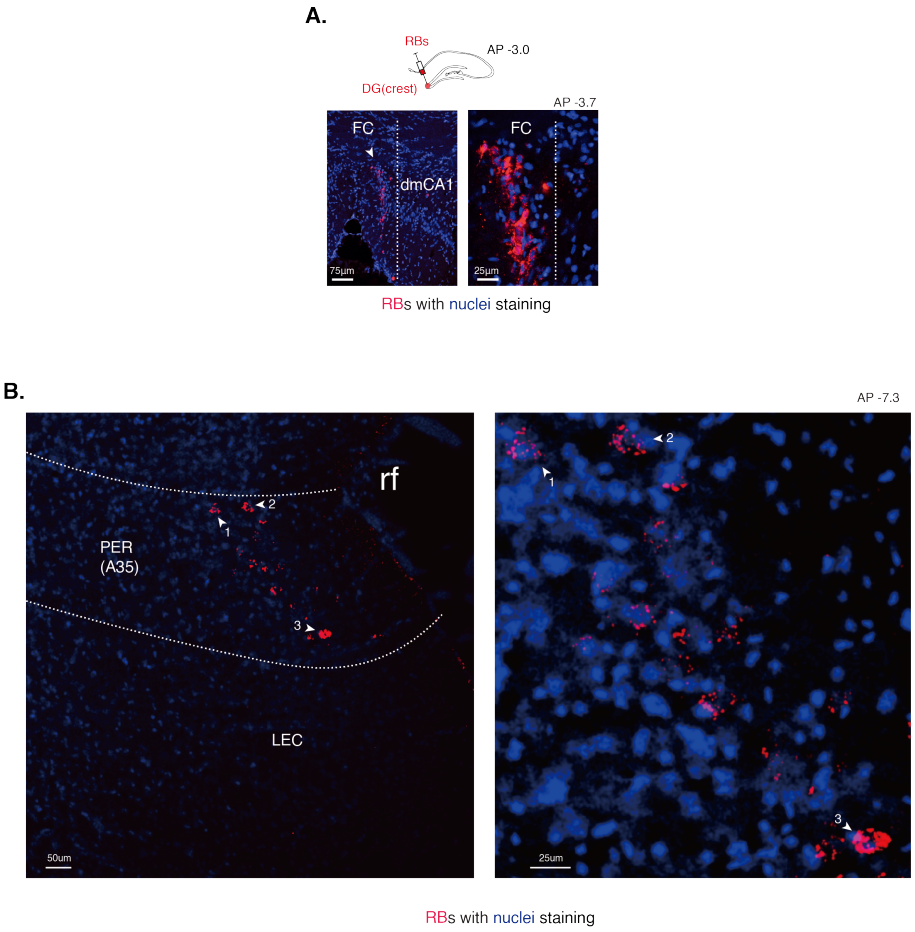


**Figure 10. Projection from FC and PER to DG** (A) injection site of retrobeads (*upper*) and labeling in FC (*lower*) are displayed. The enlarged picture is displayed in right.

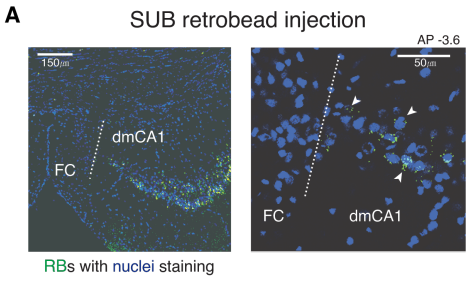


**Figure 11. Projection from CA1 to Subiculum** Projection from CA1 to subiculum. The retrobeads injected in the subiculum is labeled in dmCA1 but not in FC.

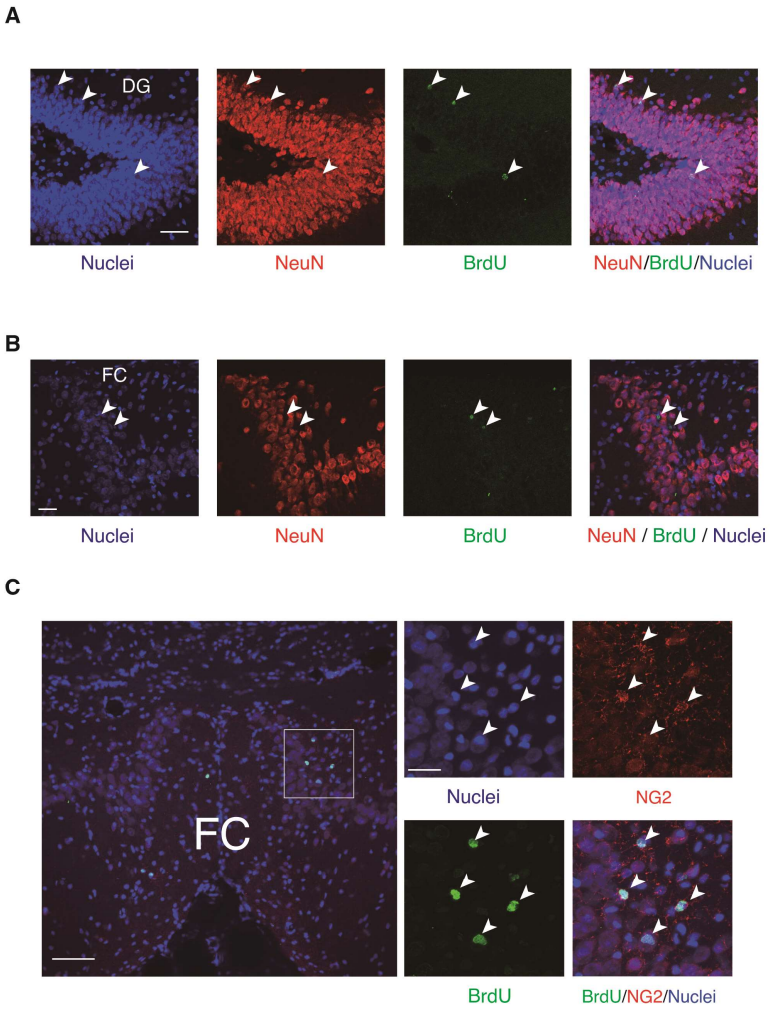


**Figure 12. No evidence of adult neurogenesis in FC** (A) Some granule cells (NeuN+, red; left) in the DG are newborn cells (BrdU+, green; middle), marked by arrowheads. A merged image of the two photomicrographs (NeuN+BrdU) with the nuclei-stained section (Hoechst staining, blue; right) showed the presence of adult-born granule cells in the DG (white; arrowheads). Scale bar: 50 μm. (B) In the FC, the locations of BrdU+ cells (arrowheads) did not overlap with the locations of NeuN+ cells. Scale bar: 30 μm. (C) BrdU-labeled cells in the FC were co-localized with NG2-labeled glial cells (oligodendroblasts; arrowhead). Scale bars: 75 μm(left) and 25 μm (right).

# Discussion

### *Fasciola cinereum*: A distinct subfield in the hippocampus

The primary issue to be identified in FC is to determine if the FC is part of a well-known hippocampal subfield, especially CA2 and DG, or independent from other subregions (Hjorth-Simonsen, 1972; Laeremans et al., 2013). Each subfield of the hippocampus was characterized by unique anatomical characteristics such as expression of genetic marker and connectivity. Therefore, it is necessary to reveal the anatomical characteristics of FC to solve the issue.

Various anatomical differences between CA1 and FC were found, suggesting an accurate border. WFS1, a neuronal marker of CA1, was found in dmCA1, but not in FC, while RGS14, a genetic marker of FC and CA2, was not found in dmCA1, suggesting that the border between FC and dmCA1 is the boundary of FC and CA1. Besides, Timm's staining and thionin staining revealed differences such as metallic reactivity and the density of neurons.

Another crucial difference is that the major outputs of FC and dmCA1 are different. dmCA1 and CA1 project to subiculum but not to DG, while FC has an efferent projection in DG but not in the subiculum. Considering these genetic markers and efferent projections collectively, I found no anatomical evidence that dmCA1 is not CA1. Nevertheless, some studies interpret the distalmost portion of dorsal CA1 as another area (Stephan, 1975; Hunsaker et al., 2008; Henriksen et al., 2010; Kjonigsen et al., 2011; Witter, 2012; Boccara et al., 2015; Kjonigsen et al., 2015; Trimper et al., 2017). For example, the region was described as mini-replica of the hippocampal formation and named FC or FC-CA area(Witter, 2012; Kjonigsen et al., 2015). Other studies have reported that the distalmost part of dorsal CA1 is subiculum (Stephan, 1975; Hunsaker et al., 2008; Trimper et al., 2017). Why is this area interpreted so differently by researchers?

The first remarkable difference between dmCA1 and distalCA1 is the thickness of the pyramidal cell layer (Slomianka et al., 2011). The cell layer of CA1 seems wide at the distalmost part comparing to the more proximal part. The thickness of the cell layer might be an important reference to distinguish different subdivisions (Swanson et al., 1978). However, it seems that the different thicknesses of the cell layers might be not due to the difference of structure or composition but to the distance difference between superficial and deep layers of CA1. It is known that the pyramidal cell layer of CA1 is divided into a superficial layer and a deep layer along the radial axis (Slomianka et al., 2011). Each cell layer can be identified using genetic markers such as Htr1a and Col11a1 (Figure 13. B-C), respectively (Soltesz and Losonczy, 2018). It has been reported that CA1 pyramidal cell layers become more distinct from septal to temporal and from proximal to distal. Therefore, the thick pyramidal cell layer in dmCA1 seems to be more appropriately interpreted as a difference along the proximodistal axis in CA1 (Slomianka et al., 2011). The laminal width might be the leading cause of confusion for the identity of the area.

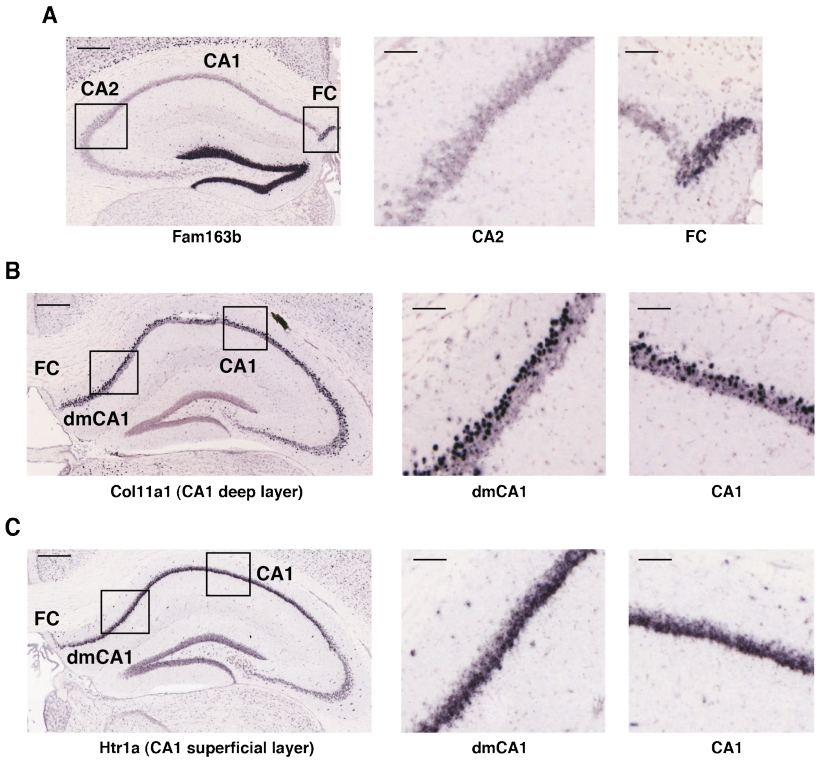


**Figure 13. *In situ* hybridization (ISH)** (A) The expression of Fam163b seems to be limited in FC and DG but not in CA2. (B) Overall hippocampi (left) and enlarged figures (right). Col11a1, a molecular marker for CA1 deep layer, is presented. The cells seem to be far from the main stem of the pyramidal cell layer in dmCA1, but largely overlapped in the more proximal part in CA1. Even though the dispersion of CA1 pyramidal cell layer in mice seems to quite less than in a rat, the ISH data of mice give an insight into the spreading of the cells. (C) The figure is the same as (B) but the labeled cells are Htr1a, a marker for CA1 superficial layer. Image credit: Allen Mouse Brain Atlas [Internet]. Seattle (WA): Allen Institute for Brain Science. © 2011. Available from: http://mouse.brain-map.org. (Lein et al., 2007). Scale bars: 300 μm (left) and 70 μm (right).

Several genetic markers for FC and CA2 including RGS14 and PCP4 (Lein et al., 2005; Dalley et al., 2008; Lee et al., 2010; Laeremans et al., 2013) are distributed widening in the superior region in a most septal portion of Cornu Ammonis (Figure 4. A). Therefore, it is possible to have an insight that in the transverse axis, the width of FC is underestimated, and more extended area (dmCA1) should be evaluated as FC. However, the insight has two problems. The first problem is that the laterally extended FC and CA2 genetic markers did not persist in the posterior part. Rather, the genetic markers suggest that the FC boundary is restricted to the medial portion than laterally extended one, and the extended area (dmCA1) expresses CA1 genetic marker (WFS1) (Figure 4. C). The second problem is that it is open to dispute that the laterally extended area in most septal part of *Cornu Ammonis* is whether CA2 or FC because the markers are found in both areas. Even though several genetic markers coexist in both areas, it is controversial to conclude that FC is CA2 because they are not the same structure in terms of anatomical connection, and some heterogenetic gene expression is suspected (Lein et al., 2005). Thanks to the Allen Institute for Brain Science, it is possible to glance at the hint about the argument. S100b, which is a genetic marker expressed in CA2 but not in FC, was observed at the septal tip of the hippocampus (Dalley et al., 2008), suggesting that the laterally extended area is CA2. On the other hand, the genetic expression of Fam163b, which seems to be expressed in FC and DG but not in CA2, did not seems to be expressed in the most septal extended area, suggesting a piece of evidence that the area is CA2 rather than FC (Figure 13. A). To sum up, the genetic expression does not support the extended boundary of FC, but instead, it supports dmCA1 is CA1.

Meanwhile, it can be argued that because dmCA1 looks different from other CA1 areas in the horizontal section, someone can think of this as a different area (*e.g.* FC) than CA1. For example, someone can claim that the FC-labelled area in parvalbumin (PV) staining section of figure 4 of Boccara et al. (2015), which is

referred to as dmCA1 in this thesis, appears to be stained darker than the area marked CA1 in the same section. However, because both CA1 and FC are stained with PV, the staining might not define the border between CA1 and FC clearly (Callahan et al., 2013). In this thesis, I did not find a clear border between FC and CA1 in PV staining (Figure 5. A-D), and PV were expressed in all of FC, dmCA1 and CA1, suggesting that the PV staining is not a suitable method to distinguish FC and CA1.

On the other hand, some researchers reported that dmCA1 in the dorsal hippocampus is a subiculum. One of the reasons for the report is maybe due to a misunderstanding of the plane that is referred to (Amaral et al., 1991; Witter and Amaral, 2004; Trimper et al., 2017). In a horizontal section of the intermediate hippocampus, the subiculum located at the distal part of CA1. However, it is not always accurate in a coronal section of the dorsal hippocampus, and it depends on the section. If someone tries to refer to the anatomical position of CA1 and subiculum in the horizontal section without considering the detailed characteristics, and apply to the coronal section of the dorsal hippocampus, the research might make a confusing result (Duvernoy et al., 2013).

Also, the point of view that considers FC and adjacent CA1 as mini-replica of the hippocampus needs to be addressed(Witter, 2012). In terms of anatomical connection, DG projects CA3, CA3 project CA1, and CA1 project to subiculum. The FC and dmCA1 region called mini-replica of the hippocampus, however, did not show similar connectivity. FC did not project to adjacent CA1, and CA1 right next to FC is also projecting to subiculum like the rest part of CA1. While CA1 and CA3 are distinguished by distinct genetic markers, genetic expression of dmCA1 and dCA1 is homogeneous(Figure 3. C). These pieces of evidence do not support the point of view that FC and dmCA1 are mini-replica of the hippocampus.

Finally, in terms of the boundary of FC, there is one more thing that needs to be considered. Although the most controversial boundary of FC is the boundary between FC and CA1, some atlas interpreted a septal tip of the dentate gyrus, which

is triangular shaped as FC in the coronal section (Paxinos and Watson, 2009). However, in this study, the area did not show the expression of RGS14 that is reliably expressed in FC and CA2 (Figure 4. B). The heterogenetic gene expression between the area and FC suggests that the most septal area of the dentate gyrus is not FC.

The next issue is that FC is an independent area or a part of other hippocampal subregions. FC is possibly interpreted as an extension of CA2 due to their genetic similarity (Lein et al., 2005; Laeremans et al., 2013). The evidence of the argument is the similarity of gene expression between both areas. As addressed above, however, it is controversial that the gene expression between both areas is the same as discussed above.

Some studies interpreted FC as a part of DG because FC is composed of granule cells (Hjorth-Simonsen, 1972). In this study, however, the efferent connection and genetic expression of FC is quite different from the granule cells in DG. In addition, evidence of adult neurogenesis in FC was not observed in this study, which is one of the major characteristics of DG. Also, It is not found any similarity between FC and CA3 in terms of efferent projection and genetic expression, which also suggested that FC and CA3 are distinct subregions.

In addition, the most noticeable difference between the FC and the other well-known hippocampal subfields is that FC did not exist along the septotemporal axis in the hippocampus (Figure 6). In the rostral part, FC located medially to CA1. In caudal part, however, it goes up to splenium, which is caudal part of the corpus callosum, and meets indusium griseum (IG) as reported previously (Hill, 1895; Das, 1971).

To sum up, based on the structural, connectional, and genetic differences, FC is an independent and distinct subfield in the hippocampus.

Finally, one of the unexpected discoveries of the study is that the projection from PER to DG was revealed (Figure 10. B). The existence of the projection was controversial in previous studies. Some studies reported the presence, while others

found no evidence of the projection (Canning and Leung, 1997; Dolorfo and Amaral, 1998; Naber et al., 1999; Witter et al., 1999; Witter et al., 2000; Vivar et al., 2012; Ohara et al., 2013). The common ground of this study and a previous study (Ohara et al., 2013) which reported the projection is that both studies injected a retrograde tracer into the crest of the dentate gyrus, which is a junction of dorsal blade and ventral blade of dentate gyrus located almost septal end. It is known that EC and DG have a topological connection (Ruth et al., 1988; Dolorfo and Amaral, 1998). Ventral DG has an intense connection with MEC, while dorsal DG has an intense connection with LEC. The projection from the PER to the septal end of DG might be an extension of the topological connection. To confirm the projection, however, a more accurate anatomical tracing study is needed (Doan et al., 2019).

**The role of direct and indirection projection in FC and DG**

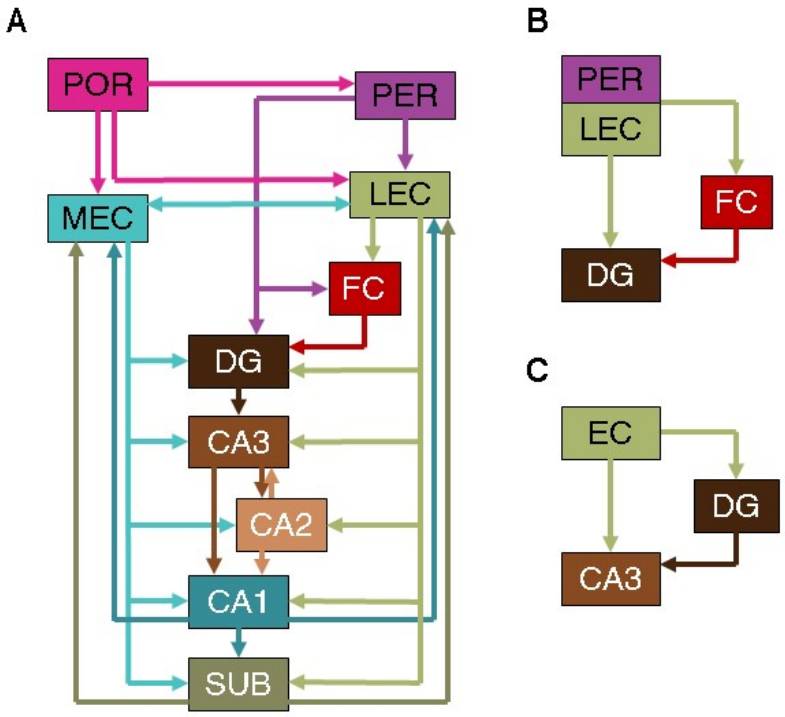


**Figure 14. Connectivity diagram of parahippocampal area and hippocampus**

(A) Overall MTL and dorsal hippocampus connectivity is shown in the diagram. The diagram is based on (Nilssen et al., 2019), but the specific layer information in a substructure is missing for simplification. The projection From CA2 to CA3 was drawn (Tzakis and Holahan, 2019). (B) A direct and indirection projection via FC from PER and EC to DG is displayed. For simplification, MEC and LEC are merged to EC. (C) A direct and indirect projection via DG from EC to CA3 is displayed.

The anatomical connectivity of FC and the connected area are quite impressive. FC has an afferent connection with LEC and PER, while FC has an efferent connection to DG. The interesting point is that the information from both LEC and PER, an information source of FC, can send their information directly to the DG regardless of FC (Figure 14). Then why the FC is needed and what is the role?

In terms of connectivity, there is FC-like structure exist in the hippocampus. It is a dentate gyrus. There are two routes to transmit information from EC layer II to CA3 (Andersen, 2007). In this case, the projection going to CA3 via DG and the projection going directly to CA3 are known to play different roles (Treves and Rolls, 1994). The projection from DG to CA3 is known to have strong synaptic weight, suggesting that the projection has a role in teaching signal or detonator (Mcnaughton and Morris, 1987). The direct projection from EC to CA3, however, is known to have plastic synapse, although its strength of synaptic input is weak. While the strong and sparsely activated DG mossy fibers activate a part of CA3 based on the input from EC, a synaptic strength between direct projection from EC to CA3 (perforant pathway) and activated CA3 can be modified easily (Marr, 1969; Mcnaughton and Morris, 1987; O'Reilly and McClelland, 1994; Treves and Rolls, 1994). The synapse between recurrent projection from CA3 to CA3 (recurrent collateral) and activated CA3 can be potentiated in the same way. Once a synaptic connection is established, the CA3 cells are able to make representation without help of DG (Treves and Rolls, 1994; Lee and Kesner, 2004a). The mechanism has been suggested as a principle of memory formation. In this case, DG input should be sparse and orthogonal, or CA3 representations should be saturated (Mcnaughton and Morris, 1987). The sparse coding and orthogonal coding is not just hypothesized model. In an electrophysiological experiment, it was reported that only a few cells (9%) were recruited for the representation of an environment and most of them are recruited to representing only one environment (GoodSmith et al., 2017).

A large number of granule cells (about $10^6$ cells) and several inhibition mechanisms (subtraction, division, and lateral inhibition) have been suggested as a mechanism of the sparse and orthogonal coding in DG, and anatomical and physiological pieces of evidence were found (Marr, 1969; Sloviter and Brisman, 1995; Rolls, 2013).

In the case of the FC, the axon of the excitatory neurons of the FC is likely to have a strong influence on the GC because the axon is located near the granule cell layer of the DG (inner one-fifth in the molecular layer), suggesting small number of synaptic input from FC is able to have an influence for DG granule cell activity. The synaptic strength between the perforant path (PP) and DG granule cell (DG GC) might have less influence than the FC due to its location is far from the soma of the granule cell. Especially, the lateral perforant pathway (lPP) from LEC project to the outer molecular layer in DG far from the granule cell layer, suggesting that the influence of the projection for the action potential activity in DG GC is weak (Witter, 2007).

Also, it is already known that the synapses between PP and granule cells in DG have plasticity (Lomo, 1971; Cunningham et al., 1996). So, the possibility is suggested that when PP is activated, the indirect excitatory projection to DG via FC has a role in helping the activation of DG granule cells by supplying excitatory postsynaptic potential (EPSP) while the direct projection modifies its synaptic strength with activated DG granule cell. Especially, the FC can help make action potential for DG GC by the input from LEC, whose direct pathway has a weak influence on action potential in DG GC, via indirect pathway as well as the input from MEC.

However, since the synaptic characteristics of FC and DG are unknown yet, further studies about the detailed synaptic connection are needed. Also, considering the relatively small size and low density of cells in FC, the number of cells in FC might be quite small, comparing to DG. The relatively small size of neurons becomes

a disadvantage for sparse coding, insisting that a different mechanism from the one described above should be suggested for FC and DG.

The next question is the cognitive function of the FC. Despite a lack of references, it is possible to infer the cognitive role based on connectivity. It was reported that PER, one of the input areas of FC, is known as an important area for object recognition and contextual scene-based choice (or object-based choice) while LEC is known for object-place associative memory and scene-based contextual learning (Barker and Warburton, 2011; Tsao et al., 2013; Wilson et al., 2013b; Park et al., 2017; Yoo and Lee, 2017). In addition, it is reported that DG, a major target of FC, has an important role in learning contextual behavior (Lee and Kesner, 2004a; Ahn and Lee, 2014). Taken together, it is reasonable to test whether FC related to associative learning of context, object, and place or not.

# Chapter 2. *Fasciola cinereum* is important for contextual memory acquisition but not for retrieval

# Introduction

The previous chapter showed the afferent and efferent connectivity of FC. the FC-connected area, PER, LEC, and DG, have an essential role in recognition and associative memory for object, place, and context (Lee and Kesner, 2004a; Barker and Warburton, 2011; Tsao et al., 2013; Wilson et al., 2013b; Ahn and Lee, 2014; Park et al., 2017; Yoo and Lee, 2017). Especially, DG, the primary intrahippocampal output of FC, is important for learning contextual behavior (Ahn and Lee, 2014). This anatomical connectivity suggests a possibility that the FC might have a cognitive role in associative memory.

In this chapter, I checked if FC is important for forming new memory during the scene-based spatial choice task that has been known as the DG-dependent memory task. In this task, rats should choose a left or right arm to get a reward in T-maze based on the scene on the monitors surrounding the maze. Rats with intact FC showed good performance in both acquisition and retrieval of contextual memory, while the rats with damaged FC showed impaired performance in acquisition but not in retrieval. Also, while the control group showed hesitation behavior when they suddenly met the novel scene, the lesion group did not show the behavior, suggesting that FC might have a role in detecting and processing novel contextual change. To sum up, the behavior result suggested that FC has an essential role in acquiring novel contextual memory.

# Materials and methods

## Subjects

Long-Evans (LE; n = 16) rats were used in the study. Rats were individually housed with a 12-12 h light-dark cycle. All behavioral experiments were conducted during the light cycle. All protocols complied with the Institutional Animal Care and Use Committee of the Seoul National University.

## Apparatus for lesion study

An elevated t-maze (72 × 8 cm for stem and 40 × 8 cm for each arm) was used. A food well (2.5 cm diameter, 0.8 cm deep) was located at the end of each arm (Figure 15). The food well was covered by a plastic washer to prevent the rat from sampling a reward in the food well from the stem. A quarter piece of cereal (Froot Loops, Kellogg's) was used as a reward. The arms of the maze were surrounded by an array of 3 LCD monitors. At the end of the stem, a start box with a guillotine door was placed. Infrared sensors were installed in front of the start box and in the stem to measure latency. The behavioral experiment was controlled by the Matlab-based custom program and the sensor data were acquired using a data acquisition device (PCI-6221, National Instrument, Austin, Texas). Five visual scenes were used in the behavioral experiments: black screen, zebra, pebbles, peacock, and palm-tree patterns. During pre-training and OLD sessions, zebra and pebble scenes were presented, and the rewarding arm was fixed to one of the arms associated with the scene (i.e., left arm for zebra scene and right arm for pebbles scene). In the NEW session, peacock and palm-tree scenes presented across trials (peacock for the left arm and palm trees for right arm). The scene pairs (zebra-pebble and peacock-palm trees) and their associated reward locations (left and right arms) were pseudo-randomly assigned to the rats. The maze was located within a circular curtained area

in which white noise was played through loudspeakers. After each session, the maze was vacuumed and swiped with 70% ethanol.

**Experiment procedure**

**Handling and shaping** After 5 days of handling and foraging in a laboratory cart, a rat experienced a habituation session in the maze. During habituation, the rat freely explored the maze and collected cereal rewards scattered throughout the maze to get familiarized with the maze and environment. Once acquainted, a shaping session started in which the rat learned to run directly to a food-well to find the reward underneath the washer covering the food-well once the start box was opened by an experimenter. Access to one of the arms was blocked by a transparent acrylic block within a session and the other arm was blocked in the next session, and so forth. When rat ran 90 trials in total in the habituation session, pre-training started.

**Pre-surgical training with old scenes** A training session was composed of sample and test blocks. There were five sample blocks (10 trials for each block). Two scenes (zebra-pebbles or peacock-palm trees) were alternately presented across the sample blocks except between the first and second blocks (i.e., black screen for the first block). Rewarding arms were identical between the first and second sample blocks. During the sample blocks, access to the unrewarded arm was blocked by a transparent acrylic block. After the last sample block, the testing block commenced (40 trials) without delay. In the testing block, both arms were accessible from the stem and one of the two scenes from the sampling block appeared pseudo-randomly across trials. When the rat reached criterion (accuracy for both scenes > 75%), the animal was assigned to either the lesion group or the control group for surgery.

**Neurotoxic lesion** Colchicine was injected into the FC for the lesion group (n = 8), whereas sterilized saline was injected in the control group (n = 8). For surgery, the rat was first anesthetized by sodium pentobarbital (Nembutal, 65 mg/kg, I.P.) and its head was fixed in a stereotaxic instrument (Kopf Instruments, Tujunga, CA). Anesthesia was maintained by 1-2% isoflurane (Piramal, Bethlehem, PA). Small burr holes were drilled to inject colchicine (7 mg/mL) or sterilized saline (0.05 μL per injection site at 10 μl/h rate; microinjection pump KDS-101, KD Scientific) through a glass pipette (HSU-2920109, Marienfield) connected to a 10 μl Hamilton syringe via polyethylene tubing (PE20, Becton Dickinson). The following coordinates were used for drug injection: 3.4 mm posterior to bregma, ±1.2 mm lateral to the midline, and 4.2 mm ventral from dura at ± 20° angle. It is well known that colchicine is a neurotoxin that selectively ablates granule cells in the dentate gyrus. Some studies reported damage outside the DG (e.g., CA1) by colchicine (Jarrard, 2002; Ahn and Lee, 2014), but I did not find any volume shrinkage with a small amount colchicine injection in other areas in the hippocampus with bare eyes inspection. After surgery, the rat rested for 3 days, and handling and cart foraging procedures began again. Ten days after surgery, the habituation session (90 trials) was carried out for 4 days to help the rat to re-adapt to the experimental situation.

**Post-surgical test (main task)** Post-surgical test conducted 14 days after surgery and the testing procedures were identical with those in the pre-surgical training except that no correction was allowed. On D14 (OLD1) and D18 (OLD2), old scenes (zebra-pebble or peacock-palm trees) were presented to test retrieval of memory. On D16 (NEW), a new pair of scenes that had not been presented during the training period was used to test memory acquisition.

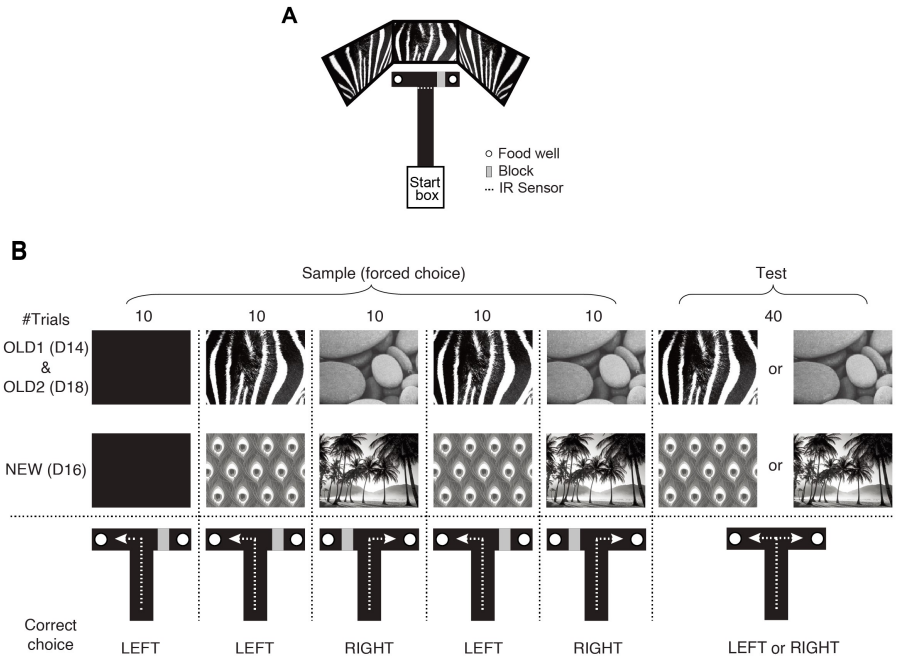


**Figure 15. Apparatus and task explanation** (A) Behavioral apparatus. The white dotted line indicates the point where the infrared beam sensors were installed. The gray rectangle represents the acrylic block used to restrict access to the arm. (B) Experimental schedule and behavioral paradigm. Rats were trained with familiar scenes before surgery. After a recovery period (14 days), rats were tested with the same scenes for one day (OLD1), then experienced two more sessions with new scenes (NEW), and re-experienced old scenes (OLD2) with a 1-day rest between sessions. In a single session, a rat experienced a total of 90 trials (50 sample trials and 40 test trials). Sample trials consisted of five blocks (10 trials per block).

**Histological analysis**

Histological procedures were the same as the ones described for the electrophysiological experiments except that only every third section was collected during sectioning. For the FC volumetry, photomicrographs taken with 10x magnification were used. The procedures for volume measurement for the FC were different from those for the other subregions (Ahn and Lee, 2014). This was largely because of the low density of cells with small cell bodies in the FC. That is, tracking the boundaries of the cell layers in the FC in the same way for other cell layers of the hippocampus did not reflect the actual volume of the FC accurately. Therefore, I converted the colored photomicrograph to black-and-white and set a threshold at which only the contours of neurons were visible. Measuring the dark areas in the photo afterward yielded a good volumetric estimate of the FC (Figure 16). One of the rats in the lesion group was excluded from the analysis for the lack of lesions. Two rats whose lesions were extensive were also excluded. As a result, five rats were assigned to the lesion group with eight rats assigned to the control group (Table 4).

**Analysis of behavioral data**

To compare behavioral performance between the control and lesion groups, a repeated-measures mixed ANOVA and t-test (both paired and unpaired) were conducted using Statview software. Latency was measured from the opening of the start-box door to displacing the washer over the food-well or to the last sensor on the track. One rat in the control group was excluded from the latency analysis due to its relative latency was too deviated from the mean of the control group more than 2 SD. But the trend was maintained even in this rat (trial 10 latency: 0.96s, trial 11 latency: 7.17s) To confirm the categorization of the lesioned rats into the normal and extensive lesion groups, a K-Mean clustering with JMP 11 (SAS; Parameter: FC volume, NEW performance, latency) conducted. For presenting the data and statistical results, mean and standard errors (mean ± S.T.E) were used. The statistical results are organized in Table 3.

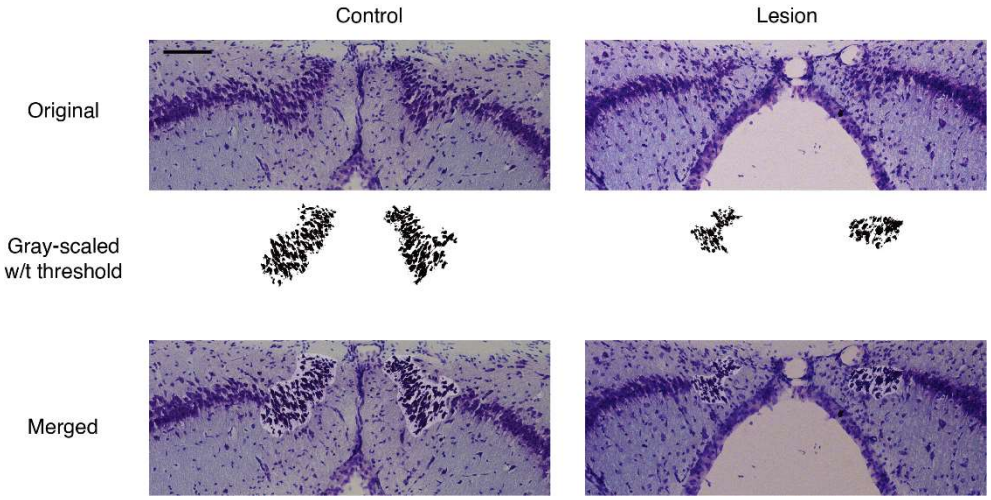


**Figure 16. Volumetric measurement of the FC** Original photomicrographs taken with 10x magnification are shown in the first row (Original). Clusters of FC cells were isolated from the background by setting an intensity threshold in the black-and-white photos of the original photomicrographs (Middle). The bottom row shows the merged photo of the two above to verify the locations of the FC in the original photos. Scale bar = 100 μm

# Results

To study the cognitive function, it is needed to establish a method to ablate the cells in FC selectively. It was reported that granule cells were composed of FC, and the granule cells in DG were selectively destroyed by injecting colchicine due to blocking microtubule-assisted axonal transport by accumulating intracellular labile Zinc (Hjorth-Simonsen and Laurberg, 1977; Goldschmidt and Steward, 1982; Lothman et al., 1982; Choi et al., 2014). Therefore, it is tested if the cells in FC are selectively destroyed by injecting colchicine, remaining adjacent CA1 unaffected. As expected, a small amount of colchicine (0.05μL/site) injected in FC made a selective lesion of FC (Figure 17).

Rats were trained to choose the left or right food well in the T-maze based on the scene on surrounding monitors to test retrieval and acquisition of contextual memory (Figure 15.A). It is reported that PER and DG are critically involved in the task, while LEC is also involved in contextual behavior with a scene (Ahn and Lee, 2014; Park et al., 2017; Yoo and Lee, 2017). The behavioral task was similar to the previous study by Ahn and Lee (2014), but some differences existed. In this task, sample blocks were added before the test block in a session that helps rats learn contextual behavior fast, and the experimenter observes novelty related behavior (Figure 15.B). Because it was reported that rats were able to learn the task eventually without DG if learning duration is too long, shortening the acquisition task period is essential for the task (Ahn and Lee, 2014). In addition, retrieval task was added again after acquisition task to test if the performance difference between retrieval and acquisition is due to lesion status change by the passage of time or the learning ability, which required in the tasks.

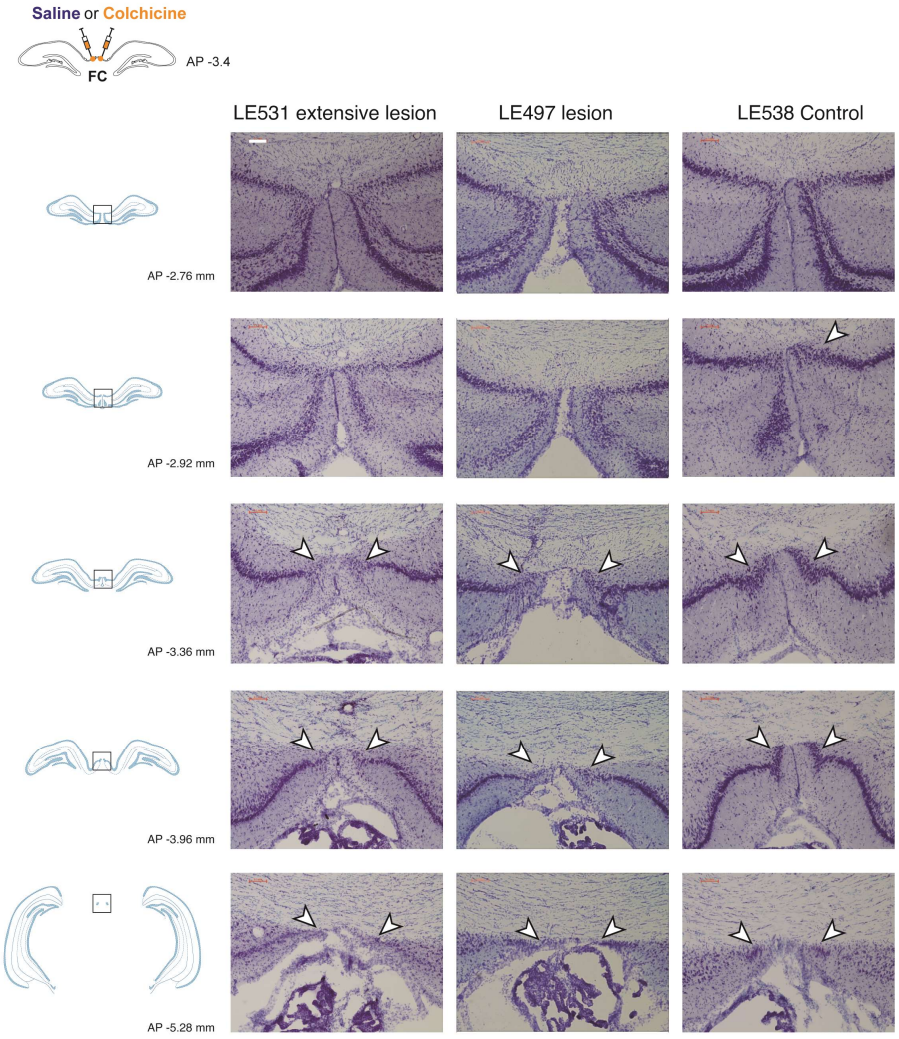


**Figure 17. A selective lesion in FC after colchicine injection** The left upper diagram describes the injection coordinate and the angle of injection needle (glass pipette). The left column shows the hippocampus diagram and distance posterior to the bregma. The next histological pictures show the center of the hippocampus of each group at the corresponding AP coordinate. The extensive lesion group is excluded in statistics due to their heterogeneous behavior (See discussion). White arrows indicate FC or the trace of FC. The diagram is modified from the atlas of Paxinos and Watson (2009). The scale bar denotes 0.1 mm.

In both tasks, the control group showed significantly higher performance than chance (P<0.05; Figure 18.A). The lesion group, however, showed impaired performance in learning novel scenes during the acquisition task while remaining the memory previously learned (Figure 18.A). This result was due neither to latency difference during acquisition test nor to different lesion status by the passage of time (Figure 18.B-C). In the second retrieval test (OLD2) which was conducted two days after the acquisition task, I found no difference in performance between groups indicating that the impairment in acquisition task is due to task requirement to learn novel scenes (Figure 18.B).

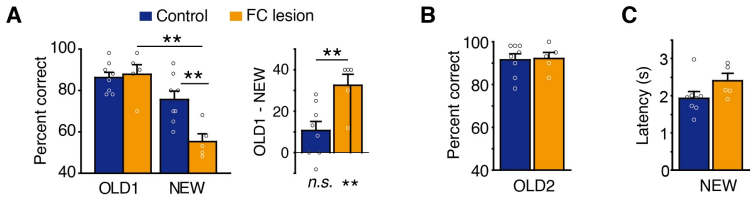


**Figure 18. Behavioral performance results during retrieval and acquisition of contextual learning** (A) Deficits in the acquisition, but not retrieval, of scene memory in the FC lesion group. Data represent means ± S.E.M. Right: Same data replotted using the difference in performance (OLD1 – NEW). (B-C) No significant difference in performance in the OLD2 session (B), and no significant difference in latency during testing in the NEW session (C) between control and lesion groups. (*p<0.05, **p < 0.01, ***p<0.001).

Rats also showed a response to the novel scene during the sample phase of the acquisition task. The control group who well-performed in sample block with familiar blank scene showed hesitation behavior when the novel scene first appeared (trial 11 in acquisition task), and the latency in the trial increased about twice compared to the latency in the previous trial (Figure 19). In the trial, there was nothing changed, including reward and brick location, but only a novel contextual scene suddenly appeared, which suggested that the rats in the control group grasped the changing contextual cue even though rats did not have to respond to it in order to get a reward. The rats in the lesion group, however, showed no such novelty-related behavior (Figure 19). The increase in latency was not maintained until the next trial (trial 12) and returning to before, suggesting that FC might have a role in detecting changing to novel context, and it might affect the learning ability (Figure 19.C). This contextual novelty-related different behavior between both groups was not shown in the retrieval task, suggesting that the hesitation behavior did not due to just contextual change but a novelty (Relative latency: $t(11)=0.9$, $P=0.42$, t-test; Control: $2.64\pm0.68$; Lesion: $1.76\pm0.77$).

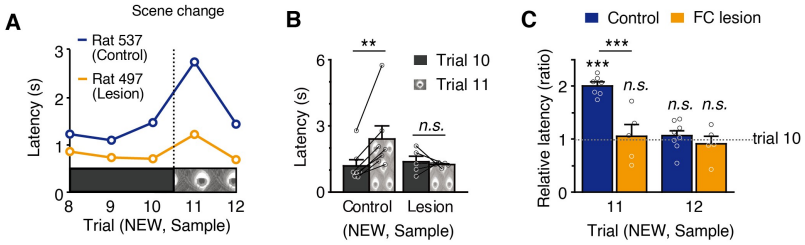


**Figure 19. The responses to the initial introduction of the novel scene**

Representative example from one rat (A) and the average latency (raw and ratio) between trial 10 and trial 11 for all rats are shown (B-C). Data represent means ± S.E.M. (*p<0.05, **p < 0.01, ***p<0.001).

**Table 3. Statistical results of T-maze lesion study** Asterisks in the p-value column indicate statistical significance. Values represent Mean ± S.E.M. AVG = average.

| Related figure | Mean±S.E.M | | N | Statistics | Post-hoc test | | Note |
|---|---|---|---|---|---|---|---|
| Figure 18.A (OLD and NEW) | OLD1, control | 86.3±2.6 | 8 | Surgical condition: F (1, 11) = 5.3, P = 0.042*, Task: F (1, 11) = 35.7, P < 0.001*; Surgical condition X task: F (1, 11) = 9.3, P = 0.011* | Control vs. Lesion in OLD1 | t (11) = 0.3, P = 0.760 | |
| | OLD1, lesion | 87.8±4.8 | 5 | | Control vs. Lesion in NEW | t (11) = 3.5, P = 0.005* | |
| | NEW1, control | 75.8±4.0 | 8 | | OLD1 vs. NEW in Control | t (7) = 2.3, P=0.054 | |
| | NEW1, lesion | 55.4±3.6 | 5 | | OLD1 vs. NEW in Lesion | t (4) = 5.9, P = 0.004* | |
| | | | | OLD1, control, t (7) = 14.0, P < 0.001*; OLD1, lesion, t (4) = 7.9, P = 0.001*; NEW1, control, t (7) = 6.4, P < 0.001*; NEW1, lesion, t (4) = 1.5, P = 0.205 | | | Comparison with chance (50%) |
| Figure 18.A (right) | control | 10.5±4.5 | 8 | t (11) = 3.1, P = 0.011* | | | |
| | lesion | 32.4±5.5 | 5 | | | | |
| Figure 18.B (OLD2) | OLD2, control | 91.6±2.7 | 8 | t (11) = 0.1, P = 0.890 | | | |
| | OLD2, lesion | 92.2±2.8 | 5 | | | | |
| Figure 18.C (NEW, latency) | control | 1.93±0.19 | 8 | t (11) = 1.6, P = 0.133 | | | |
| | lesion | 2.40±0.22 | 5 | | | | |
| Figure 19.B (trial latency, NEW) | control, trial 10 | 1.19±0.28 | 7 | Surgical condition: F (1, 10) = 0.9, P = 0.377, Trial: F (1, 10) = 6.0, P = 0.034*, Surgical condition X task: F (1, 10) = 9.4, P = 0.012* | trial 10 vs. trial 11, control | t (6) = 3.9, P = 0.008* | |
| | control, trial 11 | 2.41±0.59 | 7 | | trial 10 vs. trial 11, lesion | t (4) = 0.5, P = 0.661 | |
| | lesion, trial 10 | 1.38±0.25 | 5 | | control vs. lesion, trial 10 | t (11) = 0.6, P = 0.577 | |
| | lesion, trial 11 | 1.24±0.05 | 5 | | control vs. lesion, trial 11 | t (10) = 1.6, P = 0.131 | |
| Figure 19.C (trial latency ratio, trial 10 based) | trial 11, control | 2.01±0.07 | 7 | t (10) = 4.9, P = 0.001* | | | |
| | trial 11, lesion | 1.06±0.22 | 5 | | | | |
| | trial 12, control | 1.06±0.10 | 8 | t (11) = 0.9, P = 0.383 | | | |
| | trial 12, lesion | 0.92±0.14 | 5 | | | | |
| | | | | trial 11, control, t(6) = 14.7, P < 0.001* trial 11, lesion, t(4) = 0.3, P = 0.809 trial 12, control, t(7) = 0.7, P = 0.528 trial 12, lesion, t(4) = 0.6, P = 0.575 | | | Comparison with trial 10 (1) |

**Table 4. The statistical description of the FC volumetry** The table below shows the number of rats in each group and the volume of the FC (unit: $10^{-3}$ $mm^3$). The last two groups were excluded from analysis due to their lesion status.

| Group | N | Mean | S.T.E. |
|---|---|---|---|
| Control | 8 | 26.8 | 1.9 |
| Lesion | 5 | 11.1 | 1.8 |
| No lesion | 1 | 28.1 | |
| Extensive lesion | 2 | 6.3 | 0.2 |

# Discussion

In this study, it is revealed that FC is important for the acquisition of contextual memory, but not for the retrieval. Given that DG, the major intrahippocampal output area of FC, is also important to learning contextual behavior, it is reasonable to be inferred that FC and DG work together to form new contextual memory.

Also, it is found that rats with undamaged FC showed hesitation behavior when they first met a novel scene, but rats with destructed FC did not. Note that rats do not have to respond to the change of scene on the monitor to get a reward because the reward and acrylic brick location did not change. The behavior could be explained by latent learning in contextual retrieval theory (Hirsh, 1974). In the theory, Hirsh defined contextual retrieval as “retrieval of an item of stored information initiated by a cue which refers to but is not necessarily described within the information that is retrieved”. In this point of view, learning is processed inside a context regardless of whether contextual information is needed or not. To learn contextual cues, even when it is not necessary, is innate characteristics of the hippocampus, which called latent learning. In this task, control rats responded for change to the unexpected novel scene on the surrounding monitors, which did not need to get a reward at least in the sample phase. Considering that the rats learned the associative relation between reward locations and scenes on the monitor, The hesitative behavior might be a behavioral assay for the detection of novel contextual change and the beginning of contextual learning.

In that rats in lesion group showed less hesitation behavior and lower memory acquisition performance, FC might be an initiator for fast contextual learning by detecting an unexpected contextual change and stimulate DG granule cells to form new and orthogonal representation for the altered contextual cues.

Lastly, it should be addressed that two rats (2 rats) in the lesion group, whose remained FC volume was extremely low, showed relatively unimpaired performance in the acquisition task (Figure 17; Figure 20). How can it be explained that even though FC lesion affected the acquisition performance, the extreme damage in FC rather did not impair the acquisition performance? It is noteworthy that a similar result was reported in a monkey study (Baxter and Murray, 2001). In delayed non-matching to sample task, the authors reported that the more lesion amount of hippocampus was induced, the less behavior impairment appeared even though hippocampus lesion impaired the performance of the task while rhinal cortex lesion amount and performance deficit were correlated positively. One of the explanations for the inverse correlation was that partial hippocampal lesion could make more abnormal activity to connected structures such as the rhinal cortex, which have an important role in solving the task. Similarly, the partially damaged FC can make abnormal spiking activity such as tonic spiking or unreliable activity, which can disrupt the function of downstream. Also, if FC disappeared for a long time, the hippocampus might deform its connectivity and I/E balance to overcome the absence of FC (Keck et al., 2017). For example, the activity of inhibitory neurons in dentate gyrus might be weakened to recruit more cells to be selected for representation after FC had been disappeared. To prevent connectivity and structural change problem, an acute inactivation study should be needed for further study. Even though the two rats had a common feature that their lesion status was extensive, another possibility to consider is that even individuals of the same species may have individual differences (Lee et al., 2014).

In conclusion, this study showed that FC is important for memory acquisition but not for retrieval. Also, it was revealed that FC is important for hesitation behavior when rats first meet novel contextual change, suggesting that FC might be important for the detection of novel contextual change and initiation of the

latent learning. This study is crucial in that it revealed the cognitive function of FC for the first time.

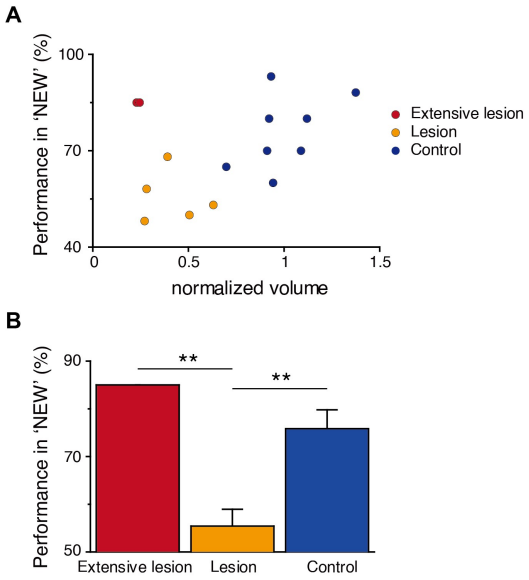


**Figure 20. The extensive lesion group showed normal performance during acquisition** (A) A raster plot for representing performance in acquisition task ('NEW') and remained FC volume relative to mean of control data. (B) Averaged performance of each group ($F(2,12) = 9.14$, $P=0.004$, ANOVA; Extensive lesion vs. Lesion: $P=0.004$; Control vs. Lesion: $P=0.004$; Extensive lesion vs. Control: $P=0.259$). Data represent means ± S.E.M. (*$p<0.05$, **$p < 0.01$, ***$p<0.001$).

# Chapter 3. FC is important for object-place associative memory

# Introduction

In previous chapters, it is discovered that FC is important for learning contextual memory. However, it is veiled whether FC is important specifically for contextual learning or there is a more general role in other kinds of learning.

Chapter 1 reported anatomical connectivity of FC that FC receives input from the perirhinal cortex, lateral entorhinal cortex, and project to dentate gyrus. It is reported that the perirhinal cortex is important for object recognition and major source of object information in the hippocampus, while the lateral entorhinal cortex and hippocampus (especially dentate gyrus) are crucial for associative memory for object and place (Lee et al., 2005; Hunsaker et al., 2008; Jo and Lee, 2010; Langston and Wood, 2010; Lee and Solivan, 2010; Barker and Warburton, 2011; Lee and Park, 2013; Lee and Jung, 2017). Therefore, the possibility is suggested that FC is also involved in the processing of associative learning of object and place, receiving the related information from the lateral entorhinal cortex and perirhinal cortex, the upstream of FC.

In these series of experiments, object recognition (OR), Object location (OL), and object-in-place (O-P) were conducted in both FC lesion group (LES) and sham lesion group (CON). The result suggested that FC is not important for object recognition, but important for object-place associative memory. These results suggested that FC is not only important for contextual memory but also has a general role in hippocampus-dependent learning.

## Materials and Methods

### Subjects

Long-Evans (LE; n = 30) rats were used in the study. Rats were individually housed with a 12-12 h light-dark cycle. All behavioral experiments were conducted during the light cycle. All protocols complied with the Institutional Animal Care and Use Committee of the Seoul National University.

### Apparatus

The experiment was carried out in a black square acrylic box (70 x 70 cm; 60 cm high). A white cue card (40 x 54 cm) was attached to the north wall. white noise was played through loudspeakers throughout the experiment for masking environmental noise. The floor of the square arena was covered with large brown paper, which is replaced between tasks and blocks to control local cues on the floor, and swept with 70% alcohol spray. Magnets were attached below the floor to locate objects in an accurate position reliably. The experiment was recorded with a digital camera (Logitech HD Pro Webcam C920, Logitech, CA, USA).

### Surgery

After three days of handling and foraging in a laboratory cart, FC lesion or sham-lesion surgery was operated. As described previous chapter, colchicine in the lesion group (n = 17) or sterilized saline in the control group (n = 13) was injected. For surgery, the rat was first anesthetized by sodium pentobarbital (Nembutal, 65 mg/kg, I.P.) and its head was fixed in a stereotaxic instrument (Kopf Instruments, Tujunga, CA). Anesthesia was maintained by 1-2% isoflurane (Piramal, Bethlehem, PA). Small burr holes were drilled to inject colchicine (7 mg/mL) or sterilized saline (0.1 μL per injection site at 10 μl/h rate; microinjection pump: Legato130, KD Scientific) through a glass pipette (1b100-4, WPI) connected to a 5μl Hamilton

syringe (7634-01, Hamilton) with adaptor (55750-01, Hamilton). The following coordinates were used for drug injection: 3.5 mm posterior to bregma, 0 mm lateral to the midline, and 3.5 mm ventral from dura with no angle through the superior sagittal sinus. After surgery, the rat rested for 6 days. Seven days after surgery, Platform habituation was conducted for 4 days.

**Experiment procedure**

On days 7 to 10, platform habituation was conducted for 15 minutes that freely explore the empty box to be habituated. From day 11, a spontaneous object exploration experiment was conducted as the below order every other day. For each task, a different set of objects were used, so no same object was repeatedly exposed in different task.

**Object location**

In this task, two identical objects were used and the objects used in the sample were not used in the test again but copy objects were used. The sample block was repeated 3 times with 3 minutes inter-block interval. In a sample block, two identical objects were located in the left upper position and right upper position, separately and rats explored the environment for 5 minutes. After 3 minutes of the last sample block, the test block started that one of the object locations is displaced to a novel place. The object to be displaced is pseudo-randomly selected by the rat. The test block lasted 5 minutes and finished. The brown paper under box was exchanged every inter-block intervals and after the experiment.

**Object-in-Place (swap)**

In this task, three different objects were used and the objects were used in the test again. The sample block was repeated 3 times with 3 minutes inter-block interval. In a sample block, three identical objects were located, separately and rats

explored the environment for 5 minutes. After 3 minutes of the last sample block, the test block started. In the test block, two objects swapped their location. The test block lasted 5 minutes and finished. The swapped objects were pseudo-randomly selected. The brown paper under box was exchanged every inter-block intervals and after the experiment.

**Object-in-Place (alternation)**

In this task, two different objects were used and the objects were not used in the test again but copy objects were used. The sample blocks were repeated 3 times with 3 minutes inter-block interval. In a sample block, two different objects were located in the left upper position and right upper position, separately and rats were allowed to explore the environment for 5 minutes. After 3 minutes of the last sample block, the test block started. In the test block, one of the objects altered to the identical object to the other one. The test block lasted 5 minutes and finished. The altered object location was pseudo-randomly selected. The brown paper under box was exchanged every inter-block intervals and after the experiment.

**Novel object recognition (1 hour)**

In this task, two identical objects were used and the objects were not used in the test again but copy objects were used. The sample block was repeated 3 times with 3 minutes inter-block interval. In a sample block, two identical objects were located in the left upper position and right upper position, separately and rats were allowed to explore the environment for 5 minutes. After 1 hour of the last sample block, the test block started. In the test block, one of the objects exchanged to the different objects. The test block lasted 5 minutes and finished. The exchanged object was pseudo-randomly selected. The brown paper under box was exchanged every inter-block intervals and after the experiment.

**Novel object recognition (5 minutes)**

The behavioral paradigm is the same as Novel object recognition (1 hour), but the inter-block interval between the last sample block and the test block is changed to 5 minutes.

**Histological analysis**

The histological procedure is the same as the lesion study on T-maze described in the previous chapter.

**Analysis of behavioral data**

The measure of exploration time for each object was conducted manually with Ethovision software (Noldus, USA) by an experimenter. The behavior that the direction of head face an object and the distance between the nose and the object is less than 3 cm is defined as an object exploration behavior. The rearing and biting behavior were not counted as exploration and excluded from data. For the three object exploration (Object-in-Place, Swap), the average time for the two swapped objects was defined as the exploration time for the target object. The discrimination index is defined as the time that subtracts target object exploration time from familiar object exploration time divided by the sum of exploration time for both objects. For the statistical comparison, the Wilcoxon signed-rank test for exploration comparison between objects and Mann-Whitney rank-sum test for discrimination index comparison between groups. The statistical analysis was conducted using Statview software and. For presenting the data and statistical results, median and interquartile range (IQR) were used. The statistical results are organized in Table 5.

# Results

The histological results verified that FC was selectively ablated by colchicine injection in the lesion group, while intact in the control group as reported in the previous chapter (Figure 21).

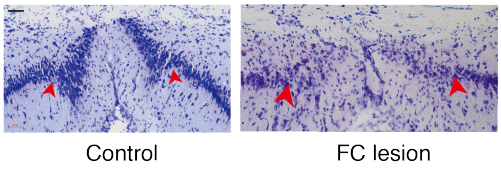


**Figure 21. Selective lesion of the FC with colchicine.** Selective lesions of the FC in the lesion group, compared with the intact FC in the control group (Nissl staining). Arrowheads mark the boundaries between the FC and dmCA1. Scale bar: 100 μm.

At first, in order to check if FC is important for object recognition memory, object recognition (OR) experiment was conducted (Figure 22.A). The experiment was consist of three sample blocks to let rats be habituated and test blocks. Each block was performed for 5 minutes and the inter-block interval in the sample was 3 minutes, while the interval between sample and test was 5 minutes. In the experiment, the lesion group showed a preference for the novel object as the control group (Figure 22.C). The results suggest that FC lesion did not impair the recognition of an object. In the previous report, however, it was reported that the dentate gyrus lesion impaired object recognition when the duration between sample and test was sufficiently long

as 1 hour, suggesting that the involvement of dentate gyrus in the task depends on the interval between sample and test (Clark et al., 2000). To test the possibility of whether FC is involved in the task when the interval is sufficiently long, the same task with the one-hour interval between sample and test was conducted again (Figure 22.B). However, the result did not differ from the previous task, suggesting that FC is not involved in object recognition itself (Figure 22.D).

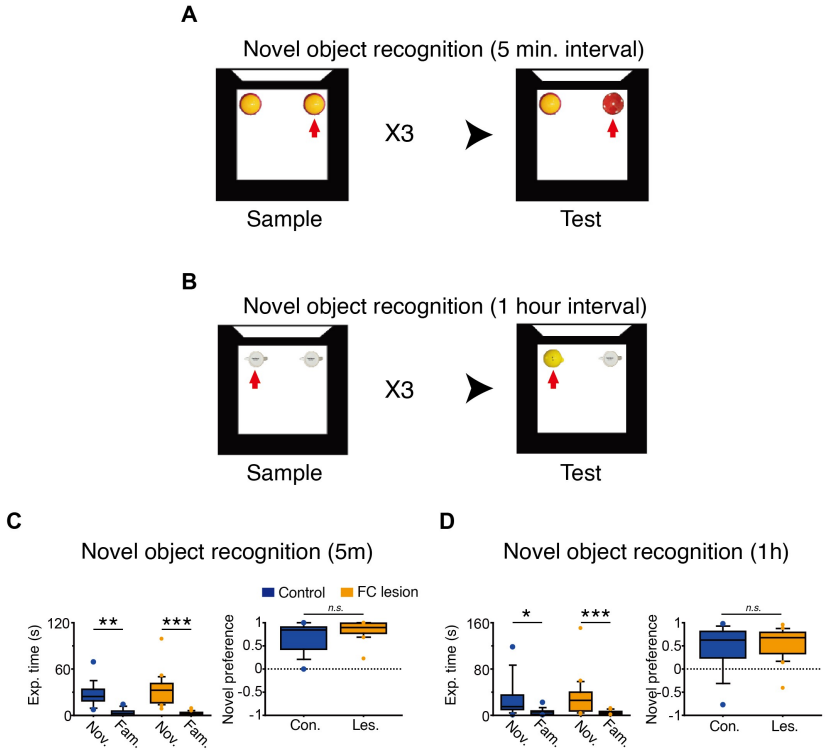


**Figure 22. FC is not important for novel object recognition** (A-B) task explanation. After three sample blocks, the test block occurred. The red arrow indicates the exchanged novel object. The interval between the last sample block and the test block is 5 minutes. (A), or 1 hour (B), separately. (C-D). Statistical results for the tasks. The plot show median value and interquartile range. The statistical comparison of exploration time is conducted in each group. (*p<0.05, **p < 0.01, ***p<0.001).

The next experiment is an object location that tests the recognition ability of a novel location of an object without the novelty of object identity. The procedure of the experiment is the same as object recognition except that object location is changed without a change of object identity (Figure 23.A). The results suggest that the control group showed a preference for the novel object location while lesion group did not, suggesting FC is important for novel place recognition (Figure 23.B).

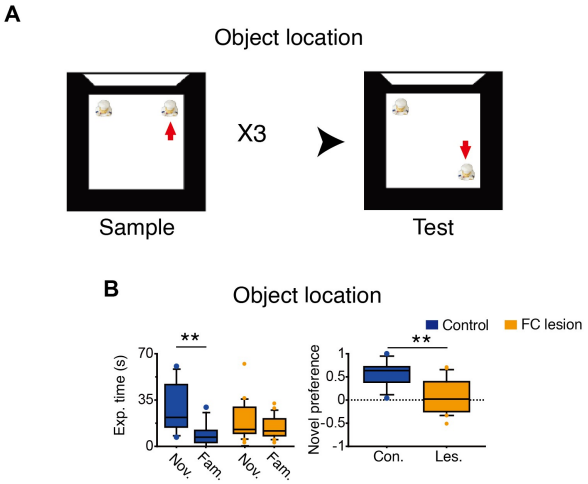


**Figure 23. FC is important to recognize a displaced object** (A) task explanation. After three sample blocks for habituation, an object displaced to a novel place. The displaced object in the figure is indicated by an arrow. (B) Statistical results for the tasks. The plot show median value and interquartile range. The statistical comparison of exploration time is conducted in each group. (*p<0.05, **p < 0.01, ***p<0.001).

The last experiment is an object-in-place task. There are two types of the object-in-place task were conventionally performed in previous studies. The one is ‘swap’ that two familiar objects swap their positions, remaining other familiar objects in the same location. Another one is ‘alternation’ that two different objects were presented in the sample, but one is altered to another one in the test (Figure 24.A-B). Although both experiments were used to test the orthodox associative memory of object and place, a detailed methodological difference has a possibility to make a different result (Packard and McGaugh, 1996; Langston and Wood, 2010). Therefore, both association tasks were conducted for cross confirmation. The result of the object-in-place task with alternation is that the control group showed a higher preference for an altered object than the remained object, while lesion group did not (Figure 24.C). The results suggest that FC is crucial for object-in-place memory. The result of another O-P memory task (swap) was similar. In the swap task, in which two objects were used for swap while another object did not change its location, the control group showed a higher preference for swapped objects than the remained object, but the lesion group did not, confirming that FC is important for object-place associative memory (Figure 24.D). To sum up, FC is important to recognize object location and learning associative memory of object and place, but not to recognize object identity.

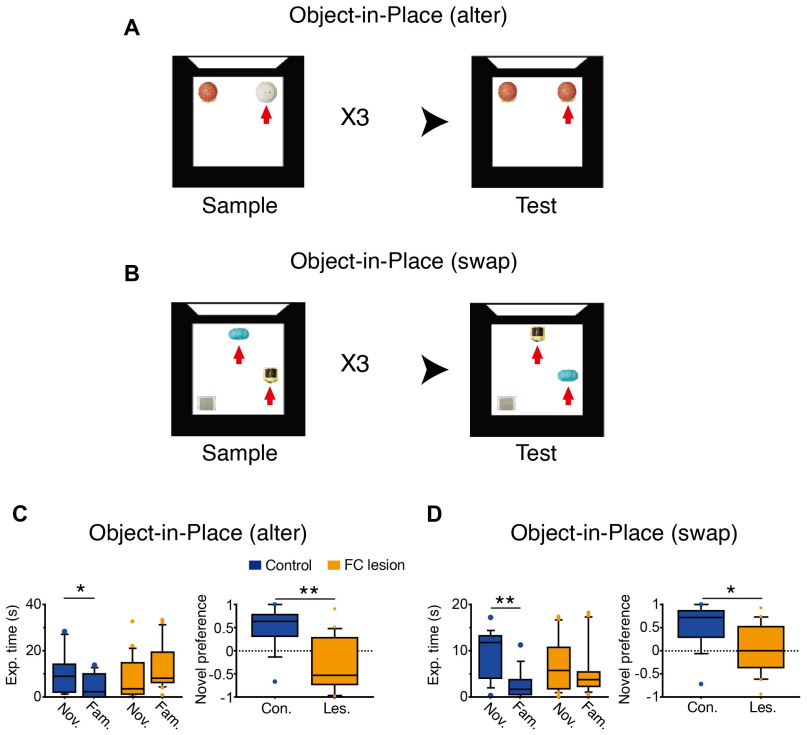


**Figure 24. FC is important for recognize object-in-place.** (A-B) task explanation. After three sample blocks, the test block occurred. The red arrow indicates the exchanged object. Unlike the novel object exploration, the exchanged object did not have a novelty but the relation between object and position was novel. The interval between the last sample block and the test block is 3 minutes. (C-D). Statistical results for the tasks. The plot show median value and interquartile range. The statistical comparison of exploration time is conducted in each group. (**$p < 0.01$).

**Table 5. Statistical results of spontaneous object exploration tasks** Asterisks in the p-value column indicate statistical significance. Values represent median (IQR). Wilcoxon signed-rank test was used for the comparison of exploration time, while the Mann-Whitney rank-sum test was used for comparison of the index.

| Task | Median (IQR) | | Statistics | Note |
|---|---|---|---|---|
| Novel object Recognition (5 min.) | Novel, Control | 24.5 (14.9) | Z = 3.180 | |
| | Fam., Control | 2.8 (5.6) | P = 0.0015* | |
| | Novel, Lesion | 32.5 (24.7) | Z = 3.621 | |
| | Fam., Lesion | 1.7 (3.3) | P = 0.0003* | |
| | Control, Index | 0.8 (0.5) | Z = 1.318 | |
| | Lesion, Index | 0.9 (0.2) | P = 0.1874 | |
| Novel object Recognition (1 hour) | Novel, Control | 15.0 (25.4) | Z = 2.411 | |
| | Fam., Control | 6.2 (5.9) | P = 0.0159* | |
| | Novel, Lesion | 26.2 (32.4) | Z = 3.337 | |
| | Fam., Lesion | 3.8 (4.1) | P = 0.0008* | |
| | Control, Index | 0.6 (0.6) | Z = 0.439 | |
| | Lesion, Index | 0.7 (0.5) | P = 0.6603 | |
| Object location | Novel, Control | 21.8 (31.9) | Z = 3.180 | |
| | Fam., Control | 7.1 (9.2) | P = 0.0015* | |
| | Novel, Lesion | 12.7 (19.8) | Z = 0.781 | |
| | Fam., Lesion | 11.7 (12.6) | P = 0.4348 | |
| | Control, Index | 0.6 (0.3) | Z = 3.160 | |
| | Lesion, Index | 0.03 (0.64) | P = 0.0016* | |
| Object-in-Place (alter) | Novel, Control | 9.0 (12.2) | Z = 2.353 | |
| | Fam., Control | 2.2 (9.9) | P = 0.0186* | |
| | Novel, Lesion | 3.6 (13.6) | Z = 1.112 | |
| | Fam., Lesion | 8.1 (13.2) | P = 0.2659 | |
| | Control, Index | 0.6 (0.5) | Z = 3.285 | |
| | Lesion, Index | 0.5 (1.0) | P = 0.0010* | |
| Object-in-Place (swap) | Novel, Control | 11.8 (9.1) | Z = 3.110 | |
| | Fam., Control | 1.7 (3.2) | P = 0.0019* | |
| | Novel, Lesion | 5.8 (9.0) | Z = 0.639 | |
| | Fam., Lesion | 3.7 (3.2) | P = 0.5228 | |
| | Control, Index | 0.7 (0.6) | Z = 2.239 | |
| | Lesion, Index | 0.0 (0.9) | P = 0.0252* | |

# Discussion

In this series of experiments, it was revealed that FC is important for place location and object-in-place tasks but not for object recognition tasks. In previous studies, it is suggested that object recognition is processed in the perirhinal cortex, and the downstream including LEC and hippocampus are not involved in object recognition (Langston and Wood, 2010; Barker and Warburton, 2011). Because FC lesion did not impair recognition of object identity and FC is one of the downstream of the perirhinal cortex, it is confirmed that the results of object recognition task also support the claim despite some controversial arguments (Clark et al., 2000; Broadbent et al., 2004).

Meanwhile, in terms of information stream, the result of object location task is quite surprising because it was reported that the upstream of FC including lateral entorhinal cortex and perirhinal cortex lesion did not impair the recognition of displaced object (Barker and Warburton, 2011; Wilson et al., 2013a), while DG lesion impairs the recognition of displaced object (Lee et al., 2005). The result suggests the possibility that FC not only delivers information from LEC to DG but also supports the learning process in DG. However, despite the controversy, another study argued that LEC is important to recognize a displaced object (Van Cauter et al., 2013).

Lastly, it is reported that the object-in-place experiment is a DG-dependent task (Lee and Solivan, 2010)[2]. FC lesion also disrupted the object-in-place experiment.

---

[2] the involvement of DG in object-in-place experiment was controversial. An experiment reported that DG is important for object-in-place memory (Lee and Solivan, 2010), while another experiment (Lee et al., 2005) reported that DG lesion did not disrupt in similar manipulation (object E). However, the unaffected

the results of the object-in-place task are interpreted in two different points of view. The first point of view is that either object and place is a single-subject to be recognized solely. In this case, in order to conclude that FC is important for the associative memory, only the association task should be impaired after FC lesion, while the recognition for both cues is intact (Wilson et al., 2013a). In this view, the results of a series of experiments are hard to support the idea that FC is important for associative memory because FC lesion not only disrupts object-place association but also place recognition. The impaired object-in-place associative memory could be interpreted as a side effect of failure for place recognition.

On the other hand, the place is able to be interpreted as a higher-dimensional cue than an object (Eichenbaum et al., 1999). In other words, the place is not defined by itself but defined by physical relationships of distance and direction with the other external cues such as white cue card and pattern of the ceiling in these experiments. In this view, the novel place recognition experiment is not a recognition experiment for single stimuli, but a different type of associative memory task that tests changed relationship between moved object and other static external cues without change of object identity. Because DG is important for hippocampal-dependent associative memory, and FC lesion disrupts the memory acquisition of DG, the impairment of the experiment could be interpreted as impairment of associative memory. In conclusion, these all three experiments are associative memory task with different methodologies (‘displacement’, ‘replacement’, and ‘swap’), and the result that FC lesion impaired the experiments suggest that FC is important for performing an associative memory task. In addition, in these series of experiments, I did not found

---

exploration time in object E that has no novelty in location and object identity but has a novelty in the associative relation might be due to presence of another object D, which moved to spatially novel place simultaneously.

a cognitive function of FC, which is independent of DG, suggesting that FC is an accessorial subregion for DG.

# Chapter 4. Electrophysiological characteristics of the *fasciola cinereum*

# Introduction

As mentioned above, the biggest obstacle for researching FC is the lack of basic knowledge about FC (Evans et al., 2015). Since little is known about the anatomical and physiological features of the area, it was challenging to hypothesize what is the role of the FC. The ambiguity of the lateral boundary is, even more, make it hard to study this area.

Whether place cells exist in FC is the major question of the research. Place cell in the hippocampus is a cell that responds to the position of the subject and has a receptive field in space (O'Keefe and Dostrovsky, 1971). Because the place cell also represents context, experience, and future behavior, it is considered as physiological evidence of cognitive map (O'Keefe and Nadel, 1978; Muller and Kubie, 1987; Muller and Kubie, 1989; Mehta et al., 2000; Pastalkova et al., 2008; Grieves et al., 2016; Park and Lee, 2016). In previous chapters, it was revealed that FC is important for several learning tasks. However, the presence of place cell in FC and whether the cognitive function was processed by place cell is vailed yet.

Theoretically, two major pathways in the medial temporal lobe were suggested as an information source of the hippocampus. By the theory, the spatial pathway is a source of spatial information and composed of POR and MEC, while the non-spatial pathway is a source of non-spatial information such as an object and composed of PER and MEC (Burwell and Amaral, 1998; Hargreaves et al., 2005). The discovery of specialized cells for recognition of egocentric spatial information in MEC including grid cell, border cell, head direction cell, speed cells has supported the theory (Fyhn et al., 2004; Hafting et al., 2005; Sargolini et al., 2006; Solstad et al., 2008; Kropff et al., 2015). In terms of anatomical connection, FC is located at the end of the non-spatial pathway (LEC and PER), suggesting FC has less spatial information, comparing to other hippocampal subregions. Therefore, it should be checked whether a place cell exists in FC as other hippocampal subregions.

In addition, the presence of sharp-wave ripples (SWR) in FC also should be inspected. It is known that sharp-wave ripple (SWR) occurs in CA3 (and some in CA2) of the hippocampus and migrate to CA1 and DG (Buzsaki, 2015; Oliva et al., 2016; Swaminathan et al., 2018). However, FC has no afferent connection with CA3. Considering the anatomical background, FC has a possibility that ripples are not observed in FC.

Also, this experiment attempts to determine whether there is a physiological difference based on the anatomical boundary between FC and dmCA1 which was described in the previous chapter. Previous studies have reported that hippocampal subregions show different physiological characteristics (Lee et al., 2004a; Lee et al., 2004b; Leutgeb et al., 2004; Vazdarjanova and Guzowski, 2004; Leutgeb et al., 2005a; Leutgeb et al., 2005b; Neunuebel and Knierim, 2014). The difference in physiological characteristics will confirm the physiological boundary.

# Materials and methods

### Subjects

Long-Evans (LE; n = 12) rats were used in the study. Rats were individually housed with a 12-12 h light-dark cycle. All behavioral experiments were conducted during the light cycle. All protocols complied with the Institutional Animal Care and Use Committee of the Seoul National University.

### Place-cell recording in a square box

The experiment was carried out in a black square acrylic box (70 x 70 cm; 60 cm high). A white cue card (40 x 54 cm) was attached to the north wall. The box was surrounded with a black curtain and white noise was played through loudspeakers throughout the experiment for masking environmental noise. The floor of the square arena was covered with large brown paper, replaced between sessions to control local cues on the floor. A digital camera, commutator (PSR-36, Neuralynx), and a custom semi-automatic feeder were all installed in the ceiling. The feeder scattered chocolate sprinkles when an experimenter pushed a switch from outside the testing room while monitoring the rat's movement.

### Hyperdrive implantation surgery

Procedures for constructing and surgically implanting the hyperdrive can be found in detail in our previous articles(Lee et al., 2018) and will be only briefly described here. A hyperdrive with 24 tetrodes was custom-made and implanted in LE rats (11-41 weeks old; n = 12). Nichrome wires were used for tetrodes (17.8 $\mu$m in diameter, A-M systems). To avoid damage in the superior sagittal sinus, the tetrode-carrying bundle of the hyperdrive was angled at 20˚ to approach the FC obliquely. The hyperdrive itself was inserted into the brain also at 10˚ angle. The surgical coordinates were pre-calculated to target the FC on the right hemisphere

with the tip of the tetrode bundle (9G or 12G stainless-steel tubing): 3.6 mm posterior to bregma and 2.2 mm lateral from midline. Stainless-steel wire coupled to the ground channel of the hyperdrive was connected to the skull screw over the cerebellum to be used as an animal ground.

**Electrophysiological recording procedures**

After seven days of recovery from surgery, tetrodes were lowered daily to target areas (FC, CA1) for about three weeks. Spiking activities from single units and local field potentials (LFPs) were fed to the data-acquisition system (Digitalynx SX, Neuralynx) through an electrode interface board (EIB-36-24TT, Neuralynx), pre-amplifier (HS-36, Neuralynx), and tether (HS-36 Litz tether, Neuralynx). Signal was digitized at 32 kHz, filtered at 600-6,000 Hz, and amplified 1,000-10,000 times. When most of the tetrodes reached the target areas, a habituation session started in the foraging box with the tether connected to the hyperdrive at least for three days, followed by foraging sessions for 6–14 days. During the foraging sessions, rats freely moved around in the square box to consume chocolate sprinkles, and the hippocampal neural signals were recorded in sync with position and head-direction information for 15 min. Neural signals were recorded during sleep in a sound-attenuating booth outside the experimental room (sleep session) before and after each behavioral recording session. The rat was allowed to sleep in the booth for at least 30 min to provide enough neural data associated with the resting period. The local field potential (LFP) data against animal ground also additionally recorded, while single units were simultaneously recorded against reference wire from ten rats. Only the LFP data against the animal ground was used for LFP analysis.

**Experiment in T-maze**

Five of twelve rats involved in electrophysiology experiments were also conducted experiments on T-maze. In one of them, well-distinguished place cells in FC were observed, so the rat was used for analysis.

**Apparatus for T-maze experiment**

An elevated t-maze (72 × 8 cm for stem and 40 × 8 cm for each arm) was used (Figure 25.A). A food well (2.5 cm diameter, 0.8 cm deep) was located at the end of each arm (Figure 25). A quarter pieces of froot loop (Kellog's) sunflower seed was used as a reward. The arms of the maze were surrounded by an array of three LCD monitors. At the end of the stem, a start box with a guillotine door was placed. Infrared sensors were installed in front of the start box and in the stem to measure latency. The behavioral experiment was controlled by the Matlab-based custom program and the sensor data were acquired using a data acquisition device (PCI-6221, National Instrument, Austin, Texas). Four visual scenes were used in the behavioral experiments: zebra, pebbles, bamboos, and mountains (Figure 25.B).

**Pre-training**

After 3 days of handling and foraging in a laboratory cart, the rat conducted foraging on the T-maze for familiarization for two days. Once acquainted, a shaping session started in which the rat trained to go straight and find a reward as well as returning after getting a reward. The reward located at the center of two arms, so the rat can see the reward directly. The shaping conducted until the rat was habituated. After the shaping for 7 days, the same behavior paradigm was conducted but the familiar scenes (zebra and pebble) on the screen were alternatively presented by blocks. The training was performed for 40 trials before surgery and 200 trials after the hyperdrive implantation surgery for two days before recording.

**Shuttling with scene alternation (familiar scenes)**

To observe a cellular activity for contextual change of FC neuron without the compound factor of behavior, I conducted the task in which scenes were altered by blocks (zebra-pebble-zebra) during the rat conducted shuttling for three days. The reward located at the center of arms for the first two days and left food well for the last day while a brick blocked the other arm. The trials in a block are 100 trials (first day) or 70 trials (other days). Other electrophysiology related setup and procedure such as sleep session before and after the experiment is the same as open field setup.

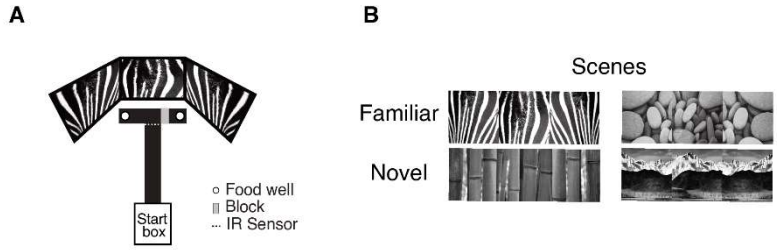


**Figure 25. Apparatus for T-maze experiment** (A) Behavioral apparatus. The white dotted line indicates the point where the infrared beam sensor was installed. The gray rectangle represents the acrylic block used to restrict access to the arm. (B) The scenes used for the tasks.

**Shuttling with scene alternation (novel scenes)**

The behavioral procedure was similar to the previous experiment, so only different procedures are described. The scenes were changed to bamboo and mountain (order: bamboos – mountains – bamboos; a block = 70 trials), and the right food well was used without cover while the other arm was blocked by a brick.

**Shuttling with scene-place alternation**

The behavioral procedure was similar to scene alternation (familiar scenes) experiment, so only different procedures are described. The experiment started with a zebra scene, and the reward was located in the left food well in the first block. The block is composed of 70 trials. At the next block, the scene on the monitor was changed to pebble while the reward location also changed to the right food well. The alternation was reversed again after the end of the second block. The experiment was performed in a day.

**Histological verification of electrode positions**

After the last recording session, the rat was killed by CO2 overdose and perfused transcardially with phosphate-buffered saline (PBS) followed by 4% v/v formalin solution. The head was fixed in formalin solution for one day before the brain was extracted. The extracted brain was fixed in 30% sucrose in 4% formaldehyde solution until it sank to the bottom of the tube at 4°C. Then, the brain was coated with gelatin and fixed in sucrose formaldehyde solution for 1-2 days. The brain was sectioned at 40 $\mu$m using a freezing microtome (HM 430, Thermo-Fisher Scientific), and every section was mounted on the glass slide and was thionin-stained. Photomicrographs were taken with a digital camera (DS-Fi1c, Nikon) attached to a microscope (Eclipse 80i, Nikon) and tetrode tracks were reconstructed three-dimensionally (Illustrator, Adobe, USA; Voxwin, UK) to match between the electrode track with the pre-configured bundle design. The recorded depth of tetrodes and physiological profiles were also considered during the reconstruction procedures.

**Unit isolation**

Single units were recorded simultaneously from the FC (n = 228) and CA1 (n = 1195), and unit isolation was manually performed using custom-written

software (WinClust) using the peaks of waveforms as a major measurements as described previously (Lee et al., 2018) while considering other parameters such as energy as well. Spikes collected during sleep sessions were also used during unit isolation for judging the stability of recording. Only the single units that meet the following criteria were included in analysis: (a) More than 50 spikes of a cluster should be identified in both the pre- and post-sleep sessions and the proportion of the number of spikes within a refractory period (1 ms) should be less than 1% of the total spikes, (b) Mean firing rate of a cluster should be less than 10 Hz to include only putative complex spiking neurons, (c) Only place cells (the number of spikes in the open field ≥ 50, spatial information ≥ 0.5 with $p$-value < 0.05; see 'Data Analysis' for details). The p-value criterion is not applied in T-maze experiments because the position was not detected in the start box that rats spend about half of the experiment time.

Spikes recorded while the animal was relatively stationary (moment velocity < 5 cm/s) were filtered out and were not used in the analysis as the previous study(Henriksen et al., 2010). For delineating the boundaries physiologically, I divided the CA1 to two subdivisions based on online atlas(Boccara et al., 2015): the distalmost part of the CA1 (dmCA1) that was regarded as the FC in some previous reports(Henriksen et al., 2010; Boccara et al., 2015) and the distal CA1 (dCA1) that is located more medially compared to the dmCA1. Only the tetrodes posterior to AP -3.0 were used for analysis.

**Electrophysiological data analysis**

Spike width is defined as the temporal distance between the peak and trough of the averaged spike waveform. Averaged spike waveform was made from all channels and spikes during recording including sleep sessions and behavior sessions. Burst index is defined by averaged spikes in 3-5 ms divided by averaged spikes 200-300 ms (Senzai and Buzsaki, 2017).

To construct a rate map, position data from the foraging session was binned into a matrix (bin size = 2.7 × 2.7 cm) and spike data were assigned to the matching bins. A rate map was calculated by diving the number of spikes by the duration of the visit per bin (firing rate). The resulting rate map was smoothed by an adaptive binning method(Skaggs et al., 1996).

In a rate map of a unit, continuous bins showing over 20% of the peak firing rate were included to define the unit's place field. At least 20 continuous bins (88.2 $cm^2$) were required for the unit's firing field to be qualified as a place field. The in-field firing rate was measured as the firing rate in the place field. The stability of a rate-map (rate map similarity) was measured as the correlation coefficient (R) between the rate maps constructed for the first half and the second half of a session (each half = 7.5 min) (Henriksen et al., 2010). For better distinguishment between subregions, the raw rate map was used for the rate map similarity analysis. In the T-maze experiment, the rate map similarity is defined as the rate map correlation coefficient between the first block and last block for the 'Same,' while first block and second block for the 'Diff.' Also, because the different place selectivity by the direction, 'outbound,' which is a direction toward reward until the sensor in front of the monitor, and 'inbound,' which is a direction toward start box' was analyzed independently. For practical reason, the time after cutting the last sensor on the track was defined as inbound in the analysis.

The spatial information of spiking activity was measured as follows (Skaggs et al., 1993).

$$\text{Spatial information} = \sum_i p_i \frac{\lambda_i}{\lambda} \log_2 \frac{\lambda_i}{\lambda} \text{ (bits/spike)},$$

where $i$ denotes the bin number, and $p_i$ and $\lambda_i$ represent the occupancy rate and the firing rate of the $i$th bin, respectively. Finally, λ denotes the mean firing rate. The probability of obtaining the spatial information score was calculated from the random distribution of spatial information using a Monte-Carlo method. That is, the spiking train of a unit was randomly shifted (minimum shifting unit = 33 s), and

spatial information was re-calculated from the generated rate-map for each shift. This procedure was repeated for 1000 times. The p-value was defined as the proportion of shuffled data above the spatial information obtained from the actual rate map. The coherence was measured as the correlation coefficient between raw rate map and reconstructed rate map, where the firing rate of each pixel was averaged firing rate of adjacent pixels. The firing rate (sleep) was measured during sleep sessions after a behavioral experiment. For statistical comparison (ANOVA, repeated-measures ANOVA, t-test, paired t-test and one-sample t-test), commercial software packages including the JMP (SAS), Statview (SAS) and Matlab (MathWorks) were used. Statistical results are organized in tables (Table 6, Table 7, and Table 8)

**Local field potential analysis**

The analysis procedure is followed by the previous report in my laboratory (Ahn et al., 2019) and custom-write Matlab (Mathworks, USA) program was used. Here, I briefly describe the different procedures. After the LFP data were down-sampled (1/16) to 2 kHz, the LFP data in 150Hz – 250Hz were filtered with a bandpass filter. The parameters for the filtering is below:

Passband edge frequency(Wp): 145Hz – 255Hz

Stopband edge frequency(Rp): 130Hz – 270Hz

Passband ripple (Rp): 3dB

Stopband attenuation (Rs): 15dB

Filter type (ftype): bandpass

These parameters were used for the Matlab functions in signal processing toolbox (Mathworks): ‘buttord’, ‘butter’ and ‘zp2sos’ in order. The filtered EEG was derived from ‘filtfilt‘ function.

**Ripple detection**

For ripple detection, filtered LFP data were smoothed by Gaussian filter, and envelops were detected. For the calculation of envelope, 'smoothdata' function was used after the Hilbert transform of LFP data (smoothing bin size: 25/2000 s). The envelope is defined as the LFP data above 1.5 times of standard deviation (STD) from the mean. For noise reduction, the data point above 11 STD was discarded from the analysis. Also, the ripple less than 20 ms was discarded, and the ripples whose interval was less than 20 ms were considered as one ripple. Once the ripple boundary for each tetrode was confirmed, the border extended to one STD from the average of the envelope. The ripple of a session is defined as the total duration of overlapped ripples recorded in CA1 area (both dCA1 and dmCA1), and the ripple detected from at least three tetrodes were included in the analysis to reduce noise.

**Ripple power measurement**

Once ripple detection is finished, the power of ripple was measured in unfiltered LFP (unit: mV) data using 'mtspectrumc' function in the Chronux 2.0 toolbox (Bokil et al., 2010). Parameters for the function is below

Frequency (Fs): 2000 Hz

TimeBandWidth and multiple Tapers (tapers): [3 5] (300ms)

Frequency to be analyzed (fpass): 300 Hz

Pad(pad): 0

Trial (trialave, not used): 1

Mean and S.T.E. (err, not used): [1 0.05]

The power in a ripple was measured by 'bandpower' function in Chronux. Because the LFP data was measured against the animal ground, body movement affected the LFP power. I noticed that the corpus callosum (CC) showed similar ripple power to CA1 when a rat awakens, while CC showed less ripple power than CA1 when the rat sleep. Therefore, I rejected the ripples whose power ratio of

averaged CA1 and averaged CC is less than 1.5. The power transformed into dB using pow2db function in Matlab (Rasmussen et al., 2017). The outburst ratio is defined as the average firing rate in the boundaries of ripples divided by the average firing rate out of ripples. Only the LFP data recorded from the post-experimental sleep session was used.

# Results

To identify the physiological characteristics of FC and distinguish the physiological boundary of the FC from CA1, I recorded each area (FC, dmCA1, CA1) simultaneously (Figure 26.A). For confirmation of the border between FC and CA1, the electrophysiological properties of the distalmost part of CA1 (dmCA1), a region considered as FC in some studies, with more proximally located distal CA1 (dCA1) and FC are compared. To target electrodes into FC while avoiding the superior sagittal sinus, the tip of hyperdrive was angled 20º medially and implanted with a 10º angle (Figure 26.A). Histological results suggested that the tetrodes targeted FC, dmCA1, and dCA1 (Figure 26.A). Some complex-spiking neurons recorded in all three parts showed place-specific spiking pattern, or place field during random foraging in a square box (Figure 27.A). However, some spike identity and firing patterns were different between FC and CA1 areas. Spikes recorded in FC showed a more narrow waveform than those of dmCA1 and dCA1 (Figure 26.B-C). Besides, the averaged firing rate, peak-firing rate, in place-field firing rate, spatial information, and reliability of FC cells were lower than dmCA1 and CA1, while the firing rate during resting sessions before and after behavior experiment did not differ (Figure 27A-C). However, no significant difference in physiological characteristics was found between dmCA1 and CA1, suggesting that those areas were not different areas. The result suggests that the distinct boundary defined by anatomical characteristics is also validated in physiologically.

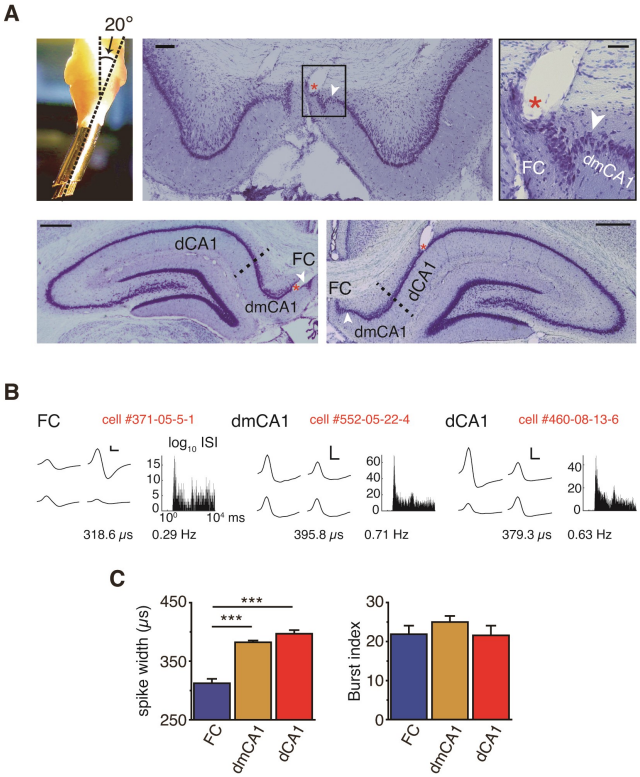


**Figure 26. Non-spatial physiological characteristics of FC comparing to CA1**

Recording electrode bundle and tetrode locations. Upper left: An angled bundle (20° medially) carrying 24 tetrodes to the FC and its neighboring hippocampal subregions was installed in the hyperdrive. Upper center: Representative example of the electrode track, showing the tetrode tip in the cell layer of the FC. Upper right: Magnified view more clearly showing the tip location (*). Tetrode tracks that recorded the distalmost CA1 (dmCA1; lower left) and distal CA1 (dCA1; lower right) regions are also shown. Scale bars: 100 μm (upper center), 50 μm (upper right) and 500 μm (lower panels). (B) Representative non-spatial properties of place cells. Representative waveforms (left) and inter-spike interval (ISI) histograms (log scale) of single units recorded from the FC, dmCA1, and dCA1 are shown. Vertical scale bar: 100 μV; horizontal scale bar: 200 μs. The numbers below the plots indicate (left to right) spike width and firing rate in a recording session during rest. (C) Comparison among the FC dmCA1 and dCA1. (***p<0.001).

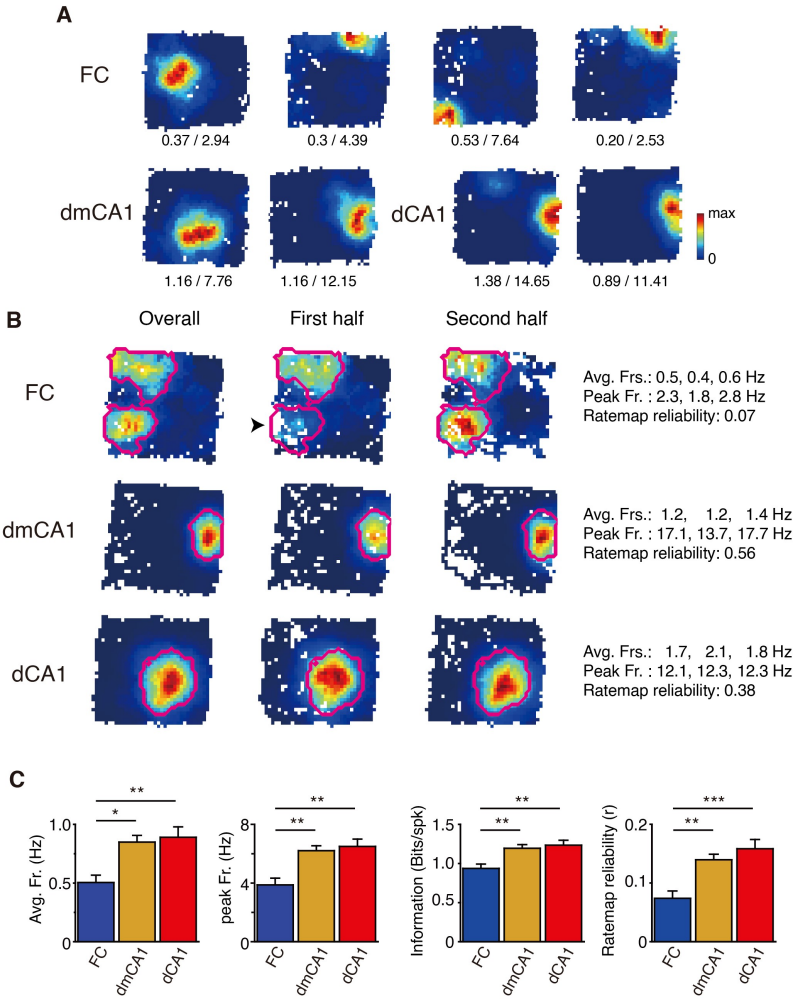
A
FC
0.37 / 2.94
0.3 / 4.39
0.53 / 7.64
0.20 / 2.53
dmCA1
dCA1
max
0
1.16 / 7.76
1.16 / 12.15
1.38 / 14.65
0.89 / 11.41
B
Overall
First half
Second half
FC
Avg. Frs.: 0.5, 0.4, 0.6 Hz
Peak Fr. : 2.3, 1.8, 2.8 Hz
Ratemap reliability: 0.07
dmCA1
Avg. Frs.: 1.2, 1.2, 1.4 Hz
Peak Fr. : 17.1, 13.7, 17.7 Hz
Ratemap reliability: 0.56
dCA1
Avg. Frs.: 1.7, 2.1, 1.8 Hz
Peak Fr. : 12.1, 12.3, 12.3 Hz
Ratemap reliability: 0.38
C
Avg. Fr. (Hz)
peak Fr. (Hz)
Information (Bits/spk)
Ratemap reliability (r)
FC
dmCA1
dCA1

**Figure 27. Spatial characteristics of FC compared to dmCA1 and dCA1.** (A) Representative place fields of principal cells in the FC, dmCA1, and dCA1, recorded during foraging in a square arena. The numbers below are mean firing rates and peak firing rates of place cells. (B) Representative place field stability of place cells in each subregion. The rate maps for 15 minutes are presented in the left column while the rate maps for the first 7.5 minutes and last 7.5 minutes are presented in center and right, separately. The color scale for a place cell is the same for three different rate maps. Average firing rate (Avg. Fr.), peak firing rate (Peak Fr.) and rete map reliability are described in right. Rate map reliability is a correlation coefficient (R) of raw rate maps of the first half and second half. The magenta lines indicate the boundary of a place field. (C) Comparison among the FC, dmCA1, and dCA1. Place cells in the FC showed different firing patterns compared to those in the dmCA1 and dCA1 in mean firing rate, peak firing rate, spatial information and rate map reliability (*$p<0.05$, **$p < 0.01$, ***$p<0.001$).

Despite some physiological differences between dmCA1 and FC, it is reasonable to worry about the possibility that the spiking of place cells recorded in FC might come from adjacent dmCA1 soma or neurites (Leutgeb et al., 2007; GoodSmith et al., 2017). In this case, the different quantitative firing properties such as firing rate and spatial information of FC and dmCA1 are explained by intra-CA1 variance, while qualitative physiological properties such as response to sharp-wave ripples remained. To confirm the possibility, the existence of sharp-wave ripples (SWRs) and outburst activity of cells were examined during SWR, which are outstanding physiological properties of CA1 during a resting session. In dmCA1, strong and noticeable ripple and outburst activity during the ripple period of CA1 place cells were observed (Figure 28) as reported (O'Keefe and Nadel, 1978; Buzsaki, 1986, 2015). About the LFP and cellular activity of FC place cell, however, the ripple events were sparse and weak, and cells seemed to respond weakly for ripple events (Figure 28). In quantitative comparison, the ripple power of FC showed significantly lower than dmCA1 and dCA1 but similar to CC, suggesting that the ripple might due to volume conductive signal (Figure 28.E). The SWR-outburst rate, which is the ratio of in-SWR firing rate and out-SWR firing rate, the place cells showed significantly less than dmCA1 and dCA1, suggesting that the characteristics of FC are qualitatively, as well as quantitatively, different from CA1 areas (Figure 28). In conclusion, the place cells recorded in FC were not an illusion of spikes from CA1 regions but were from FC. However, it should be also noticed that despite significant low SWR-outburst rate, compared to the CA1 region, the discharge rate in the ripple period was higher about twice than in the out-ripple period in FC, suggesting FC also was affected by ripple from the indirect way such as volume conduction or EC projection.

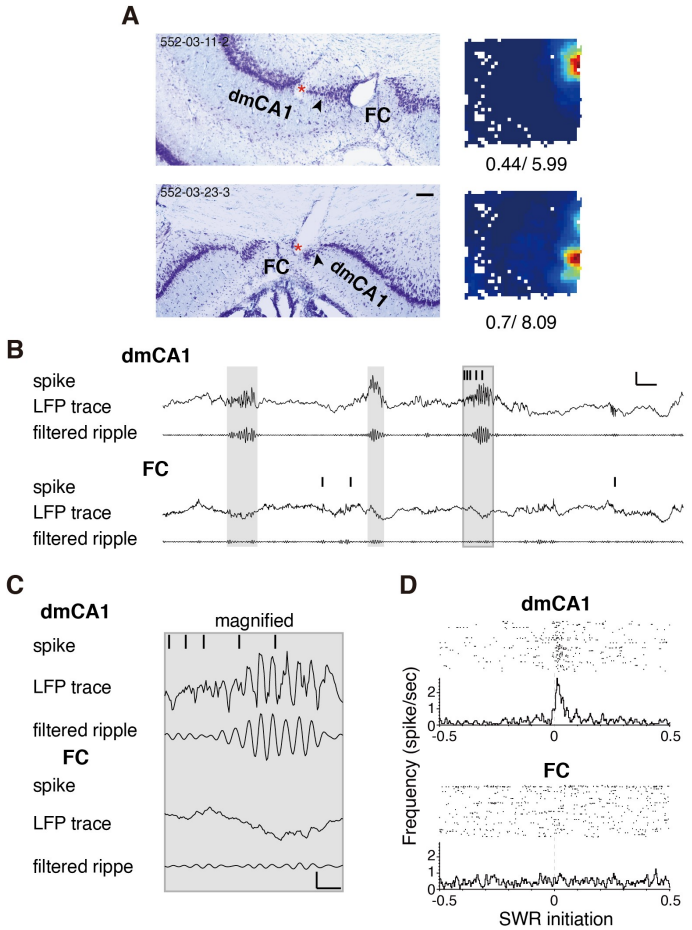
A
552-03-11-2
dmCA1
FC
0.44/ 5.99
552-03-23-3
FC
dmCA1
0.7/ 8.09
B
dmCA1
spike
LFP trace
filtered ripple
FC
spike
LFP trace
filtered ripple
C
dmCA1
magnified
spike
LFP trace
filtered ripple
FC
spike
LFP trace
filtered rippe
D
dmCA1
Frequency (spike/sec)
2
1
0
-0.5
0
0.5
FC
SWR initiation
E
whole TT
TT with PC
PC activity in SWR
SWR power (dB)
-20
-30
-40
***
FC
dmCA1
dCA1
CC
SWR outburst ratio
16
8
0

**Figure 28. SWR and single-unit response** (A) The histological verification for tetrode locations and firing rate maps in simultaneously recorded cells in both dmCA1 (*upper*) and FC (*lower*). The upper left characters in histology denote the single unit ID. The red asterisks denote the recording location. The numbers below the firing rate map indicate mean firing rate and peak firing rate. The scale bar denotes 0.1 mm. (B) Spike train and LFP trace for both units in (A) during the resting session after the foraging experiment. The raw LFP trace and band-pass filtered LFP (range: 150-250 Hz) are presented. The gray zones indicate the SWR period. The vertical and horizontal scale bar denotes 400 μv and 50 ms. (C) The enlarged figure of the last SWR event in (B). The vertical and horizontal scale bars denote 200 μv and 100 ms. (D) A peri-event time histogram (PETH) and raster plot (PETR) aligned to SWR onset timing for the representative cells presented in (A) and (B) are displayed. (E) Statistical results for population ripple power and outburst ratio are shown. Averaged ripple power recorded in all tetrodes located in each area (*left*) and the tetrodes recording place cells (PC, *center*). The SWR outburst ratio is defined as the average firing rate in the SWR period divided by the average firing rate out of ripple events. (*$p<0.05$, **$p < 0.01$, ***$p<0.001$).

In the previous chapter, it was revealed that FC is important for contextual learning and fast detection of contextual change. How can this structure be involved in learning, especially for contextual learning? In order to reveal how the FC represent contextual cue and respond to contextual change, I recorded FC single units to investigate how the cells of FC coded contextual information (Figure 29). During presenting the context as A-B-A' block on the screen front of T-maze, a rat was shuttling back and forward, and the responses of the cells were observed. The three experiments were conducted:

1) The reward comes from the same location regardless of the scene with old scenes (Figure 29.B).

2) The same as the first experiment except presenting novel scene (Figure 29.C)

3) Reward located altered by a scene on the monitor in each block (Figure 29.D)

In these experiments, however, I observed that the place cell in this task responded to the place and time interaction (Figure 29.A-D). For example, the cell in Figure 29.A is place cell apparently. However, the responses to the same scenes (block 1 and –block 3) were hugely different. Some cells showed sudden global remapping, showing a presence, absence, or location changing and maintained for several ten minutes (Figure 29.A-D). Some showed global remapping when the scene was changed, while others not. Even the cells which responded to the changing scene did not show a similar firing pattern between the same scenes (block 1 and block 3). This dissimilarity of representation between the same scenes was also observed statistically (Figure 29.E). Even in a familiar scene alternation task, the firing patterns in both the same scenes showed lower rate map similarity than that of a completely different block 1-block 2 scene pairs. In order to check whether the unstable place field is due to the change of unstable cluster, I looked at the waveform at the resting session before and after the experiment, but no difference was observed (Figure 29.A). Taken together, the result suggests that FC does not store a representation for a context even though it maintains the representation for a while.

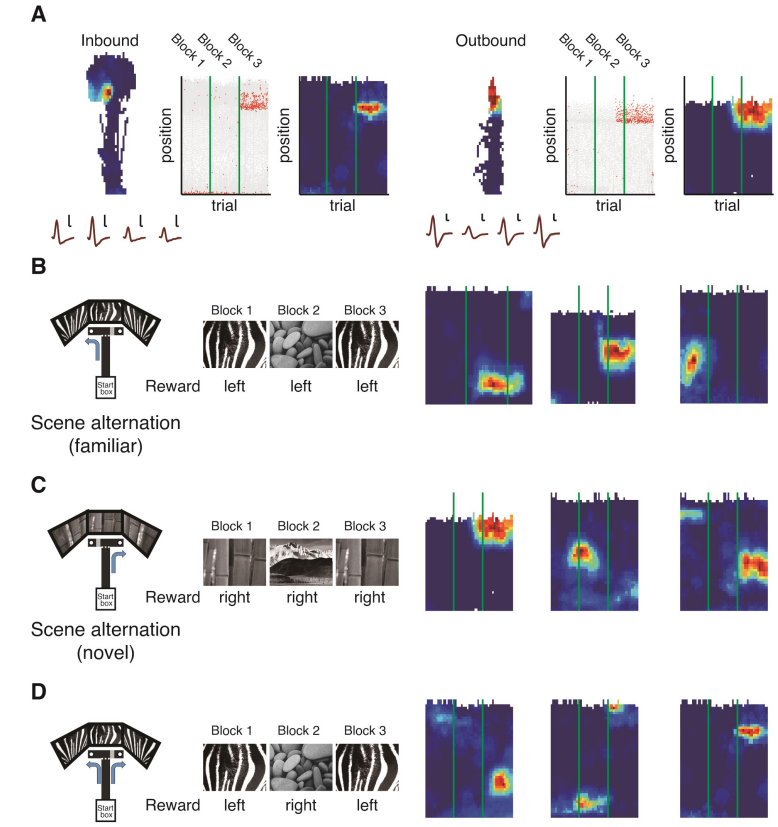
A
Inbound
Block 1
Block 2
Block 3
position
trial
Outbound
B
Block 1
Block 2
Block 3
Start box
Reward
left
left
left
Scene alternation
(familiar)
C
right
right
right
Scene alternation
(novel)
D
left
right
left
Scene-place alternation

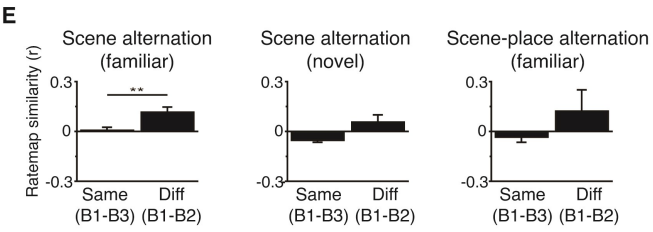
E
Scene alternation
(familiar)
Scene alternation
(novel)
Scene-place alternation
(familiar)
Ratemap similarity (r)
0.3
0
-0.3
**
Same
(B1-B3)
Diff
(B1-B2)

**Figure 29. FC place cells showed global remapping regarding or regardless of contextual cue change and did not rescued** (A) Representative rate maps and spike maps of global remapping. The reward location and contextual scene on the monitor were identical in block 1 and block 3 while the contextual scene was changed in block 2. Each block was separately presented by a green vertical line. The overall 2D rate map in inbound or outbound are represented left and the trial-position spike map and rate map is presented to the center and right. To confirm the stability of the unit, the average spikes of each tetrode channel on before and after sleep sessions are presented below 2D rate map (gray: pre-sleep, brown: post-sleep) Horizontal scale bars denote 0.1 ms while vertical scale bar denotes 100μV. Note that the left cell showed global remapping right next to the change of the contextual scene while the right cell changed during the second block. Also, note that the place field maintained for a moment, while did not replicate in the same conditions (block 1 and block 3). (B-D) three different tasks and representative firing patterns. The reward location and used scenes for blocks are presented left while trial-position rate maps are presented right. As described above, the place cells showed global remapping regarding or regardless of block change and tasks. (E) Statistical comparison between the same conditions (Same) and the different conditions (Diff). Note that the rate map similarity between the same conditions never higher than different conditions, suggesting that FC did not rescue the representation about context or context-associated place after global remapping. (*$p<0.05$, **$p < 0.01$, ***$p<0.001$).

**Table 6. Statistical results of the electrophysiology experiment (Square field).**Asterisks in the p-value column indicate statistical significance. Bonferroni correction was conducted (corrected alpha = 0.166). Values represent Mean ± S.E.M. AVG = average.

| Measurement | FC | dmCA1 | dCA1 | F | df | p-value | FC/dmCA1 | FC/dCA1 | dmCA1/dCA1 |
|---|---|---|---|---|---|---|---|---|---|
| Spike width (μs) | 312.9±6.8 | 381.9±3.5 | 397.0±5.9 | 40.8 | 2, 311 | P<0.0001* | P<0.0001* | P<0.0001* | P=0.0171 |
| Burst index | 21.8±2.2 | 25.0±1.6 | 21.5±2.5 | 1.0 | 2, 311 | P=0.3697 | | | |
| Firing-rate (sleep, Hz) | 0.47±0.08 | 0.56±0.04 | 0.70±0.07 | 2.765 | 2, 311 | P=0.0645 | | | |
| AVG. firing rate (square field, Hz) | 0.50±0.07 | 0.85±0.06 | 0.89±0.09 | 3.740 | 2, 311 | P=0.0248* | P=0.0140* | P=0.0086* | P=0.6433 |
| Peak firing rate (Hz) | 3.86±0.46 | 6.21±0.35 | 6.51±0.481 | 5.414 | 2, 311 | P=0.0049* | P=0.0030* | P=0.0017* | P=0.5981 |
| Spatial information (Bits/Spike) | 0.94±0.06 | 1.20±0.05 | 1.23±0.06 | 4.170 | 2, 311 | P=0.0163* | P=0.0094* | P=0.0056* | P=0.6316 |
| Spatial coherence | 0.35±0.03 | 0.49±0.02 | 0.53±0.03 | 9.581 | 2, 311 | P<0.0001* | P=0.0004* | P<0.0001* | P=0.1523 |
| Stability | 0.57±0.04 | 0.64±0.02 | 0.62±0.03 | 0.820 | 2, 311 | P=0.4414 | | | |
| Number of field | 1.45±0.11 | 1.51±0.06 | 1.39±0.07 | 0.920 | 2, 311 | P=0.3997 | | | |
| Field size ($cm^2$) | 640.9±61.6 | 699.7±33.6 | 759.8±47.6 | 1.126 | 2,455 | P=0.3253 | | | |
| In-field firing rate (Hz) | 1.58±0.17 | 2.53±0.12 | 2.78±0.20 | 7.217 | 2,455 | P=0.0008* | P=0.0014* | P=0.0002* | P=0.2544 |

**Table 7. Statistical result of the electrophysiological experiment (SWR).**

Asterisks in the p-value column indicate statistical significance. Bonferroni correction was conducted (corrected alpha is 0.008 for ripple power comparison and 0.166 for outburst ratio). Note that rows and columns are transposed, comparing to Table 6. Values represent Mean ± S.E.M. AVG = average.

| Measurement | SWR power (dB) (All tetrodes) | SWR power (dB) (TT with PC only) | SWR outburst ratio |
|---|---|---|---|
| FC | -36.437±0.335 | -35.145±0.499 | 2.234±0.194 |
| dmCA1 | -28.340±0.353 | -26.176±0.563 | 11.144±0.747 |
| dCA1 | -29.466±0.299 | -26.525±0.346 | 13.805±1.708 |
| CC | -35.922±0.319 | -35.922±0.319 | - |
| F | 146.850 | 132.472 | 13.447 |
| df | 3,587 | 3,292 | 2,247 |
| p-value | P<0.0001* | P<0.0001* | P<0.0001* |
| FC/dmCA1 | P<0.0001* | P<0.0001* | P<0.0001* |
| FC/dCA1 | P<0.0001* | P<0.0001* | P<0.0001* |
| FC/CC | P=0.3776 | P=0.3838 | - |
| dmCA1/dCA1 | P=0.0117 | P=0.6556 | P=0.0883 |
| dmCA1/CC | P<0.0001* | P<0.0001* | - |
| dCA1/CC | P<0.0001* | P<0.0001* | - |
| Ourburst ratio compared to chance (chance = 1) | | | |
| FC | | | t(34) = 6.3, P<0.0001* |
| dmCA1 | | | t(127) = 13.6, P<0.0001* |
| CA1 | | | t(86) = 86, P<0.0001* |

**Table 8. Statistical result of the electrophysiological experiment (T-maze)** A comparison between correlation coefficient (r) that indicate the similarity between rate maps are described in the table. Asterisks in the p-value column indicate statistical significance. Values represent Mean ± S.E.M. AVG = average.

| Scene alternation (familiar) | |
|---|---|
| #Place cell in FC | 21 |
| Block 1 – Block 3 (same) | 0.007±0.017 |
| Block 1 – Block 2 (diff.) | 0.115±0.031 |
| Statistics | t(18) = -3.660, P=0.0018* |
| | |
| Scene alternation (novel) | |
| #Place cell in FC | 8 |
| Block 1 – Block 3 (same) | -0.053±0.013 |
| Block 1 – Block 2 (diff.) | 0.057±0.044 |
| Statistics | t(7) = -2.196, P = 0.0641 |
| | |
| Scene-place alternation | |
| #Place cell in FC | 5 |
| Block 1 – Block 3 (same) | -0.035±0.032 |
| Block 1 – Block 2 (diff.) | 0.121±0.129 |
| Statistics | t(4) = -1.145, P = 0.3162 |

# Discussion

### The physiological border between CA1 and FC

In this experiment, a significant difference was found between FC and dmCA1 place cells, but no difference was found between dmCA1 and distal CA1 (dCA1). Place cells were found in all of the subregions as reported in other hippocampal subregions (O'Keefe and Dostrovsky, 1971; Jung and McNaughton, 1993; Lee and Kesner, 2004b; Leutgeb et al., 2004; Mankin et al., 2015; GoodSmith et al., 2017). However, the spike width of place cell in FC was narrower than in CA1 areas (dmCA1 and dCA1), and the spatial information and firing rate (both average rate and peak firing rate) were significantly lower than CA1 areas. Also, strong sharp-wave ripples (SWR) and corresponding activity of place cells were observed in CA1 areas, while only weak power in the frequency band and inconsistent activity of place cells were detected in FC. These physiological characteristics suggested that FC is a physiologically distinct area, comparing to adjacent CA1, and the anatomical boundary and physiological boundary were agreed upon.

### Place information in FC

There are some points to be addressed about the physiological properties of FC. First, there were place cells in FC. O'Keefe and Nadal claimed that cognitive map is constructed in the hippocampus and the existence of place cell was the critical basis of the theory (O'Keefe and Nadel, 1978). Because the place is one of the critical components of episodic memory, the discovery of place cell in FC suggested that FC might have a critical role in episodic memory (Nyberg et al., 1996; Tulving, 2002). However, in a theoretical view, spatial information in the hippocampus comes from spatial pathways including POR and MEC, while non-spatial information comes from non-spatial pathways including PER and LEC (Burwell and Amaral, 1998; Hargreaves et al., 2005; Eichenbaum et al., 2007). In this study, however, it is found

that place cells in FC that got information from the non-spatial pathway (PER and LEC) represented spatial information by showing place fields. How the place cells exist in the FC?

The first simple explanation for the incongruence between theoretical view and this study is that MEC labeling after retrograde tracer injection was overlooked in this study. In a previous study, it was described that degenerations of synaptic terminals in FC were observed after contralateral EC lesion and ipsilateral MEC lesion, suggesting a synaptic connection between MEC and FC (Zimmer and Hjorth-Simonsen, 1975), despite no presentation of evidence of MEC projection. To confirm the projection, a precise further anatomical study is needed.

On the other hand, it is possible that the conventional spatial pathway model is not an accurate model for the MTL information stream. Several studies suggested that even though MEC sends its rich spatial information to the hippocampus, it seems not to be the only source of the spatial information (Fyhn et al., 2004; Hafting et al., 2005; Sargolini et al., 2006; Solstad et al., 2008; Kropff et al., 2015). For example, it is reported that the rat with extensive MEC lesion had place cells in the hippocampus as control rats while the disruption of place information was restricted, while both LEC and MEC lesion impaired spatial representation in the hippocampus (Brun et al., 2008; Hales et al., 2014). Also, the MEC-lesion rats did not show impairment of object displacement task, which is a hippocampus-dependent task and require allocentric spatial recognition (Barker and Warburton, 2011). In addition, in LEC, object location, a trace of object location, and object vector information in the egocentric frame was found (Deshmukh and Knierim, 2011; Lu et al., 2013; Tsao et al., 2013; Wang et al., 2018). These researches suggested that place information in FC might be retrieved from other structures such as LEC as well as MEC. In addition, a recent anatomical connection study revealed that the projection from POR to MEC is weak and did not project to dorsomedial MEC where grid cells were found. Instead,

POR sends its strong projection to LEC, which shakes a critical base of the spatial and non-spatial pathway theory (Doan et al., 2019).

In conclusion, the observed spatial information in FC is possibly derived from LEC.

**Unfavorable characteristics of FC for memory consolidation**

It is noteworthy that FC showed only week power in the ripple band (150-250Hz), and the cells in the region showed less activity than CA1. It is known that sharp-wave ripple (SWR) occurs in CA3 (and some in CA2) of the hippocampus and migrate to CA1 and DG (Buzsaki, 2015; Oliva et al., 2016; Swaminathan et al., 2018). Therefore, SWR is observed in all the subfields of the hippocampus. However, FC is exceptional. The small ripple power observed in the FC was not different from the power from the CC, and the reactivity of cells in the FC showed an only small increase during the ripple events, comparing to neighboring CA1, suggesting the possibility that it was just volume conducted signal or came from indirect pathway via LEC. This is probably because FC does not have an intrahippocampal afferent connection to supply ripple signal. Considering that the SWR in the hippocampus is important for memory consolidation, the lack of ripple in the FC makes an unfavorable environment for synaptic plasticity (Buzsaki, 2015). RGS14 which is expressed in FC and CA2 also has a role in blocking the synaptic plasticity. It is reported that synaptic plasticity of the synapse between CA2 pyramidal neuron and Schaffer collateral which is a projection from CA3 did not occur in normal mice, while it was possible in RGS14 knock-out mice (Lee et al., 2010). Meanwhile, synaptic modification between both the perforant pathway and *temporo-ammonic* and CA2 is possible in normal mice, suggesting the gene block a specific synaptic modification (Caruana et al., 2012). Putting this information together, the pieces of evidence suggested a possibility that this small area (FC) might not be the major structure where the formation of memory takes place. This possibility was supported

by shuttling tasks with scene alternations. In the tasks, FC place cells do not code the scene itself despite some cells showed remapping followed by scene changes. In this case, it needed to be checked whether the cell code represents the scene itself, or the scene in the temporal context, or the amount of change. It was reported that hippocampus place cells code the same visual scene or object configuration differently when different cues presented together change (Park and Lee, 2016; Lee et al., 2018).

In other cases, the trigger, which made the cells remap, is unknown and it might be uncontrolled factors such as fatigue, scanning, satiety, accumulated experience, or continuously variable input from LEC (Caruana et al., 2012; Tsao et al., 2018). The position of place field in FC lasted for a moment and suddenly changed to another location, disappeared, or appeared, meaning FC did not store a representation of context and place for a long time. Are these cells able to help contextual learning?

**Again Marr: FC can help orthogonal representation in DG**

Before answering these questions, it is necessary to see how DG works in learning.

1) DG has representations of contexts and places and maintained even for days (Liu et al., 2012; Neunuebel and Knierim, 2014; GoodSmith et al., 2017; Hainmueller and Bartos, 2018; GoodSmith et al., 2019).

2) Synaptic plasticity occurs between DG and PP (Lomo, 1971; Moser et al., 1993; Cunningham et al., 1996).

3) Sparse coding is maintained through feedback inhibition (or lateral inhibition) of neurons (Sloviter and Brisman, 1995; Kesner and Rolls, 2015).

4) DG show orthogonal representations, or pattern separation, even when the inputs are similar (Marr, 1971; Mcnaughton and Morris, 1987; Treves and Rolls, 1992; O'Reilly and McClelland, 1994; Treves and Rolls, 1994; GoodSmith et al., 2017).

Before address FC, it should be addressed that some computational model considered DG as a just pattern separator for memory acquisition in hippocampal CA3, and some lesion studies supported the idea by reporting the intact behavioral performance during retrieval but impaired in acquisition after DG lesion (Treves and Rolls, 1992; Lee and Kesner, 2004a; Ahn and Lee, 2014). However, this theoretical prediction and physiological pieces of evidence, suggesting DG is important for acquisition but not for retrieval, did not gainsay that DG store memory representation (Lee and Jung, 2017). The stable representation in DG is caused by synaptic plasticity between PP and DG by non-linearity in the NMDA receptors and competitive feedback inhibition, which help not only orthogonal and sparse but also stable stimulation to output area (CA3) during learning (Kesner and Rolls, 2015).

The discrete change and random-like activity of FC cells might be helpful for the orthogonalization, or pattern separation of DG. The orthogonal representation of DG is largely explained from two perspectives. The first point of view from David Marr suggests that the number of DG cells is higher than that of EC cells that send inputs to the DG (Marr, 1971). Therefore, sparse coding may occur in DG. The second aspect is that sparse coding by feedback inhibition and synaptic change between the perforant pathway and DG can create an orthogonal representation (Kesner and Rolls, 2015). The two seem similar in support of the orthogonal representation, but there are significant differences.

Before describing the model in Figure 30, some definitions of terms, which used in the model, should be introduced.

- Input: a pattern of stimulation for DG granule cell from the perforant pathway. For convenience, however, the input is not defined by the source, but patterns of net EPSP and candidates of each unit in the model when not considering synaptic change by potentiation.

- Representation: a subset of units (granule cells) that represent an input. In the model in Figure 30 and Figure 31, the number of units for representation is hypothesized as three.
- Candidates: a group of units that have a potential to be a representation. In the model the potential means sufficient net EPSP (excitatory postsynaptic potential) above an arbitrary threshold that a granule cell makes action potential. It is hypothesized that the probability to be selected as a representation of each unit in the candidate is the same if a representation for the input is not yet established. It is hypothesized that if representation for the input is established, the cell will be selected and activated again.
- Similar inputs: the inputs whose candidates are largely overlapped.
- Orthogonal representations: the representations that the cells included in the representations for inputs are unique.

In the model, what I suggest as a role of FC is to enlarge the pool of candidates by supply EPSP in random granule cells that not included in candidates due to insufficient EPSP. A scenario that explains how FC works is below.

Figure 30.A shows a procedure to make a representation by feedback inhibition and synaptic change for two inputs A and B. The graph shows 100 hypothetical DG granule cells (DG GCs) that respond to input A from the perforant pathway (PP). Cell 1 is the one that receives the least input and hardly spikes, while cell 100 is the cell that gets most excitatory input from input A. Because action potentials are probabilistic, it is not clear which cell will cause the spike on candidates, but once a few cells are activated, two major change will occur. The inhibitory interneurons in DG will inhibit others while NMDA receptors in active cells strengthen the synaptic weight between PP and representation in DG. These two factors cause sparse coding and help synaptic plasticity between PP related to input A and few activated DG GCs to be reselected with significantly higher probability than other cells when the same input comes in the future. Next, consider

the case where input B is similar to input A, but not equal. Although the responses of the cells are not the same as the input A, the input stimulates similar populations, and not much different group of cells would be among candidates for activation (overlapped inputs). In other words, Even though different cells could be selected in both representations due to the probabilistic spiking and lateral inhibition as mentioned above, the candidates would be overlapped when the stimulation source is only P.P.

However, if random excitatory input adds in DG, even if the input is contents free, it could change of candidate pools radically (Figure 30. B). If certain cells receive the excitatory input from FC that should have been excluded from candidates due to lack of excitatory input, the cells will have a possibility to make action potential. In this case, more cells can be recruited in candidates for input A than the pool of cells to be active only by PP. Besides, if the pool of candidates becomes large, the probability that the cells, which getting sufficient input from PP, are selected become relatively low, suggesting that the orthogonality of representation is maximized.

Furthermore, the cells in FC showed radical change to discrete pattern by time, suggesting that when another input B comes in, other cells can be stimulated by the FC and be included in the pool of candidate for input B. Thanks to these random-like and discrete pattern change of FC, the pool of candidates can be larger, supporting higher probability to be orthogonalized. The increasing size of the pool will help to make the orthogonal representation suggested by Marr (Marr, 1971).

Then what happens if the same input A comes back later, i.e. on retrieval (Figure 30.C). If FC stimulates the same cells as when input A, which came before, there should be no problem. Even when FC stimulates other cells, however, the representing cells may not be affected if the cells constructed synaptic weight strongly before as suggested in assumption. In this case, regardless of FC, the same

cells will be selected without being affected. Even if FC is lost, it may not be significantly affected.

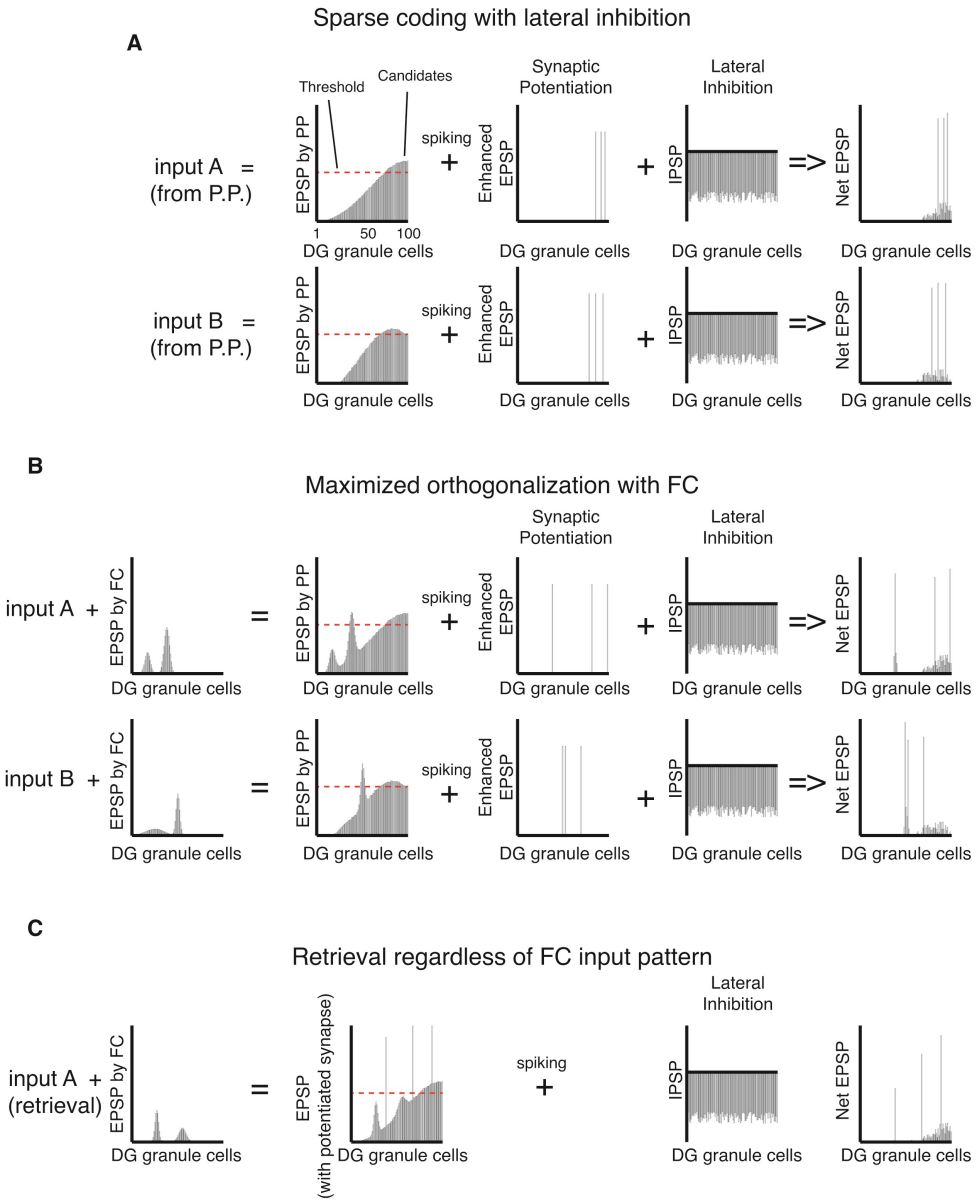
A
Sparse coding with lateral inhibition
input A =
(from P.P.)
Threshold
Candidates
EPSP by PP
1
50
100
DG granule cells
spiking
+
Synaptic
Potentiation
Enhanced
EPSP
Lateral
Inhibition
IPSP
=>
Net EPSP
input B =
(from P.P.)
B
Maximized orthogonalization with FC
input A +
EPSP by FC
=
input B +
C
Retrieval regardless of FC input pattern
input A +
(retrieval)
EPSP
(with potentiated synapse)

**Figure 30. Orthogonal representation in DG can be maximized by random FC input while not disturbing retrieval.** (A) The scenario that sparse coding occurred by lateral inhibition. In this scenario, the input is defined not as input itself, but a group of candidates who have a possibility to be selected to represent the inputs because their EPSP is above an arbitrary threshold. In this sense, the first graph shows the candidates of input A and B. The second and third graphs show two phenomena that occur as action potential (spike) arise and representation for the input is formed. The first one is synaptic plasticity to enhance the efficiency of the synapse between PP and DG. The second one is lateral inhibition which suppresses the firing of other cells in the surroundings and makes the representations exclusively firing. The final graph shows that if the same input comes again after the representation is formed, the cells that already form the representation can be reselected due to potentiated synapse. (B) This scenario is the same as (A), but FC input randomly supplies additional EPSP to DG. In this case, the pool of candidates can be large. Because of the randomized firing pattern of FC, a different group of cells can be included in the pool of candidates when different input (input B) occurred. Even though the enlargement of the candidate pool did not give a guarantee of orthogonal representation, it can make the possibility higher that orthogonal representations are formed for similar inputs. (C) This scenario shows that the same cells can be selected for representation even if FC gives input to a different set of cells when the same input A comes. When the EPSP supplied from FC is smaller than the input from the potentiated synapse, the representation can be maintained and the noise from FC can be discarded.

**Table 9. Numeric description of scenario in Figure 30.**

| | without FC | with FC | difference by |
|---|---|---|---|
| cells above threshold in A | 25 | 30 | 20.00% |
| cells above threshold in B | 27 | 32 | 18.52% |
| total cells above threshold | 30 | 40 | 33.33% |
| overlapped cells | 22 | 22 | 0.00% |
| overlap proportion of candidates(%) | 73.33% | 55.00% | -25.00% |
| representation of A* | 2,300 | 4,060 | 76.52% |
| representation of B* | 2,925 | 4,960 | 69.57% |
| Total representation pairs** | 6,727,500 | 20,137,600 | 199.33% |
| orthogonal representation pairs*** | 4,885,385 | 16,176,720 | 231.12% |
| orthogonal representation pairs(%) | 72.62% | 80.33% | 10.62% |
| overlap pairs | 1,842,115 | 3,960,880 | 115.02% |
| overlap pairs(%) | 27.38% | 19.67% | -28.17% |

* the size of a representation for input is 3 in the model.

** representation pair means the pair of representation for both A and B representation

*** orthogonal pair means the representation pair without shared cells for both A and B representation

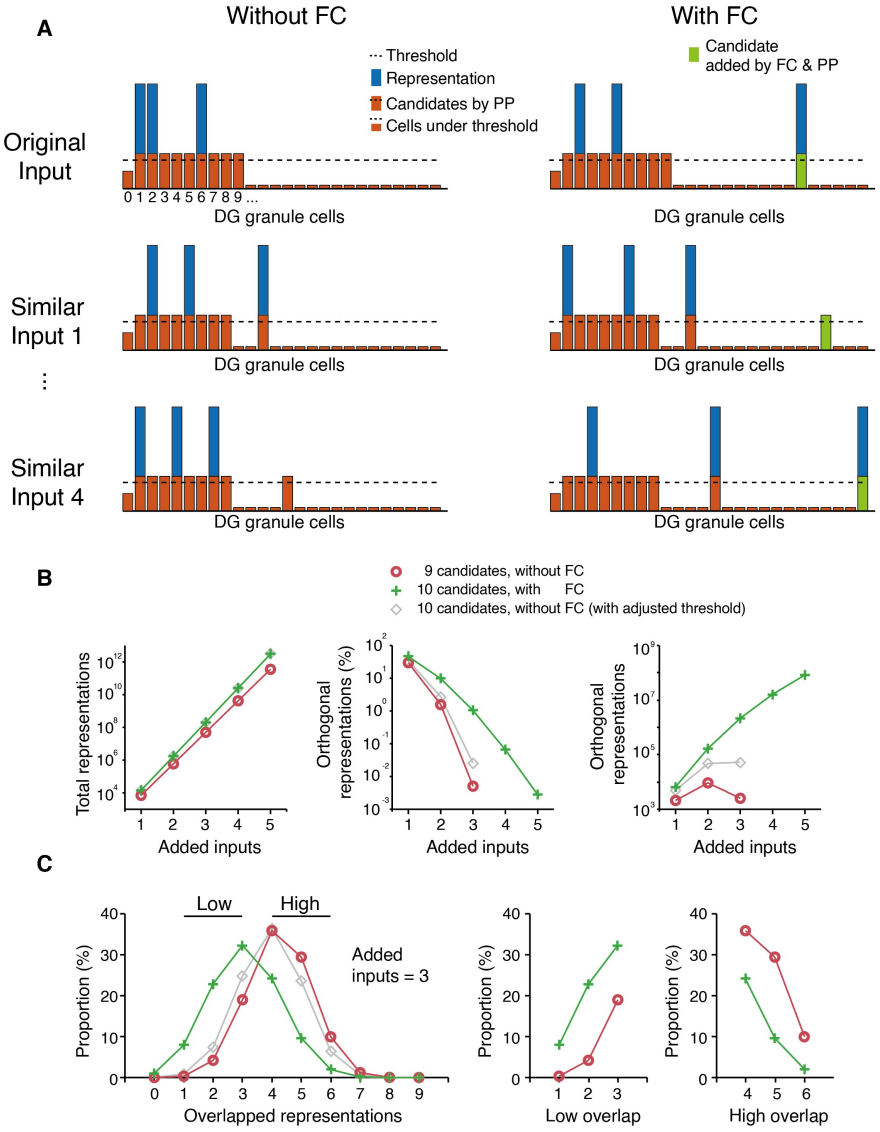
A
Without FC
With FC
Threshold
Representation
Candidates by PP
Cells under threshold
Candidate added by FC & PP
Original Input
Similar Input 1
Similar Input 4
0 1 2 3 4 5 6 7 8 9 ...
DG granule cells
B
9 candidates, without FC
10 candidates, with FC
10 candidates, without FC (with adjusted threshold)
Total representations
Orthogonal representations (%)
Orthogonal representations
Added inputs
C
Low
High
Added inputs = 3
Proportion (%)
Overlapped representations
Low overlap
High overlap

**Figure 31. FC has the advantage of reducing the overlap of representations between overlapped multi inputs.** A scenario with six largely overlapped but distinct inputs exist. In this scenario, nine cells are included in a candidate and three cells in the candidate are selected for representation. Only one cell is different from input and unique. In 'with FC' scenario (right), one cell is added to the candidate, so the candidate is ten in the scenario. For simplification, it is assumed that the additional candidates by PP input and FC & PP input are orthogonal. (B) Count of the combination for total representations, the proportion of orthogonal representations and orthogonal representations. The data is from the above multi-input scenario, but '10 candidates, without FC' scenario comes from a hypothetic scenario to match the number of the selected candidate by PP with 'with FC' scenario. In the last scenario, the additional cell is assumed that overlapped by input. The scenario assumes that more cells are included in the candidate due to the change of inhibition and excitation balance in DG (DG GC #0). (C) The proportion of overlapped representations in a case that 'added input' is three *(Left)*. If FC exists (green), the probability that the representations are separated is higher than 'without FC (Red and Gray)' ('Low' section in *Left*; *Center*). Also, the FC can reduce the probability that the representations are overlapped ('High section in *Left*; *Right*)

However, it should be considered if the model is practical. In the scenario suggested above the pool of both input A and B was increased by 33.33%, while the overlapped pair just decreased by 28.17% and the proportion of orthogonal representation is increased by 10.62% (Table 9) even though the number of orthogonal representation is increased to more than 3 times.

The impact of FC is maximized when largely overlapped multi-inputs need to be distinguished. Figure 31.A shows scenarios of overlapped multi inputs. In the scenario, it is assumed that the number of candidates for each input is nine, while eight of them are overlapped and one of them is orthogonal. The size of representation is three, while the number of cells that included in the candidate by FC stimulation is one (For calculation the number of the case, the cells added by FC in each input are assumed to be orthogonal). In this scenario, without FC, there is no orthogonal representation when additional input is more than three (Figure 31.B). With FC, however, the number of orthogonal representation exists and increased even when the largely overlapped input is added even though the proportion of orthogonal representation is decreased (Figure 31.B). What happens, if the size of the candidate increases without FC. For example, the modification of inhibition and excitation balance (I/E balance) can adjust the level of threshold and make the pool of candidates increase. In this case, however, the newly included cell could be tended to overlap with other candidates by other similar input, because it is recruited only by the similar PP input. In Figure 31.B the number of orthogonal cases and the proportion is shown (10 candidates, without FC. The number of candidates is matched to 'with FC' scenario and it is assumed that the newly included cell is the exactly same by inputs). If the number of candidates is matched to FC, the number of orthogonal representations in this scenario should be less than in the 'with FC' scenario due to its random and orthogonal recruitment. Also, as described in this scenario, if the threshold is lower due to weakening inhibition, the sparse coding in dentate gyrus could be impaired because it needs strong inhibition. It has a possibility

to impair the representations of downstream (Mcnaughton and Morris, 1987). The extensive lesion group in Chapter. 2 might be the case. If it is, this model predicts that the extensive lesion group will show impairment when it is required to separate many inputs.

Even though the representation is not orthogonal, the presence of FC can minimize the overlap of the representation in the scenario (Figure 31. C). Comparing to 'without FC', 'with FC' scenario shows a higher probability that overlaps between representations are the low and lower probability that representations for inputs are largely overlapped.

To sum up, if FC has an important role in a cognitive function, it could contribute to memory acquisition by increase the pool of candidates in DG but not to memory retrieval (Figure 32).

How does this principle explain the scene learning on T-maze presented above? Unfortunately, it is difficult to measure exactly what the input of the PP is, and it is not realistically possible to reproduce the same input of PP for experiments *in vivo*. However, it is reasonable to consider that the input from PP to the hippocampus have scene information with others (e.g. position, static room cues, internal state such as hunger, exhausting) because both source and target areas are important for scene-based learning and behavior (O'Keefe and Dostrovsky, 1971; Hirsh, 1974; Kim and Fanselow, 1992; Lee and Kesner, 2004b; Hafting et al., 2005; Brun et al., 2008; Barker and Warburton, 2011; Lu et al., 2013; Tsao et al., 2013; Ahn and Lee, 2014; Yoo and Lee, 2017). Inputs containing this scene information can enter the DG along with numerous other information. In this case, they may come in largely overlapped input, which can be orthogonalized by FC with the mechanism as shown earlier. Considering only the scene and position factor in the outbound direction, the number of inputs is crudely guessed. It is reported that the lateral inhibition lasts more than 150 ms (Sloviter and Brisman, 1995), suggesting a possibility that a representation lasts more than 150 ms and the next representation

will be presented after that. The average latency from the start box to the sensor front of the screen is 3.43 seconds, suggesting about 23 (=3.43/0.15) inputs make a representation in the stem, assuming that the duration of lateral inhibition is 150 ms (Figure 25.A). Suppose that the velocity of the rat is constant, and considering that the distance of the stem is 72 cm, the representation will last for 3.1 cm (=72 cm / 23) and changed. This series of representations is a possible basis of place field in DG granule cell.

Considering two scenes, 46 orthogonal representations for inputs are expected on the outbound stem. In this situation, FC might have a role in making orthogonal representation for each input. Also, this viewpoint suggests a link between spatial representation that the representation of memory is consists of a pool of active cells and global remapping that the change of external input is represented by moving, presence or absence of place field. They do not contradict in this viewpoint that global remapping is explained in a single cell for several inputs while spatial representation is explained by multi cells in an input (Kubie et al., 2019).

This model requires many assumptions. The assumptions include that.

- Projection from FC to DG gives net excitatory input to DG GCs.
- The input of FC is strong enough to affect the selection of the active candidates but weaker than the input from the potentiated synapse.
- FC will help synaptic potentiation between PP and DG GCs

It is also difficult to calculate how much FC affects orthogonalization quantitatively due to the lack of metric information. These points should be revealed in further studies. This model is meaningful in that it explains the role and operating principle of FC based on its anatomical and physiological evidence.

Lastly, the difference between the FC-DG model suggested in this chapter and the previous DG-CA3 model (Treves and Rolls, 1992). Even though both models have a common point that explains how upstream structure affect the

selection of cells for a representation, the working mechanisms are different. In the DG-CA3 model, DG gives a sparse, orthogonal and strong input to CA3, so the cells which receive both PP and mossy fiber input are selected for representation. In this case, the sparse and orthogonal input is possible due to a large pool and sparse coding in DG. Also, it is known that the mossy fiber input to CA3 decidedly makes pyramidal cells in CA3 active. In this case, the mossy fiber input should be reliable for a perforant pathway input, unless the representation of CA3 for input from the perforant pathway becomes unstable. The stable representation in DG was reported by empirical studies (Neunuebel and Knierim, 2014; Hainmueller and Bartos, 2018). In the FC-DG model, however, the pool of FC is small, and the representation of FC place cell showed unexpected change even when external cues are not changed. But, the model suggested that this change helps FC stimulate various cells in DG for the enlarging pool of candidates. In other words, FC conducts pattern separation in a temporal axis that stimulates a different subset of DG GCs for temporally distant similar inputs (or the same inputs) as well as different inputs, while DG conducts pattern separation in a spatial axis that select orthogonal subset of neurons for an input. Also, as described above, if FC decidedly activates DG GCs, it will cause catastrophic unstable representation in DG, following in CA3. However, it was reported that representation in DG for input is stable, suggesting the input from FC might not be strong to definitely activate DG GCs. Even though the FC stimulation did not guarantee pattern separation in DG, it will help to reduce overlap between representations for similar inputs by enlarging the pool of candidates (Figure 32).

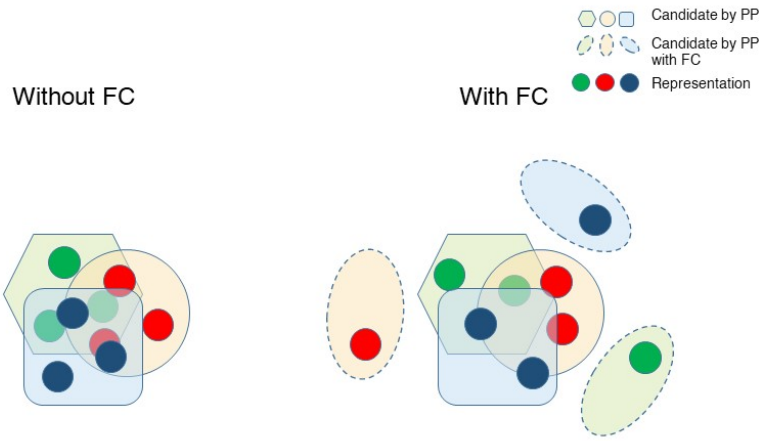


**Figure 32. The schematic diagram for representing the role of FC.** 'Without FC' scenario presents three largely overlapped inputs (left). In this case, the representations for each input have a possibility to be largely overlapped. 'With FC' scenario showed expanded candidate for each input by the stimulation of under threshold cells (right). The expanded candidates can reduce the probability of representation overlap.

# General discussion

In this study, I revealed several anatomical and physiological features and suggested a working model. Also, it was revealed that FC is important to perform various DG-dependent memory tasks, supporting the suggested model. In addition, the series of experiments suggest proper anatomical boundary between CA1 and FC based on various staining methods, anatomical connection, physiological properties, and colchicine sensitivity.

# Implication

This thesis has four important implications. The first one is that this thesis defines the lateral boundary of FC and identify anatomical and physiological features. Also, It revealed the cognitive functions of FC. It introduces a new connectional and functional circuit of the hippocampus that has not been known. In short, this thesis updates the anatomical and functional circuit of the hippocampus.

The second importance is that this thesis suggested a new neural mechanism. It is reported that firing patterns in some area in the brain looks continually changed. Until now, this has been proposed as time coding (Mankin et al., 2015; Tsao et al., 2018). However coding the time itself, rather than coding the interval from a particular temporal cue, is not available to the subject because the time does not come back. I think, the name ‘time coding’ comes from the point of view of experimenters who replay a neural activity of a particular time zone using a computer, which the subject never meet again and decode. In this thesis, I proposed a new concept that the firing pattern can increase the pool of candidates that could be selected for representation in downstream. Even though I suggested the model only for FC, the same mechanism might be noteworthy for the study of CA2 that show similar firing patterns.

The next importance is that in the FC lesion study, it is reported that the lesion group showed impaired memory acquisition after lesion surgery, but intact

memory retrieval. The symptom is similar to anterograde amnesia (Scoville and Milner, 1957). This suggests a possibility that the cause of some patients with anterograde amnesia is damaged FC. Until now, because it is not known that FC is important for learning, it has not been possible to inspect FC damage. This thesis is the first study to begin investigating and treating these patients.

Finally, there is a similarity between brain and neural network-based artificial intelligence models. For example, it is reported that convolution neural network model is inspired by single-cell recording from the visual cortex, and reinforcement learning is inspired by research into animal learning (Zhang et al., 2016; Hassabis et al., 2017). The perspective suggests that the discovery of new neural circuits and the presentation of new mechanisms of the brain will help the development of artificial intelligence as well as neuroscientists. In this sense, the discovery of FC circuit and the newly proposed working model will contribute greatly to the development of artificial intelligence.

# Limitation

Although the presented working model, explains the results of experiments from this study, it should be verified because the model was constructed too many assumptions.

Regarding the anatomical connection, a detailed study should be needed. For example, a part of the projection from the parahippocampal cortex to FC might be a long-range inhibitory projection. While this thesis and some previous studies showed the projection from LEC to FC (Hjorth-Simonsen, 1972; Hjorth-Simonsen and Laurberg, 1977; Li et al., 2017), the study of Basu and colleagues (Basu et al., 2016) showed a long-range inhibitory projection from LEC in FC in supplementary figure 8. Despite the effort, upwards spread in the tracing studies can not help making confusing noise. So, precise anatomical study and cross-check should be needed.

In *invivo* electrophysiology study, I found a discontinuous and sudden change of place field in a place cell. It is to be worthy of attention that how the discrete representations with sudden change appear and what makes it. Also, how the representation is maintained for a short time (from a few minutes to dozens of minutes) is repaid. In addition, it is necessary to verify whether the pool of candidates is actually expanded by FC.

In the lesion study, it should be noted that two rats in the lesion group with extensive FC lesion did not show impairment during memory acquisition. One possibility is that if the FC is completely ablated, the I/E balance of DG may have changed so that the remaining areas can cover to some extent for homeostasis (Ramirez and Stein, 1984; Baxter and Murray, 2001; Kim and Baxter, 2001; Lavenex et al., 2007; Otchy et al., 2015). So, it should be confirmed by further inactivation study, which does not affect the permanent change of I/E balance. In addition, the model predicts that the acceptable number of overlapping inputs and the amount of input overlapping of complete FC lesion group with permanently changed I/E balance to cover absent FC will be different from the control group (Figure 31.B-C, gray). This prediction needs to be checked in further study.

In the model, the role of FC is described as playing a role similar to a random number generator to enlarge the pool of candidates for representation without consideration of the contents in it. Although the model is designed to focus on the sudden changes of representations of FC place cells, it must not be overlooked that the FC is not an area that exhibits a content-free and random firing pattern. The presence of a place cell suggests that the cells code with allocentric references (Eichenbaum et al., 1999). The limitation of the model is that it does not reveal how such information is used downstream especially in DG.

In addition, it should be addressed that the validation of the model suggested in the thesis is challenging. The model predicts that if synaptic potentiation occurs, observation of a candidate for input may not be possible. There is a technical

difficulty in observing the subthreshold potential of DG multiunit simultaneously with blocking synaptic potentiation to see if the concept of candidate exists in a real brain. Also, the implementation of the parahippocampal cortex and hippocampus, including FC, on the artificial neural network model will be helpful to find out whether the model is practical for learning. If the model is correct, it will be possible to rescue the function of FC by stimulating DG as FC does, which stimulates a variety of cells by time and change of external input with proper strength.

Although the projection from FC to DG is double-checked, the area projected by FC is only the part of the septal tip in DG, which means the other most part in DG did not receive the projection of FC. It raises a question of whether the crest in the septal tip of DG has a specialized function for memory or not. For a better understanding of how DG works, the functional differences between the area where FC project and others in DG should be inspected in further study.

# Bibliography

Ahn JR, Lee I (2014) Intact CA3 in the hippocampus is only sufficient for contextual behavior based on well-learned and unaltered visual background. Hippocampus 24:1081-1093.

Ahn JR, Lee HW, Lee I (2019) Rhythmic Pruning of Perceptual Noise for Object Representation in the Hippocampus and Perirhinal Cortex in Rats. Cell reports 26:2362-2376 e2364.

Amaral DG, Dolorfo C, Alvarez-Royo P (1991) Organization of CA1 projections to the subiculum: a PHA-L analysis in the rat. Hippocampus 1:415-435.

Andersen P (2007) The hippocampus book. Oxford ; New York: Oxford University Press.

Arnold F (1838) Untersuchungen im Gebiete der Anatomie und Physiologie: mit besonderer Hinsicht auf seine anatomischen Tafeln: Höhr.

Aronov D, Nevers R, Tank DW (2017) Mapping of a non-spatial dimension by the hippocampal-entorhinal circuit. Nature 543:719-722.

Barker GRI, Warburton EC (2011) When Is the Hippocampus Involved in Recognition Memory? The Journal of Neuroscience 31:10721-10731.

Basu J, Zaremba JD, Cheung SK, Hitti FL, Zemelman BV, Losonczy A, Siegelbaum SA (2016) Gating of hippocampal activity, plasticity, and memory by entorhinal cortex long-range inhibition. Science 351:aaa5694.

Baxter MG, Murray EA (2001) Opposite relationship of hippocampal and rhinal cortex damage to delayed nonmatching-to-sample deficits in monkeys. Hippocampus 11:61-71.

Boccara CN, Kjonigsen LJ, Hammer IM, Bjaalie JG, Leergaard TB, Witter MP (2015) A three-plane architectonic atlas of the rat hippocampal region. Hippocampus 25:838-857.

Bokil H, Andrews P, Kulkarni JE, Mehta S, Mitra PP (2010) Chronux: a platform for analyzing neural signals. Journal of neuroscience methods 192:146-151.

Brinks H, Conrad S, Vogt J, Oldekamp J, Sierra A, Deitinghoff L, Bechmann I, Alvarez-Bolado G, Heimrich B, Monnier PP, Mueller BK, Skutella T (2004) The repulsive guidance molecule RGMa is involved in the formation of afferent connections in the dentate gyrus. The Journal of neuroscience : the official journal of the Society for Neuroscience 24:3862-3869.

Broadbent NJ, Squire LR, Clark RE (2004) Spatial memory, recognition memory, and the hippocampus. PNAS 101:14515-14520.

Brun VH, Leutgeb S, Wu HQ, Schwarcz R, Witter MP, Moser EI, Moser MB (2008) Impaired spatial representation in CA1 after lesion of direct input from entorhinal cortex. Neuron 57:290-302.

Burwell RD (2001) Borders and cytoarchitecture of the perirhinal and postrhinal cortices in the rat. Journal of Comparative Neurology 437:17-41.

Burwell RD, Amaral DG (1998) Cortical afferents of the perirhinal, postrhinal, and entorhinal cortices of the rat. The Journal of comparative neurology 398:179-205.

Buzsaki G (1986) Hippocampal sharp waves: Their origin and significance. Brain Research 398:242-252.

Buzsaki G (2015) Hippocampal sharp wave-ripple: A cognitive biomarker for episodic memory and planning. Hippocampus 25:1073-1188.

Callahan LS, Thibert KA, Wobken JD, Georgieff MK (2013) Early-life iron deficiency anemia alters the development and long-term expression of parvalbumin and perineuronal nets in the rat hippocampus. Dev Neurosci 35:427-436.

Canning KJ, Leung LS (1997) Lateral entorhinal, perirhinal, and amygdala-entorhinal transition projections to hippocampal CA1 and dentate gyrus in the rat: a current source density study. Hippocampus 7:643-655.

Caruana DA, Alexander GM, Dudek SM (2012) New insights into the regulation of synaptic plasticity from an unexpected place: hippocampal area CA2. Learning & memory 19:391-400.

Choi BY, Lee BE, Kim JH, Kim HJ, Sohn M, Song HK, Chung TN, Suh SW (2014) Colchicine induced intraneuronal free zinc accumulation and dentate granule cell degeneration. Metallomics : integrated biometal science 6:1513-1520.

Clark RE, Zola SM, Squire LR (2000) Impaired recognition memory in rats after damage to the hippocampus. Journal of Neuroscience 20:8853-8860.

Cunningham AJ, Murray CA, O'Neill LA, Lynch MA, O'Connor JJ (1996) Interleukin-1 beta (IL-1 beta) and tumour necrosis factor (TNF) inhibit long-term potentiation in the rat dentate gyrus in vitro. Neurosci Lett 203:17-20.

Dalley R, Ng L, Guillozet-Bongaarts A (2008) CA2 Pyramidal Layer. Nature Precedings.

Das GD (1971) Experimental studies on the postnatal development of the brain. I. Cytogenesis and morphogenesis of the accessory fascia dentata following hippocampal lesions. Brain Res 28:263-282.

Deshmukh SS, Knierim JJ (2011) Representation of non-spatial and spatial information in the lateral entorhinal cortex. Frontiers in behavioral neuroscience 5:69.

Doan TP, Lagartos-Donate MJ, Nilssen ES, Ohara S, Witter MP (2019) Convergent Projections from Perirhinal and Postrhinal Cortices Suggest a Multisensory Nature of Lateral, but Not Medial, Entorhinal Cortex. Cell reports 29:617-627 e617.

Dolorfo CL, Amaral DG (1998) Entorhinal cortex of the rat: topographic organization of the cells of origin of the perforant path projection to the dentate gyrus. The Journal of comparative neurology 398:25-48.

Duvernoy H, Cattin F, Risold P-Y (2013) Anatomy. In: The Human Hippocampus, pp 39-68. Berlin, Heidelberg: Springer Berlin Heidelberg.

Eichenbaum H, Yonelinas AP, Ranganath C (2007) The medial temporal lobe and recognition memory. Annual review of neuroscience 30:123-152.

Eichenbaum H, Dudchenko P, Wood E, Shapiro M, Tanila H (1999) The hippocampus, memory, and place cells: is it spatial memory or a memory space? Neuron 23:209-226.

Evans PR, Dudek SM, Hepler JR (2015) Regulator of G Protein Signaling 14: A Molecular Brake on Synaptic Plasticity Linked to Learning and Memory. Progress in molecular biology and translational science 133:169-206.

Fyhn M, Molden S, Witter MP, Moser EI, Moser MB (2004) Spatial representation in the entorhinal cortex. Science 305:1258-1264.

Gilbert PE, Kesner RP, Lee I (2001) Dissociating hippocampal subregions: double dissociation between dentate gyrus and CA1. Hippocampus 11:626-636.

Girard F, Venail J, Schwaller B, Celio MR (2015) The EF-hand Ca(2+)-binding protein super-family: a genome-wide analysis of gene expression patterns in the adult mouse brain. Neuroscience 294:116-155.

Goldschmidt RB, Steward O (1982) Neurotoxic effects of colchicine: differential susceptibility of CNS neuronal populations. Neuroscience 7:695-714.

GoodSmith D, Lee H, Neunuebel JP, Song H, Knierim JJ (2019) Dentate Gyrus Mossy Cells Share a Role in Pattern Separation with Dentate Granule Cells and Proximal CA3 Pyramidal Cells. The Journal of neuroscience : the official journal of the Society for Neuroscience 39:9570-9584.

GoodSmith D, Chen X, Wang C, Kim SH, Song H, Burgalossi A, Christian KM, Knierim JJ (2017) Spatial Representations of Granule Cells and Mossy Cells of the Dentate Gyrus. Neuron 93:677-690 e675.

Grieves RM, Wood ER, Dudchenko PA (2016) Place cells on a maze encode routes rather than destinations. Elife 5.

Hafting T, Fyhn M, Molden S, Moser MB, Moser EI (2005) Microstructure of a spatial map in the entorhinal cortex. Nature 436:801-806.

Hainmueller T, Bartos M (2018) Parallel emergence of stable and dynamic memory engrams in the hippocampus. Nature 558:292-296.

Hales JB, Schlesiger MI, Leutgeb JK, Squire LR, Leutgeb S, Clark RE (2014) Medial entorhinal cortex lesions only partially disrupt hippocampal place cells and hippocampus-dependent place memory. Cell reports 9:893-901.

Hargreaves EL, Rao G, Lee I, Knierim JJ (2005) Major dissociation between medial and lateral entorhinal input to dorsal hippocampus. Science 308:1792-1794.

Hassabis D, Kumaran D, Summerfield C, Botvinick M (2017) Neuroscience-Inspired Artificial Intelligence. Neuron 95:245-258.

Haug FM (1974) Light microscopical mapping of the hippocampal region, the pyriform cortex and the corticomedial amygdaloid nuclei of the rat with Timm's sulphide silver method. I. Area dentata, hippocampus and subiculum. Z Anat Entwicklungsgesch 145:1-27.

Hendrickson ML, Rao AJ, Demerdash ON, Kalil RE (2011) Expression of nestin by neural cells in the adult rat and human brain. PloS one 6:e18535.

Henriksen EJ, Colgin LL, Barnes CA, Witter MP, Moser MB, Moser EI (2010) Spatial representation along the proximodistal axis of CA1. Neuron 68:127-137.

Hill A (1895) IV. The fasciola cinerea; its relation to the fascia dentata and to the nerves of lancisi. Proceedings of the Royal Society of London 58:98-103.

Hirsh R (1974) The hippocampus and contextual retrieval of information from memory: a theory. Behav Biol 12:421-444.

Hjorth-Simonsen A (1972) Projection of the lateral part of the entorhinal area to the hippocampus and fascia dentata. The Journal of comparative neurology 146:219-232.

Hjorth-Simonsen A, Zimmer J (1975) Crossed pathways from the entorhinal area to the fascia dentata. I. Normal in rabbits. The Journal of comparative neurology 161:57-70.

Hjorth-Simonsen A, Laurberg S (1977) Commissural connections of the dentate area in the rat. The Journal of comparative neurology 174:591-606.

Huang CH, Chen CC, Siow TY, Hsu SH, Hsu YH, Jaw FS, Chang C (2013) High-resolution structural and functional assessments of cerebral microvasculature using 3D Gas DeltaR2*-mMRA. PloS one 8:e78186.

Humpel C, Lippoldt A, Chadi G, Ganten D, Olson L, Fuxe K (1993) Fast and widespread increase of basic fibroblast growth factor messenger RNA and protein in the forebrain after kainate-induced seizures. Neuroscience 57:913-922.

Hunsaker MR, Rosenberg JS, Kesner RP (2008) The role of the dentate gyrus, CA3a,b, and CA3c for detecting spatial and environmental novelty. Hippocampus 18:1064-1073.

Igarashi KM, Ito HT, Moser EI, Moser MB (2014) Functional diversity along the transverse axis of hippocampal area CA1. FEBS letters 588:2470-2476.

Itoh N, Yazaki N, Tagashira S, Miyake A, Ozaki K, Minami M, Satoh M, Ohta M, Kawasaki T (1994) Rat FGF receptor-4 mRNA in the brain is expressed preferentially in the medial habenular nucleus. Brain research Molecular brain research 21:344-348.

Jarrard LE (2002) Use of excitotoxins to lesion the hippocampus: update. Hippocampus 12:405-414.

Jinde S, Zsiros V, Jiang Z, Nakao K, Pickel J, Kohno K, Belforte JE, Nakazawa K (2012) Hilar mossy cell degeneration causes transient dentate granule cell hyperexcitability and impaired pattern separation. Neuron 76:1189-1200.

Jo YS, Lee I (2010) Disconnection of the hippocampal-perirhinal cortical circuits severely disrupts object-place paired associative memory. The Journal of

neuroscience : the official journal of the Society for Neuroscience 30:9850-9858.

Jung MW, McNaughton BL (1993) Spatial selectivity of unit activity in the hippocampal granular layer. Hippocampus 3:165-182.

Keck T, Toyoizumi T, Chen L, Doiron B, Feldman DE, Fox K, Gerstner W, Haydon PG, Hubener M, Lee HK, Lisman JE, Rose T, Sengpiel F, Stellwagen D, Stryker MP, Turrigiano GG, van Rossum MC (2017) Integrating Hebbian and homeostatic plasticity: the current state of the field and future research directions. Philosophical transactions of the Royal Society of London Series B, Biological sciences 372.

Kesner RP, Rolls ET (2015) A computational theory of hippocampal function, and tests of the theory: new developments. Neuroscience and biobehavioral reviews 48:92-147.

Kim JJ, Fanselow MS (1992) Modality-specific retrograde amnesia of fear. Science 256:675-677.

Kim JJ, Baxter MG (2001) Multiple brain-memory systems: the whole does not equal the sum of its parts. Trends in neurosciences 24:324-330.

Kjonigsen LJ, Leergaard TB, Witter MP, Bjaalie JG (2011) Digital atlas of anatomical subdivisions and boundaries of the rat hippocampal region. Front Neuroinform 5:2.

Kjonigsen LJ, Lillehaug S, Bjaalie JG, Witter MP, Leergaard TB (2015) Waxholm Space atlas of the rat brain hippocampal region: three-dimensional delineations based on magnetic resonance and diffusion tensor imaging. Neuroimage 108:441-449.

Kohara K, Pignatelli M, Rivest AJ, Jung HY, Kitamura T, Suh J, Frank D, Kajikawa K, Mise N, Obata Y, Wickersham IR, Tonegawa S (2014) Cell type-specific genetic and optogenetic tools reveal hippocampal CA2 circuits. Nature neuroscience 17:269-279.

Kreuzberg MM, Deuchars J, Weiss E, Schober A, Sonntag S, Wellershaus K, Draguhn A, Willecke K (2008) Expression of connexin30.2 in interneurons of the central nervous system in the mouse. Molecular and cellular neurosciences 37:119-134.

Kropff E, Carmichael JE, Moser MB, Moser EI (2015) Speed cells in the medial entorhinal cortex. Nature 523:419-424.

Kubie JL, Levy ERJ, Fenton AA (2019) Is hippocampal remapping the physiological basis for context? Hippocampus.

Laeremans A, Nys J, Luyten W, D'Hooge R, Paulussen M, Arckens L (2013) AMIGO2 mRNA expression in hippocampal CA2 and CA3a. Brain structure & function 218:123-130.

Langston RF, Wood ER (2010) Associative recognition and the hippocampus: differential effects of hippocampal lesions on object-place, object-context and object-place-context memory. Hippocampus 20:1139-1153.

Lavenex P, Lavenex PB, Amaral DG (2007) Spatial relational learning persists following neonatal hippocampal lesions in macaque monkeys. Nature neuroscience 10:234-239.

Lee HW, Lee SM, Lee I (2018) Neural Firing Patterns Are More Schematic and Less Sensitive to Changes in Background Visual Scenes in the Subiculum than in the Hippocampus. The Journal of neuroscience : the official journal of the Society for Neuroscience 38:7392-7408.

Lee I, Kesner RP (2004a) Encoding versus retrieval of spatial memory: double dissociation between the dentate gyrus and the perforant path inputs into CA3 in the dorsal hippocampus. Hippocampus 14:66-76.

Lee I, Kesner RP (2004b) Differential contributions of dorsal hippocampal subregions to memory acquisition and retrieval in contextual fear-conditioning. Hippocampus 14:301-310.

Lee I, Solivan F (2010) Dentate gyrus is necessary for disambiguating similar object-place representations. Learning & memory 17:252-258.

Lee I, Park SB (2013) Perirhinal cortical inactivation impairs object-in-place memory and disrupts task-dependent firing in hippocampal CA1, but not in CA3. Frontiers in neural circuits 7:134.

Lee I, Rao G, Knierim JJ (2004a) A double dissociation between hippocampal subfields: differential time course of CA3 and CA1 place cells for processing changed environments. Neuron 42:803-815.

Lee I, Hunsaker MR, Kesner RP (2005) The role of hippocampal subregions in detecting spatial novelty. Behav Neurosci 119:145-153.

Lee I, Yoganarasimha D, Rao G, Knierim JJ (2004b) Comparison of population coherence of place cells in hippocampal subfields CA1 and CA3. Nature 430:456-459.

Lee JW, Jung MW (2017) Separation or binding? Role of the dentate gyrus in hippocampal mnemonic processing. Neuroscience and biobehavioral reviews 75:183-194.

Lee KJ, Park SB, Lee I (2014) Elemental or contextual? It depends: individual difference in the hippocampal dependence of associative learning for a simple sensory stimulus. Frontiers in behavioral neuroscience 8:217.

Lee SE, Simons SB, Heldt SA, Zhao M, Schroeder JP, Vellano CP, Cowan DP, Ramineni S, Yates CK, Feng Y, Smith Y, Sweatt JD, Weinshenker D, Ressler KJ, Dudek SM, Hepler JR (2010) RGS14 is a natural suppressor of both synaptic plasticity in CA2 neurons and hippocampal-based learning and memory. Proceedings of the National Academy of Sciences of the United States of America 107:16994-16998.

Lein ES, Callaway EM, Albright TD, Gage FH (2005) Redefining the boundaries of the hippocampal CA2 subfield in the mouse using gene expression and 3-dimensional reconstruction. The Journal of comparative neurology 485:1-10.

Lein ES et al. (2007) Genome-wide atlas of gene expression in the adult mouse brain. Nature 445:168-176.

Leutgeb JK, Leutgeb S, Moser M-B, Moser EI (2007) Pattern Separation in the Dentate Gyrus and CA3 of the Hippocampus. Science 315:961-966.

Leutgeb JK, Leutgeb S, Treves A, Meyer R, Barnes CA, McNaughton BL, Moser MB, Moser EI (2005a) Progressive transformation of hippocampal neuronal representations in "morphed" environments. Neuron 48:345-358.

Leutgeb S, Leutgeb JK, Treves A, Moser M-B, Moser EI (2004) Distinct Ensemble Codes in Hippocampal Areas CA3 and CA1. Science 305:1295-1298.

Leutgeb S, Leutgeb JK, Barnes CA, Moser EI, McNaughton BL, Moser MB (2005b) Independent codes for spatial and episodic memory in hippocampal neuronal ensembles. Science 309:619-623.

Li N, Qiao M, Zhao Q, Zhang P, Song L, Li L, Cui C (2016) Effects of maternal lead exposure on RGMa and RGMb expression in the hippocampus and cerebral cortex of mouse pups. Brain Res Bull 127:38-46.

Li Y, Xu J, Liu Y, Zhu J, Liu N, Zeng W, Huang N, Rasch MJ, Jiang H, Gu X, Li X, Luo M, Li C, Teng J, Chen J, Zeng S, Lin L, Zhang X (2017) A distinct entorhinal cortex to hippocampal CA1 direct circuit for olfactory associative learning. Nature neuroscience 20:559-570.

Lippoldt A, Andbjer B, Rosen L, Richter E, Ganten D, Cao Y, Pettersson RF, Fuxe K (1993) Photochemically induced focal cerebral ischemia in rat: time dependent and global increase in expression of basic fibroblast growth factor mRNA. Brain Res 625:45-56.

Liu X, Ramirez S, Pang PT, Puryear CB, Govindarajan A, Deisseroth K, Tonegawa S (2012) Optogenetic stimulation of a hippocampal engram activates fear memory recall. Nature 484:381-385.

Lomo T (1971) Potentiation of monosynaptic EPSPs in the perforant path-dentate granule cell synapse. Exp Brain Res 12:46-63.

Lothman EW, Stein DA, Wooten GF, Zucker DK (1982) Potential mechanisms underlying the destruction of dentate gyrus granule cells by colchicine. Exp Neurol 78:293-302.

Lu L, Leutgeb JK, Tsao A, Henriksen EJ, Leutgeb S, Barnes CA, Witter MP, Moser MB, Moser EI (2013) Impaired hippocampal rate coding after lesions of the lateral entorhinal cortex. Nature neuroscience 16:1085-1093.

Mankin EA, Diehl GW, Sparks FT, Leutgeb S, Leutgeb JK (2015) Hippocampal CA2 Activity Patterns Change over Time to a Larger Extent than between Spatial Contexts. Neuron 85:190-201.

Marcus JN, Aschkenasi CJ, Lee CE, Chemelli RM, Saper CB, Yanagisawa M, Elmquist JK (2001) Differential expression of orexin receptors 1 and 2 in the rat brain. The Journal of comparative neurology 435:6-25.

Mark LP, Daniels DL, Naidich TP, Yetkin Z, Borne JA (1993) The hippocampus. AJNR American journal of neuroradiology 14:709-712.

Marr D (1969) A theory of cerebellar cortex. J Physiol 202:437-470.

Marr D (1971) Simple memory: a theory for archicortex. Philosophical transactions of the Royal Society of London Series B, Biological sciences 262:23-81.

Mattis J, Tye KM, Ferenczi EA, Ramakrishnan C, O'Shea DJ, Prakash R, Gunaydin LA, Hyun M, Fenno LE, Gradinaru V, Yizhar O, Deisseroth K (2011) Principles for applying optogenetic tools derived from direct comparative analysis of microbial opsins. Nature methods 9:159-172.

Mcnaughton BL, Morris RGM (1987) Hippocampal Synaptic Enhancement and Information-Storage within a Distributed Memory System. Trends in neurosciences 10:408-415.

Mehta MR, Quirk MC, Wilson MA (2000) Experience-dependent asymmetric shape of hippocampal receptive fields. Neuron 25:707-715.

Morris RG, Garrud P, Rawlins JN, O'Keefe J (1982) Place navigation impaired in rats with hippocampal lesions. Nature 297:681-683.

Moser E, Moser MB, Andersen P (1993) Synaptic potentiation in the rat dentate gyrus during exploratory learning. Neuroreport 5:317-320.

Muller RU, Kubie JL (1987) The effects of changes in the environment on the spatial firing of hippocampal complex-spike cells. The Journal of neuroscience : the official journal of the Society for Neuroscience 7:1951-1968.

Muller RU, Kubie JL (1989) The firing of hippocampal place cells predicts the future position of freely moving rats. The Journal of neuroscience : the official journal of the Society for Neuroscience 9:4101-4110.

Naber PA, Witter MP, Lopez da Silva FH (1999) Perirhinal cortex input to the hippocampus in the rat: evidence for parallel pathways, both direct and indirect. A combined physiological and anatomical study. The European journal of neuroscience 11:4119-4133.

Neunuebel JP, Knierim JJ (2014) CA3 retrieves coherent representations from degraded input: direct evidence for CA3 pattern completion and dentate gyrus pattern separation. Neuron 81:416-427.

Nilssen ES, Doan TP, Nigro MJ, Ohara S, Witter MP (2019) Neurons and networks in the entorhinal cortex: A reappraisal of the lateral and medial entorhinal subdivisions mediating parallel cortical pathways. Hippocampus 29:1238-1254.

Nyberg L, McIntosh AR, Cabeza R, Habib R, Houle S, Tulving E (1996) General and specific brain regions involved in encoding and retrieval of events: what, where, and when. Proceedings of the National Academy of Sciences of the United States of America 93:11280-11285.

O'Keefe J, Dostrovsky J (1971) The hippocampus as a spatial map: Preliminary evidence from unit activity in the freely-moving rat. Brain Res 34:171-175.

O'Keefe J, Nadel L (1978) The hippocampus as a cognitive map. Oxford: Clarendon Press.

O'Reilly RC, McClelland JL (1994) Hippocampal conjunctive encoding, storage, and recall: avoiding a trade-off. Hippocampus 4:661-682.

Ohara S, Sato S, Tsutsui K, Witter MP, Iijima T (2013) Organization of multisynaptic inputs to the dorsal and ventral dentate gyrus: retrograde trans-synaptic tracing with rabies virus vector in the rat. PloS one 8:e78928.

Oliva A, Fernandez-Ruiz A, Buzsaki G, Berenyi A (2016) Role of Hippocampal CA2 Region in Triggering Sharp-Wave Ripples. Neuron 91:1342-1355.

Otchy TM, Wolff SB, Rhee JY, Pehlevan C, Kawai R, Kempf A, Gobes SM, Olveczky BP (2015) Acute off-target effects of neural circuit manipulations. Nature 528:358-363.

Packard MG, McGaugh JL (1996) Inactivation of Hippocampus or Caudate Nucleus with Lidocaine Differentially Affects Expression of Place and Response Learning. Neurobiology of learning and memory 65:65-72.

Park EH, Ahn JR, Lee I (2017) Interactions between stimulus and response types are more strongly represented in the entorhinal cortex than in its upstream regions in rats. Elife 6.

Park SB, Lee I (2016) Increased Variability and Asymmetric Expansion of the Hippocampal Spatial Representation in a Distal Cue-Dependent Memory Task. Hippocampus 26:1033-1050.

Parkinson JK, Murray EA, Mishkin M (1988) A selective mnemonic role for the hippocampus in monkeys: memory for the location of objects. The Journal of neuroscience : the official journal of the Society for Neuroscience 8:4159-4167.

Pastalkova E, Itskov V, Amarasingham A, Buzsaki G (2008) Internally Generated Cell Assembly Sequences in the Rat Hippocampus. Science 321:1322-1327.

Paxinos G, Watson C (2009) The rat brain in stereotaxic coordinates: compact sixth edition: New York, NY: Academic Press.

Rajasethupathy P, Sankaran S, Marshel JH, Kim CK, Ferenczi E, Lee SY, Berndt A, Ramakrishnan C, Jaffe A, Lo M, Liston C, Deisseroth K (2015) Projections from neocortex mediate top-down control of memory retrieval. Nature 526:653-659.

Ramirez JJ, Stein DG (1984) Sparing and recovery of spatial alternation performance after entorhinal cortex lesions in rats. Behavioural brain research 13:53-61.

Rasmussen R, Jensen MH, Heltberg ML (2017) Chaotic Dynamics Mediate Brain State Transitions, Driven by Changes in Extracellular Ion Concentrations. Cell Syst 5:591-603 e594.

Rolls ET (2013) A quantitative theory of the functions of the hippocampal CA3 network in memory. Frontiers in cellular neuroscience 7:98.

Ruth RE, Collier TJ, Routtenberg A (1988) Topographical relationship between the entorhinal cortex and the septotemporal axis of the dentate gyrus in rats: II. Cells projecting from lateral entorhinal subdivisions. The Journal of comparative neurology 270:506-516.

Sargolini F, Fyhn M, Hafting T, McNaughton BL, Witter MP, Moser M-B, Moser EI (2006) Conjunctive Representation of Position, Direction, and Velocity in Entorhinal Cortex. Science 312:758-762.

Schmidtmer J, Engelkamp D (2004) Isolation and expression pattern of three mouse homologues of chick Rgm. Gene Expression Patterns 4:105-110.

Scoville W, B,, Milner B (1957) Loss of recent memory after bilateral hippocampal lesions. JNeurolNeurosurgPsychiatry 20:11-21.

Senzai Y, Buzsaki G (2017) Physiological Properties and Behavioral Correlates of Hippocampal Granule Cells and Mossy Cells. Neuron 93:691-704 e695.

Skaggs WE, McNaughton BL, Gothard KM, Markus EJ (1993) An information-theoretic approach to deciphering the hippocampal code. In: Advances in neural information processing systems 5. (Hanson SJ, Cowan JD, Giles CL, eds), pp 1030-1037. San Mateo, CA: Morgan Kaufmann.

Skaggs WE, McNaughton BL, Wilson MA, Barnes CA (1996) Theta phase precession in hippocampal neuronal populations and the compression of temporal sequences. Hippocampus 6:149-172.

Slomianka L, Amrein I, Knuesel I, Sorensen JC, Wolfer DP (2011) Hippocampal pyramidal cells: the reemergence of cortical lamination. Brain structure & function 216:301-317.

Sloviter RS, Brisman JL (1995) Lateral inhibition and granule cell synchrony in the rat hippocampal dentate gyrus. The Journal of neuroscience : the official journal of the Society for Neuroscience 15:811-820.

Solstad T, Boccara CN, Kropff E, Moser M-B, Moser EI (2008) Representation of Geometric Borders in the Entorhinal Cortex. Science 322:1865-1868.

Soltesz I, Losonczy A (2018) CA1 pyramidal cell diversity enabling parallel information processing in the hippocampus. Nature neuroscience 21:484-493.

Stephan H (1975) Allocortex. Berlin Heidelberg 1975: Springer, Berlin, Heidelberg.

Steward O (1976) Topographic organization of the projections from the entorhinal area to the hippocampal formation of the rat. The Journal of comparative neurology 167:285-314.

Sun Y, Nitz DA, Holmes TC, Xu X (2018) Opposing and Complementary Topographic Connectivity Gradients Revealed by Quantitative Analysis of Canonical and Noncanonical Hippocampal CA1 Inputs. eNeuro 5.

Swaminathan A, Wichert I, Schmitz D, Maier N (2018) Involvement of Mossy Cells in Sharp Wave-Ripple Activity In Vitro. Cell reports 23:2541-2549.

Swanson LW (2014) Neuroanatomical Terminology: a lexicon of classical origins and historical foundations: OUP Us.

Swanson LW (2018) Brain maps 4.0-Structure of the rat brain: An open access atlas with global nervous system nomenclature ontology and flatmaps. The Journal of comparative neurology 526:935-943.

Swanson LW, Wyss JM, Cowan WM (1978) An autoradiographic study of the organization of intrahippocampal association pathways in the rat. The Journal of comparative neurology 181:681-715.

Treves A, Rolls ET (1992) Computational constraints suggest the need for two distinct input systems to the hippocampal CA3 network. Hippocampus 2:189-199.

Treves A, Rolls ET (1994) Computational analysis of the role of the hippocampus in memory. Hippocampus 4:374-391.

Trimper JB, Galloway CR, Jones AC, Mandi K, Manns JR (2017) Gamma Oscillations in Rat Hippocampal Subregions Dentate Gyrus, CA3, CA1, and Subiculum Underlie Associative Memory Encoding. Cell reports 21:2419-2432.

Tsao A, Moser MB, Moser EI (2013) Traces of experience in the lateral entorhinal cortex. Current biology : CB 23:399-405.

Tsao A, Sugar J, Lu L, Wang C, Knierim JJ, Moser MB, Moser EI (2018) Integrating time from experience in the lateral entorhinal cortex. Nature 561:57-62.

Tulving E (2002) Episodic memory: from mind to brain. Annu Rev Psychol 53:1-25.

Tzakis N, Holahan MR (2019) Social Memory and the Role of the Hippocampal CA2 Region. Frontiers in behavioral neuroscience 13:233.

Van Cauter T, Camon J, Alvernhe A, Elduayen C, Sargolini F, Save E (2013) Distinct roles of medial and lateral entorhinal cortex in spatial cognition. Cerebral cortex 23:451-459.

van den Heuvel DM, Hellemons AJ, Pasterkamp RJ (2013) Spatiotemporal expression of repulsive guidance molecules (RGMs) and their receptor neogenin in the mouse brain. PloS one 8:e55828.

Vazdarjanova A, Guzowski JF (2004) Differences in hippocampal neuronal population responses to modifications of an environmental context: evidence for distinct, yet complementary, functions of CA3 and CA1

ensembles. The Journal of neuroscience : the official journal of the Society for Neuroscience 24:6489-6496.

Vigers AJ, Baquet ZC, Jones KR (2000) Expression of neurotrophin-3 in the mouse forebrain: insights from a targeted LacZ reporter. The Journal of comparative neurology 416:398-415.

Vivar C, Potter MC, Choi J, Lee JY, Stringer TP, Callaway EM, Gage FH, Suh H, van Praag H (2012) Monosynaptic inputs to new neurons in the dentate gyrus. Nature communications 3:1107.

von Heimendahl M, Rao RP, Brecht M (2012) Weak and nondiscriminative responses to conspecifics in the rat hippocampus. The Journal of neuroscience : the official journal of the Society for Neuroscience 32:2129-2141.

Wang C, Chen X, Lee H, Deshmukh SS, Yoganarasimha D, Savelli F, Knierim JJ (2018) Egocentric coding of external items in the lateral entorhinal cortex. Science 362:945-949.

Wilson DI, Watanabe S, Milner H, Ainge JA (2013a) Lateral entorhinal cortex is necessary for associative but not nonassociative recognition memory. Hippocampus 23:1280-1290.

Wilson DIG, Langston RF, Schlesiger MI, Wagner M, Watanabe S, Ainge JA (2013b) Lateral entorhinal cortex is critical for novel object-context recognition. Hippocampus:n/a-n/a.

Witter M (2012) Chapter 5 - Hippocampus. In: The Mouse Nervous System (Watson C, Paxinos G, Puelles L, eds), pp 112-139. San Diego: Academic Press.

Witter MP (2007) The perforant path: projections from the entorhinal cortex to the dentate gyrus. 163:43-61.

Witter MP, Amaral DG (2004) The hippocampal formation. In: The rat nervous system., 3rd. Edition (Paxinos G, ed), pp 635-704. Amsterdam: Elsevier.

Witter MP, Naber PA, Lopes da Silva F (1999) Perirhinal cortex does not project to the dentate gyrus. Hippocampus 9:605-606.

Witter MP, Naber PA, van Haeften T, Machielsen WC, Rombouts SA, Barkhof F, Scheltens P, Lopes da Silva FH (2000) Cortico-hippocampal communication by way of parallel parahippocampal-subicular pathways. Hippocampus 10:398-410.

Wood ER, Dudchenko PA, Robitsek RJ, Eichenbaum H (2000) Hippocampal neurons encode information about different types of memory episodes occurring in the same location. Neuron 27:623-633.

Yoo SW, Lee I (2017) Functional double dissociation within the entorhinal cortex for visual scene-dependent choice behavior. Elife 6.

Zhang T, Zeng Y, Zhao D, Wang L, Zhao Y, Xu B (2016) Hmsnn: Hippocampus inspired memory spiking neural network. In: 2016 IEEE International Conference on Systems, Man, and Cybernetics (SMC), pp 002301-002306: IEEE.

Zimmer J, Hjorth-Simonsen A (1975) Crossed pathways from the entorhinal area to the fascia dentata. II. Provokable in rats. The Journal of comparative neurology 161:71-101.

# Acknowledgments (감사의 말)

먼저, 지도 교수님 이신 이인아 교수님께 감사의 말씀을 드립니다. 교수님의 지도 덕분에, 연구자로서 갖춰야 하는 여러 능력들을 갖출 수 있었습니다. 또한, 저는 FC 연구를 하면서 다양한 종류의 실험을 해보고, 다양한 문헌들을 읽으면서, 어떤 실험이 필요한지, FC 가 어떻게 작동할 수 있는지에 대하여 다양한 생각과 상상을 해 볼 수 있었습니다. 남들이 잘 알지 못하고 참고 문헌도 거의 없는 새로운 영역을 개척하면서 힘든 적도 있고, 여러가지 한계를 느낄 때도 있었지만, 돌이켜 보면, 이 연구를 하면서 새로운 것을 밝히고, FC 의 작동 원리를 고민해 보던 시간이 저에게 매우 소중하고, 즐거운 시간이었습니다. 이 연구의 시작은 교수님께서 2013 년에 FC 에 대해 아는 바가 없는 것 같으니 우리가 알아보자는 그 말씀에서 시작하였습니다. 이러한 연구를 할 수 있도록 기회를 주신 점에도 감사를 드리고 싶습니다. 또한 이 졸업논문은 많은 분들의 도움 없이는 나올 수 없었습니다. 고려대학교의 선웅 교수님과 이화여자대학교의 이은수 교수님께서는 이 연구에서 중요한 파트인 해부학 연구를 하는데 많은 조언을 해주시고 실험에 큰 도움을 주셨습니다. 또한 우리 연구실을 졸업한 현석이는 해부학 연구와 참고 문헌 탐색에 큰 도움이 되었습니다. 우리 연구실의 유승우 박사님과 홍열이, 은영이 에게도 행동 실험 및 분석에 큰 공헌을 하였기에 감사하다는 말을 전하고 싶습니다. 또한 카이스트의 정민환 교수님, 정영석 박사님과 윤미루 학생도 이 연구를 지지해 주시고, 연구에 많은 도움을 주셨습니다. 이러한 도움에 감사하다는 이야기를 전해 드리고 싶습니다. 추가로 전기 생리학 연구에 필요한 수술을

알려주신 안재롱 박사님. 실험 환경 셋업에 도움을 주었던 승우, 연진이. 행동 실험을 도와주었던 재민이. 해부학 실험에서 synaptic connection 을 확인하는 방법에 대한 아이디어를 제공해준 은혜, LFP 분석에 도움을 주었던 수민이, 자료의 해석 및 model 과 관련한 discussion 에 적극적으로 의견을 내 주었던 충희 형, 요섭이, 현우에게도 감사하다는 이야기를 전하고자 합니다. 우리 연구실이 연구에 적합한 환경이 될 수 있도록 연구 환경을 유지하는데 힘써준 보나, 동구, 혜리, 희승, 소희, 승배, 수빈이 에게도 역시 감사의 이야기를 남기고 싶습니다. RA 로 연구에 도움을 주었던 류경규, 김지욱, 홍성현 학생에게도 감사의 인사를 전하고 싶습니다.

또한, 제가 생활 할 수 있고 성장할 수 있도록 많은 지지와 도움을 주신 부모님께 감사의 말씀을 전하고 싶습니다. 또한 많은 지지와 응원을 보내준 누나와 매형, 그리고 잘 자라고 있는 서윤이와 다윤이 에게도 고마움을 표현하고 싶습니다. 마지막으로 저의 삶을 주관하시는 하나님께 감사 드립니다.

이 박사학위논문에 실린 자료 중 일부는 정현석과 이은영의 석사학위논문에도 사용되었음을 밝힙니다.

# Abstract in Korean

소대회 (fasciola cinereum)는 해마의 하위 구조 중 하나로, 다른 해마의 하위 구조들에 비해 상대적으로 잘 알려지지 않은 미지의 영역이다. 기존의 연구들에서 해마의 하위 구조들의 고유한 연결 및 생리학적 특성이 인지적인 기능, 특히 학습과 기억에, 중요하다는 것이 알려진 바 있다. 하지만 소대회의 연결 관계 및 생리학적 특성에 대해서는 거의 알려진 바가 없기 때문에, 이것의 인지적인 기능이 무엇일지 예상하는 것은 매우 어렵다. 따라서, 이 연구에서는 소대회의 해부학적 연결 관계 및 생리학적 특성을 밝히고, 인지적인 기능이 무엇인지 알아내고자 하였다. 이 연구의 해부학 실험에서 소대회가 비주위 피질과 측면 내 후각 피질에서 정보를 받고 치상회로 정보를 전달한다는 것을 알아내었다. 소대회와 연결된 영역들이 학습과 기억에 중요한 영역이기 때문에, 소대회 역시 학습에 중요한지 알아보기 위해, 소대회를 선택적으로 없앤 쥐를 이용하여, 치상회가 중요하다고 알려져 있는 맥락 학습 실험을 진행 하였다. 예상대로, 이 쥐는 이미 배운 것을 회상하는 데는 대조 군과 큰 차이를 보이지 않았지만, 새로운 맥락 학습을 하는 데는 어려움을 겪는다는 것을 확인할 수 있었다. 이것을 통해 소대회가 맥락 학습에 중요하다는 것을 알게 되었다. 마지막으로 소대회가 맥락 학습에 특화된 영역인지 다른 종류의 치상회가 중요하다고 알려져 있는 실험에도 중요한지 알아보기 위해 사물-장소 연상 기억을 요구하는 실험들과 사물의 재인 능력을 알아보는 실험들을 진행 하였다. 그 결과 소대회가 사물을 재인하는 능력에는 영향을 미치지 않지만, 사물과 장소의 연상 기억을 요구하는 실험들에서는 중요하다는 것을 알게 되었다. 이를 통해 소대회가 맥락 학습뿐만

아니라, 다른 일반 적인 치상회 의존적인 학습 들에서 중요한 역할을 한다는 것을 발견 하였다. 또한 전기 생리학 실험에서, 자유롭게 움직이는 쥐의 소대회에 있는 개별 신경세포들의 전기생리학적 활동을 관찰하여 보았을 때, 그것은 해마의 다른 곳에서 관찰되는 신경세포들과 마찬가지로 장소 선택적인 발화 활동을 보인다는 것, 즉 장소 세포가 존재함을 발견하였으며 그것이 인접한 CA1 영역과 비교하였을 때 차이가 있음을 확인하였다. 또한, 소대회에서 발견되는 장소 세포를 쥐가 T 모양의 미로를 왕복하는 행동을 하는 동안 관찰 하였을 때, 이 장소 세포가 표상하는 위치가 주변 장면의 변화와 동기화 되어 변화하거나 혹은 상관 없이 변화하는 것을 관찰할 수 있었다. 나는 이러한 관찰을 토대로, 소대회가 인지적인 기능이 있다면, 이러한 특성이 치상회의 학습 능력에 도움을 줄 수 있지만 이미 학습한 것을 회상하는 데는 관여하지 않을 수 있음 설명하는 모델을 새롭게 제시 하였다.

**이 연구의 중요성:** 이 연구는 기존의 연구에서 상대적으로 소홀히 다루어진 소대회의 해부학적, 생리학적, 인지적 특성들에 대해 처음으로 밝히고 이것의 작동 기전에 관해 제시한 연구라는 점에서 기념비적인 연구라고 할 수 있다. 이러한 발견 및 새로운 모델의 제시는 해마의 구조 및 기능에 관한 이해를 넓혔다. 그 뿐 아니라 소대회가 손상된 쥐에서 전향성 기억상실증과 유사한 증상이 나타나는 것을 확인할 수 있다. 이는 전향성 기억 상실증의 기존에 알려지지 않은 잠재적인 원인을 찾았다는 점에서, 이 원인으로 인한 병의 치료의 시작이 될 수 있는 연구이다. 또한 이 연구에서 새롭게 제시된 모델은 뇌모사 인공지능의 제작에 큰 영감을 불어넣을 것으로 예상된다.